DISSERTATION ZUR ERLANGUNG DES DOKTORGRADES
DER FAKULTÄT FÜR BIOLOGIE
DER LUDWIG-MAXIMILIANS-UNIVERSITÄT MÜNCHEN

Histone Acetylation as a Barrier to Cell Fate Reprogramming via Nuclear Transfer

Vorgelegt von
ANA JANEVA, M.Sc.
aus Skopje

2025

Diese Dissertation wurde angefertigt
unter der Leitung von Dr. Eva Hörmanseder
am Institut für Epigenetik und Stammzellen
des Helmholtz Zentrums München

Erstgutachterin: Prof. Dr. Maria-Elena Torres-Padilla
Zweitgutachter: Prof. Dr. John Parsch

Tag der Abgabe: 28.07.2025
Tag der mündlichen Prüfung: 09.12.2025

Eigenständigkeitserklärung

Hiermit versichere ich an Eides statt, dass die vorliegende Dissertation mit dem Titel „**Histone Acetylation is a Novel Barrier to Cell Fate Reprogramming via Somatic Cell Nuclear Transfer**“ von mir selbstständig verfasst wurde und dass keine anderen als die angegebenen Quellen und Hilfsmittel benutzt wurden. Die Stellen der Arbeit, die anderen Werken dem Wortlaut oder dem Sinne nach entnommen sind, wurden in jedem Fall unter Angabe der Quellen (einschließlich des World Wide Web und anderer elektronischer Text- und Datensammlungen) kenntlich gemacht. Weiterhin wurden alle Teile der Arbeit, die mit Hilfe von Werkzeugen der künstlichen Intelligenz de novo generiert wurden, durch Fußnote/Anmerkung an den entsprechenden Stellen kenntlich gemacht und die verwendeten Werkzeuge der künstlichen Intelligenz gelistet. Die genutzten Prompts befinden sich im Anhang. Diese Erklärung gilt für alle in der Arbeit enthaltenen Texte, Graphiken, Zeichnungen, Kartenskizzen und bildliche Darstellungen.

München, 28.07.2025
(Ort / Datum)

Ana Janeva
(Vor und Nachname in Druckbuchstaben).

Ana Janeva
(Unterschrift)

Affidavit

Herewith I certify under oath that I wrote the accompanying Dissertation myself.
Title: “**Histone Acetylation is a Novel Barrier to Cell Fate Reprogramming via Somatic Cell Nuclear Transfer**“. In the thesis no other sources and aids have been used than those indicated. The passages of the thesis that are taken in wording or meaning from other sources have been marked with an indication of the sources (including the World Wide Web and other electronic text and data collections). Furthermore, all parts of the thesis that were de novo generated with the help of artificial intelligence tools were identified by footnotes/ annotations at the appropriate places and the artificial intelligence tools used were listed. The prompts used were listed in the appendix. This statement applies to all text, graphics, drawings, sketch maps, and pictorial representations contained in the Work.

Munich, 28.07.2025
(Location/date)

Ana Janeva
(First and last name in block letters)

Ana Janeva
(Signature)

“Two things fill the mind with ever new and increasing admiration and awe, the more often and steadily we reflect upon them: the starry heavens above me and the moral law within me. I do not seek or conjecture either of them as if they were veiled obscurities or extravagances beyond the horizon of my vision; I see them before me and connect them immediately with the consciousness of my existence.”

— Immanuel Kant

Table of Contents

1. Summary

Cell fates are established during embryonic development and differentiation. Under physiological conditions in healthy organisms, cell fates rarely change, and any changes are often considered abnormal. Specific experimental manipulations, initially performed by John Gurdon in 1958, demonstrated that cell fates can be reversed to totipotency by injecting somatic nuclei into an enucleated *Xenopus laevis* egg and give rise to fertile adults in a process known as somatic cell nuclear transfer (SCNT). This process has low efficiency, as the cloned embryos often do not survive or demonstrate developmental abnormalities. The failure of cloned embryos to develop and survive has partly been attributed to a phenomenon known as epigenetic memory, referring to the aberrant expression of genes indicative of the transcriptional profile of the donor cell, or the failure of genes to accurately re-activate in the newly generated cell types, which is thought to be dependent on the propagation of chromatin marks. The failure of genes to activate their expression in reprogrammed cells has widely been attributed to 'repressive' chromatin features in the starting cell type, yet the phenomenon in which genes maintain an active chromatin and transcription state from the donor cell to the reprogrammed cell, has not been fully addressed yet. This phenomenon has in part been attributed to the persistence of trimethylation at histone H3 lysine K4 (H3K4me3) around the transcription start site (TSS) of genes that fail to downregulate their expression in reprogramming, so-called ON-memory genes. Currently, however, it is unknown which factors, and which 'active' chromatin marks contribute to ON-memory, acting alongside or together with H3K4me3, to form an "epigenetic barcode" that stabilizes cell fate specific gene expression and prevents cell fate reprogramming. To address this question, our group has previously developed Digital Reprogramming, a computational model capable of predicting reprogramming resistance and identifying epigenetic barriers from chromatin and transcriptome data in donor nuclei and wild-type target cells. With this approach, acetylation on Histone H3 lysine 27 (H3K27ac) was identified as a potential novel barrier to reprogramming and was thus chosen as the focus of this project. Reducing H3K27ac levels using p300/CBP inhibitors in donor cells before reprogramming correlated with an improved downregulation of genes linked to H3K27ac-modified enhancers during reprogramming. Importantly, these effects were accompanied by an improvement in the embryonic development of the resulting NT embryos. Taken together, these findings implicate H3K27ac as a protective mechanism maintaining cell fates and acting as a barrier to cell fate changes during reprogramming.

2. Zusammenfassung

Das Zellschicksal wird während der Embryonalentwicklung und Zelldifferenzierung festgelegt. Unter physiologischen Bedingungen in gesunden Organismen ändern sich die Zellidentitäten nur selten, und solche Änderungen werden oft als abnormal betrachtet. Durch spezifische experimentelle Manipulationen, die erstmals 1958 von John Gurdon durchgeführt wurden, konnte gezeigt werden, dass das Zellschicksal durch Injektion somatischer Zellkerne in ein entkerntes Ei von *Xenopus laevis* zurück in einen totipotenten Zustand umgewandelt werden kann, sodass in einem als somatischer Zellkerntransfer bekannten Prozess fruchtbare, geklonte erwachsene Tiere entstehen. Dieses Verfahren ist wenig effizient, da die geklonten Embryonen oft nicht überleben oder Entwicklungsanomalien aufweisen. Das Scheitern der Entwicklung und des Überlebens geklonter Embryonen wird zum Teil auf ein Phänomen zurückgeführt, das als epigenetisches Gedächtnis bekannt ist und sich auf die abweichende Expression von Genen bezieht, die auf das Transkriptionsprofil der Spenderzelle hinweisen, oder darauf, dass Gene in den neu erzeugten Zelltypen nicht richtig reaktiviert werden. Das Versagen von Genen, ihre Expression in reprogrammierten Zellen zu aktivieren, wurde weithin auf „repressive“ Chromatinmerkmale im Ausgangszelltyp zurückgeführt, doch das Phänomen, dass Gene einen aktiven Chromatin- und Transkriptionszustand von der Spenderzelle bis zur reprogrammierten Zelle beibehalten, ist noch nicht vollständig erforscht. Dieses Phänomen wurde zum Teil auf die Persistenz der Trimethylierung an Histon H3 Lysin K4 (H3K4me3) um die Transkriptionsstartstelle (TSS) von Genen zurückgeführt, die ihre Expression bei der Reprogrammierung nicht herunterregulieren, so genannte ON-Memory-Gene. Derzeit ist jedoch nicht bekannt, wie ON-Memory auf molekularer Ebene übertragen wird. Es ist unklar, welche Faktoren und welche „aktiven“ Chromatinmarkierungen zu ON-Memory beitragen und neben oder zusammen mit H3K4me3 einen „epigenetischen Barcode“ bilden, der die zellschicksalspezifische Genexpression stabilisiert und die Reprogrammierung des Zellschicksals verhindert. Um diese Frage zu klären, hat unsere Gruppe Digital Reprogramming entwickelt, ein Computermodell, das in der Lage ist, Reprogrammierungsresistenz vorherzusagen und epigenetische Barrieren anhand von Chromatin- und Transkriptomdaten in Spenderkernen und Wildtyp-Zielzellen zu identifizieren. Mit diesem Ansatz wurde die Acetylierung am Histon H3-Lysin 27 (H3K27ac) als potenzielle neue Barriere für die Reprogrammierung identifiziert und als Schwerpunkt dieses Projekts ausgewählt. Die Verringerung von H3K27ac mit Hilfe von p300/CBP-Inhibitoren in Spenderzellen vor der Reprogrammierung korrelierte mit einer verbesserten Herunterregulierung von Genen, die mit H3K27ac-modifizierten Enhancern verbunden sind, während der Reprogrammierung. Wichtig ist, dass diese Effekte mit einer Verbesserung der embryonalen Entwicklung der resultierenden NT-Embryonen einhergingen. Zusammengefasst deuten diese Ergebnisse darauf hin, dass H3K27ac als

Schutzmechanismus fungiert, der das Zellschicksal aufrechterhält und während der Reprogrammierung als Barriere gegen Veränderungen des Zellschicksals wirkt.

3. Introduction

3.1. Cell fate establishment and reprogramming

The earliest developmental stage of sexually reproducing organisms is the zygote, which is generated upon the fusion of a male and a female gamete. All cell types of an organism are formed from the totipotent zygote, which ultimately gives rise to a fertile adult organism (Condic, 2014). During development, the zygote undergoes multiple rounds of cell division. Its potency, i.e., the ability of a cell to differentiate into different cell types of an organism, is gradually restricted and eventually lost (Lu & Zhang, 2015), as cellular identities emerge. The integration of developmental signals, along with the establishment of transcription factor (TF) networks and a set of epigenetic characteristics, stabilizes cellular identities during lineage commitment (Atlasi & Stunnenberg, 2017; Bell et al., 2024; Perrimon et al., 2012; Spitz & Furlong, 2012; Zaret & Mango, 2016). Importantly, cell identities are stably inherited by daughter cells during mitosis (Escobar et al., 2021; Gonzalez et al., 2021; Palozola et al., 2019; Stewart-Morgan et al., 2020).

Early models of cellular differentiation posited an irreversible process (Waddington, 2014). In his influential landscape model, Waddington described cells as marbles rolling down an inclined surface with branching valleys, where each bifurcation represents a cell fate decision. The cell's journey through these valleys symbolizes differentiation toward terminal states, with surrounding hills illustrating barriers that prevent cell fate reversal or change. This model attributed differentiation to unidirectional changes in genetic and epigenetic traits that progressively restrict cellular potential (Figure 1).

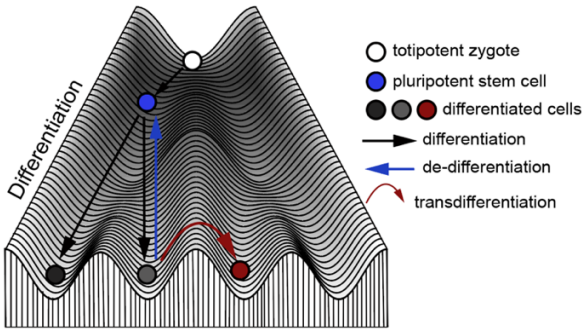

Figure 1: Waddington landscape. The Waddington landscape model depicting cell differentiation. A totipotent zygote (white circle) gradually loses potency and develops into pluripotent stem cells (blue circle) which further differentiate into specialized cell types (black, red circles). Arrows indicate differentiation (black arrow), de-differentiation (blue arrow), and transdifferentiation (red arrow) trajectories between cell states. The landscape topography represents cell fate decisions.

Nowadays, it is known that cell differentiation is not irreversible, and cell fates are plastic (

Figure ***1***), owing to several experimental procedures that have demonstrated the conversion of differentiated cells into undifferentiated cells. Examples of such procedures are somatic cell nuclear transfer (SCNT) (Gurdon et al., 1958), cell-cell fusion (Blau et al., 1983) and transcription factor (TF) overexpression (Takahashi & Yamanaka, 2006). All these experiments entail *nuclear reprogramming*, which describes a switch in gene activity from the starting cell type to that of an earlier developmental stage or another cell type (Gurdon & Melton, 2008). Moreover, pluripotent and totipotent cells generated via nuclear reprogramming can differentiate and in the case of SCNT, give rise to a cloned organism (Gurdon et al., 1958; Takahashi & Yamanaka, 2006).

The ability to generate cells using nuclear reprogramming is instrumental in understanding the mechanisms that establish and stably maintain cell fates under physiological conditions (Brumbaugh et al., 2019). In the context of disease, deriving and differentiating cell lines for *in vitro* studies allows disease modeling, organoid studies and drug testing (Mall & Wernig, 2017; Nakatsukasa et al., 2025). Moreover, nuclear reprogramming is the foundation for developing cell replacement therapies in which injured or defective cells can be replaced by healthy cells, which have been produced from another cell type (Gurdon & Melton, 2008). The ability to produce such cells from the patient that requires them, circumvents the issue of rejection commonly faced with transplants, as there is no genetic incompatibility. Given these far-reaching implications for understanding stem cell biology, as well as regenerative medicine and disease modeling, understanding the molecular mechanisms underlying reprogramming is of essence, and has been the goal of several decades of research to date (Götz & Torres-Padilla, 2025).

3.2. Somatic cell nuclear transfer (SCNT)

Somatic Cell Nuclear Transfer (SCNT), or briefly Nuclear Transfer (NT) is defined as an experimental procedure in which the nucleus of a differentiated cell, termed donor nucleus, is transplanted into an enucleated recipient egg. Thereby, the reprogramming activities of the egg reverse the somatic nucleus to a totipotent state, which gives rise to new cell types of an embryo and ultimately, an adult organism (Gurdon et al., 1958; Gurdon & Uehlinger, 1966). The first attempts at NT were carried out by Briggs and King in the frog species *Rana pipiens* (R. Briggs & King, 1952). At the time, transplanting a differentiated nucleus to replace the totipotent nucleus of the zygote was considered a key experiment to solve the question of whether all cells of an organism house the same set of genes (reviewed in (M. S. Oak & Hörmanseder, 2022)). If the embryo derived from a transplanted nucleus developed, this would confirm that the genetic material remains

intact during development, and that differentiation does not compromise the plasticity of the nucleus. Briggs and King introduced blastula nuclei into enucleated eggs from *Rana pipiens* and obtained living tadpoles, but this was not the case when transplanting differentiated nuclei from neurula-stage endoderm cells. Thus, they concluded that the properties of a nucleus that permit embryonic development are decreased or eliminated after a certain point in differentiation (R. Briggs & King, 1952).

John Gurdon revisited this approach in a different frog species, *Xenopus laevis,* and demonstrated that differentiated nuclei could support normal development and give rise to sexually mature adult frogs (Figure 2) (Elsdale et al., 1960; Gurdon et al., 1958; Gurdon & Uehlinger, 1966). This finding contradicted Briggs and King and showed that even nuclei from advanced developmental stages, such as tadpoles, can support the normal growth of NT embryos. A key control in this experiment was the use of donor nuclei from an *X. laevis* strain containing only one nucleolus, thus making the resultant NT embryos easily distinguishable from wildtype strains with two nucleoli per nucleus (Elsdale et al., 1960). This proved that the UV-induced enucleation prior to SCNT indeed destroyed the chromosomes of the egg, and they did not participate in the development of the NT embryos. These experiments led to the conclusion that during cell differentiation, the genome remains intact and that almost all cells house the same set of genes (Elsdale et al., 1960; Gurdon et al., 1958; Gurdon & Uehlinger, 1966). Several decades later, cloning was achieved in mammals, and the early results from *Xenopus* were reproduced. The first cloned mammals were mouse embryos (Tsunoda et al., 1987; Wakayama et al., 1998), bovine embryos (Prather et al., 1987), sheep (Campbell, McWhir, et al., 1996) and pigs (Polejaeva et al., 2000).

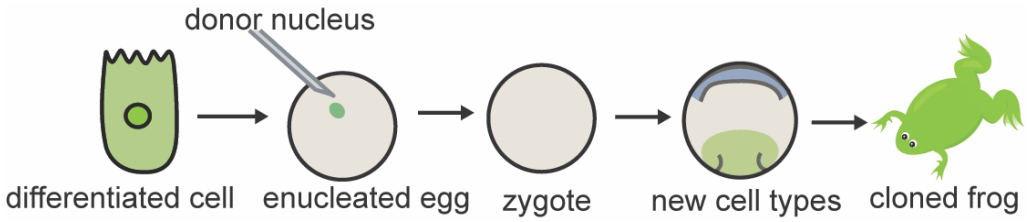

Figure 2: Schematic overview of the Nuclear Transfer procedure in Xenopus laevis: Endoderm cells from a neurula-stage donor embryo are injected into an enucleated egg, giving rise to a totipotent zygote, which then differentiates into new cell types and ultimately produces a cloned adult organism.

3.2.1. A molecular insight into nuclear transfer reprogramming

SCNT-reprogramming involves multiple molecular mechanisms, including maternal cytoplasmic factors, transcription factors, chromatin remodelers, histone

variants, DNA replication processes, and metabolic changes, while the genomic sequence of the donor nucleus remains intact (Gurdon, 2013; Matoba & Zhang, 2018; M. S. Oak & Hörmanseder, 2022; Pasque, Jullien, et al., 2011). Matoba & Zhang have proposed to define SCNT-reprogramming as the cellular and molecular events that occur in the transferred somatic nucleus before the next major developmental event takes place in the cloned embryo (Matoba & Zhang, 2018). This major developmental event is the activation of zygote-driven transcription, termed zygotic genome activation (ZGA) (Jukam et al., 2017; Matoba & Zhang, 2018). It is important to note that the timing of ZGA strongly varies across species. While mouse embryos undergo major ZGA after only one cell division, *X. laevis* embryos undergo 12 cell divisions before transcription resumes (Hörmanseder et al., 2013). This species-specific difference creates distinct contexts in which reprogramming occurs upon SCNT: the extended pre-ZGA window in *Xenopus* involves multiple rounds of rapid DNA replication which can dilute chromatin marks and other epigenetic information from the donor nucleus, possibly introducing replication-dependent changes beyond the direct effects of the egg cytoplasm.

Despite these complexities, defining SCNT reprogramming as the molecular events preceding ZGA remains useful to distinguish the direct reprogramming effects of the egg cytoplasm from the subsequent developmental processes, as the activation of the zygotic genome introduces additional, transcription-dependent epigenetic changes (Matoba & Zhang, 2018). Such transcription-dependent processes can obscure the distinct reprogramming events driven solely by the egg cytoplasm. However, it is worth noting that many developmental processes in the cloned embryo are likely influenced by both the reprogramming events before ZGA and the proper execution of ZGA itself. For instance, the interplay between these initial reprogramming processes and intrinsic properties of the donor nucleus may collectively impact genome activation. Furthermore, ZGA represents a critical developmental milestone for the transition from maternal to embryonic control (Jukam et al., 2017; Vastenhouw et al., 2019). Therefore, the following section describing NT to *Xenopus laevis* eggs and mouse oocytes will focus on the molecular events that reprogram the somatic nucleus before the cloned embryo resumes transcription.

3.2.1.1. Nuclear reprogramming in *Xenopus*

While the vertebrate egg cytoplasm has the remarkable ability to reprogram somatic nuclei and support the development of NT embryos, the cellular and molecular mechanisms that facilitate or inhibit this process are poorly understood (Hörmanseder, 2021; Matoba & Zhang, 2018; M. S. Oak & Hörmanseder, 2022). In amphibians, the term oocyte refers to a precursor cell of mature eggs, which are incompetent for fertilization. Amphibian oocytes contain a nucleus called germinal vesicle (GV) that hosts an

abundance of components necessary to support early embryonic development. Such immature oocytes are arrested at the prophase of meiosis I, and hormones such as progesterone can trigger their release into meiosis I and into the metaphase of meiosis II, at which they are arrested again (Ferrell, 1999). Then, oocytes are considered mature and ready for fertilization, marking a stage termed egg in *Xenopus*, similar to the MII oocyte in mammals (Hörmanseder et al., 2013). Therefore, when using mature eggs as recipients in NT reprogramming, this can be referred to as egg-NT (M. S. Oak & Hörmanseder, 2022).

The mechanisms of nuclear reprogramming in *Xenopus* can be studied using three complementary experimental systems: egg-NT, oocyte-NT and egg extracts (Hörmanseder, 2021; Miyamoto, 2019; M. S. Oak & Hörmanseder, 2022; Tokmakov et al., 2016). In egg-NT, the somatic nuclei are microinjected into mature UV-enucleated eggs. This is then followed by embryonic development through rapid, transcriptionally silent cell divisions until zygotic genome activation. This system provides a direct readout of the reprogramming success by monitoring and quantifying embryonic development. However, there are several caveats in attempting to study mechanistic aspects of nuclear reprogramming in egg-NT (M. S. Oak & Hörmanseder, 2022). A prime example is the transition from the somatic to early embryonic cell cycle upon injection to an egg. While somatic cells are largely mitotically quiescent, early embryonic divisions in *Xenopus* rapidly oscillate between DNA replication and mitosis with no detectable G-phases (Hörmanseder et al., 2013). Such rapid cycling may lead to chromosomal damage in the donor nucleus due to incomplete DNA replication (M. S. Oak & Hörmanseder, 2022). Together with the fact that early *Xenopus* embryos are transcriptionally inactive until the mid-blastula transition, egg-NT reprogramming of somatic nuclei is mainly associated with the induction of DNA replication and mitotic transition (Tokmakov et al., 2016), making it challenging to study transcriptional reprogramming events in this system (M. S. Oak & Hörmanseder, 2022).

In contrast, when somatic nuclei are transplanted into the GV of oocytes (oocyte-NT), they undergo extensive transcriptional reprogramming without DNA replication, cell division, or protein synthesis (Halley-Stott et al., 2010). Such oocytes are characterized by high transcriptional activity and contain a high abundance of maternal RNAs and proteins capable of supporting early development (Halley-Stott et al., 2010; Tokmakov et al., 2016). In nuclear reprogramming experiments using oocytes, up to several hundred somatic nuclei can be injected directly into the GV, reaching about 400 µm in diameter. The high transcriptional activity and ability to accept hundreds of nuclei make oocyte-NT particularly suited for studying transcriptional mechanisms and resistance to reprogramming (M. S. Oak & Hörmanseder, 2022). Additionally, *Xenopus* oocytes can transcriptionally reprogram incoming nuclei from different species, such as mammalian

nuclei (Halley-Stott et al., 2010). In this case, many genes that are normally inactive in the donor nucleus are rapidly activated upon exposure to the GV, for example pluripotency genes. Moreover, this system allows manipulation of endogenous reprogramming factors by knockdown or overexpression approaches, and is thus highly useful in dissecting the kinetics and molecular mechanisms of transcriptional reprogramming (Halley-Stott et al., 2013). The use of two distinct species as donor and recipient allows the measurement of induced transcripts without background from maternal transcripts (Halley-Stott et al., 2010). Hence, much of the mechanistic insight about nuclear reprogramming in *Xenopus* has been obtained from oocyte-NT.

Complementing these *in vivo* approaches, cell-free extracts prepared from *Xenopus* eggs have proven beneficial in dissecting reprogramming mechanisms. In an attempt to circumvent the limitation of the low number of reprogrammed cells obtained by a NT experiment, reprogramming systems using egg and oocyte extracts have been developed to allow mechanistic studies of reprogramming (Miyamoto, 2019; Tokmakov et al., 2016). Cells incubated with egg extracts are considered only partially reprogrammed, as this process can induce only some aspects of reprogramming, such as DNA replication and chromatin decondensation in the absence of transcription (Miyamoto, 2019; M. S. Oak & Hörmanseder, 2022). However, egg extracts retain many activities of intact eggs, therefore providing a valuable system to recapitulate molecular events of reprogramming (Tokmakov et al., 2016), while being highly biochemically tractable and amenable to perturbations. For instance, it is possible to remove specific maternal factors from egg extracts by immunodepletion, which is still very challenging to perform in live eggs (Miyamoto, 2019). Moreover, fractionation of extracts can also be used to identify egg factors that facilitate certain reprogramming events (Miyamoto, 2019). It has also been shown that pre-exposure of donor cells to egg extracts can enhance the efficiency of subsequent NT (Ganier et al., 2011).

	Oocyte-NT	**Egg-NT**	**Egg Extract**
Generating new cell types	no	yes	no
DNA replication	no	yes	yes
Transcriptional reprogramming	yes	yes	no
Protein synthesis	no	yes	yes
Donor cells per recipient	hundreds	one	scalable
Species (donor/recipient)	different	same	flexible
Yield	high	low	high
Manipulation of reprogramming factors	yes	no	yes

Table 1: Summary of the key properties of nuclear reprogramming in *Xenopus laevis*, oocyte-NT, egg-NT and egg extract.

The following sections describe the molecular events occurring after NT to eggs, which have been elucidated through combined insights from all three experimental systems in the frog. In *Xenopus* egg-NT, the eggs are enucleated using UV light, which does not damage the rest of the egg apart from the chromosomes due to its low penetrance and large size of the egg (Gurdon, 1960c). The microinjection of the donor nucleus during an SCNT-experiment simultaneously activates the egg, similar to sperm entry in normal fertilization. The first event taking place after the injection of the donor nucleus into the egg and oocyte is the increase in nuclear volume (Gurdon, 1968) or chromatin decompaction. This is thought to set the stage for subsequent DNA replication and transcription (Gurdon & Wilmut, 2011). Similar to somatic nuclei injected to eggs, an increase in nuclear volume has also been observed in sperm soon after fertilization in frogs and mammals (Gurdon & Wilmut, 2011).

The next event following NT to *Xenopus* eggs is DNA replication of the transplanted nuclei, preceding the first mitotic cell division. In the *Xenopus* embryo, the first cell division is prolonged and takes about 90 min, followed by a series of rapid cell divisions every 30 min (Hörmanseder et al., 2013). Interestingly, the DNA synthesis-inducing activity of eggs can force even differentiated and rarely or nondividing cells to replicate their DNA (Graham et al., 1966). The introduction of a slowly dividing differentiated cell into a rapidly dividing egg can be seen as the first challenge that needs to be overcome for a successful NT experiment. The suddenly rapid cell division could lead to separation of only partially replicated chromosomes, which in turn leads to damaged cleavage nuclei and abnormal cleavage (King & DiBerardino, 1965). Some of the early attempts to improve NT outcomes in *Xenopus* involved performing “serial NT” (Gurdon, 1960a), a procedure in which the nuclei of cleaved or partially cleaved NT blastulae are injected into eggs. Such subsequent NT has been beneficial for improving NT outcomes and is thought to provide the NT embryo a second chance to complete DNA replication and develop further (M. S. Oak & Hörmanseder, 2022). Studies using egg extract-induced reprogramming confirmed that differentiated erythrocytes inefficiently replicate in *Xenopus* eggs but replicate as readily as sperm nuclei if they have undergone a previous round of mitosis before reprogramming (Lemaitre et al., 2005). This study suggested that exposure to a mitotic environment remodels the chromatin by shortening of chromatin loops and closer spacing of replication origins, similar to the chromatin of sperm nuclei and the early *Xenopus* embryo. In summary, preconditioning the somatic cell chromatin to an embryonic state before reprogramming seems beneficial, although additional factors that restrict reprogramming are likely at play. After 12 rapid and

transcriptionally silent cell cycles, the embryo reaches the mid-blastula transition, the zygotic genome is activated, and transcription resumes.

While NT to *Xenopus* eggs has been useful to gain insights into DNA replication in reprogramming, mechanistic insights into chromatin remodeling and transcriptional reprogramming have been obtained from the complementary, highly tractable, systems of oocyte-NT and egg-extract exposure. For instance, large-scale chromatin decompaction of the condensed somatic chromatin is considered a prerequisite for successful reprogramming (Matoba & Zhang, 2018; Pasque, Jullien, et al., 2011). Such decompaction is considered necessary to activate downstream gene expression by facilitating TF-binding to their genomic targets. In biochemical experiments using egg extract to induce reprogramming, the decompaction of chromatin following the exposure to the egg has been attributed to the H2A-H2B histone chaperone nucleoplasmin (Tamada et al., 2006). In addition, gain of H3K14 acetylation and the displacement of heterochromatin proteins such as HP1β and TIF1β can be observed, which is indicative of chromatin opening (Tamada et al., 2006). In the early stages of reprogramming by oocytes, the somatic transcriptional machinery is lost, as visible by the loss of somatic RNA Pol II and TATA-binding protein (TBP), along with repression of somatic genes (Jullien et al., 2014). Next, the somatic linker histone H1 is replaced by oocyte-specific linker histone B4, which promotes chromatin decondensation in eggs and oocytes (Jullien et al., 2010). In addition, the replication-independent histone variant H3.3., previously associated with active transcription, has been found to be necessary for efficient oocyte-NT reprogramming (Jullien et al., 2012). The macroH2A histone variant correlated with transcriptional repression is replaced from somatic nuclei following NT to oocytes (Pasque, Halley-Stott, et al., 2011). Lastly, the oocyte transcriptional machinery is activated by binding of the oocyte-specific TBP2, RBP1, and increased levels in phosphorylated RNA Pol II, reflecting transcriptional activity (Jullien et al., 2014).

Noteworthy, nuclear actin is enriched in the GV of oocytes, where it plays a role in transcriptional activation and chromatin remodeling (Ulferts et al., 2024). Upon NT to *Xenopus* oocytes, filamentous actin is formed in the transplanted nuclei, as revealed by live-imaging studies (Miyamoto et al., 2011). Such nuclear actin polymerization, involving the actin signaling proteins Toca-1 and Wave1, has been identified as a key step in the reactivation of the pluripotency TF *Oct4/Pou5f1* upon NT to oocytes (Miyamoto et al., 2011, 2013). Moreover, Wave1 associates with active transcriptional machineries through multiple interactions. It binds to the SET domain of MLL, an H3K4me3 methyltransferase. Wave1 also interacts with the phosphorylated serine 2 residue of RNA Pol II, which is associated with transcriptional elongation. Through these interactions, Wave1 enhances the efficiency of transcriptional reprogramming by oocytes (Miyamoto et al., 2013). Collectively, these studies in oocyte-NT and egg-extract systems reveal a coordinated

series of molecular events involving histone variant exchange, chromatin remodeling, and actin-mediated transcriptional activation that work synergistically to enable nuclear reprogramming.

3.2.1.2. SCNT reprogramming in mouse

While the field of nuclear reprogramming was pioneered by amphibian cloning, the mouse has become one of the most widely studied models for mammalian SCNT-reprogramming in a research context (Kishigami & Wakayama, 2009). Moreover, many mechanistic insights of the reprogramming process, some of which have also be found to be conserved in the frog, have been discovered in the context of mouse SCNT-reprogramming. Thus, the following sections detail reprogramming processes and mechanisms revealed through mouse studies as an example for mammalian SCNT.

Unlike in frog, the enucleation of the oocytes is usually performed manually in mouse NT, as UV irradiation may also damage the maternal cytoplast (Li et al., 2004). Upon introduction to the enucleated mammalian oocyte, the donor nucleus undergoes rapid nuclear membrane breakdown and forms condensed metaphase-like chromosomes in a process known as premature chromosome condensation (PCC), which is triggered by M-phase promoting factors (MPF) in the ooplasm (Campbell, Loi, et al., 1996). Most chromatin-associated proteins dissociate from the genome during PCC (Matoba & Zhang, 2018). Later, the oocytes are activated by adding strontium chloride ($SrCl_2$) to the medium, which mimics the natural Ca^{2+} signals induced by fertilization (Matoba & Zhang, 2018). This is a noteworthy difference to the SCNT procedure in *Xenopus,* as the injection of the donor nucleus and the activation of the oocyte are two separate events in the mouse and occur simultaneously in the frog where microinjection is sufficient to activate the recipient egg. After activation using $SrCl_2$ in lieu of the sperm-borne phospholipase C zeta 1 PLCZ1 in natural fertilization, the MPF levels decline, and expansion of the transplanted nucleus can be observed. Lacking the maternal and paternal pronuclei typically found after fertilization, a varying number of pronuclei termed pseudo-pronuclei (PPN) are formed once the donor nucleus enters G1 phase and forms a nuclear membrane. The PPN then incorporates a large amount of maternal proteins and drastic changes in chromatin structure and protein association are thought to occur as a consequence (Matoba & Zhang, 2018).

In contrast to the fast embryonic cell divisions in frog, the first cell division in mouse embryos takes about 20 h. In fertilized zygotes, the first DNA replication is characterized by slower fork speed compared to that of more differentiated cells (Nakatani, 2025; Nakatani et al., 2022), and occurs about 5-6 h post fertilization, continuing for 6-7 h (Yamauchi et al., 2009). A recent study reported that hydroxyurea (HU) treatment, which

correlates with reduced replication fork speed, had beneficial effects on mouse SCNT (Nakatani et al., 2022). HU-treated SCNT embryos showed improved developmental rates at the blastocyst stage and revealed increased activation of reprogramming-resistant regions (Matoba et al., 2014). Thus, this work suggests a beneficial role for replication dynamics in mouse SCNT reprogramming. In frog, the role and contribution of replication fork speed for reprogramming efficiency still needs to be determined.

The donor cell chromatin undergoes extensive remodelling within 12 h post-activation (Djekidel et al., 2018). This remodelling includes widespread histone replacement, rearrangements in nucleosome positioning and reprogramming of chromatin accessibility to accommodate the transition from the somatic to the totipotent cell (Djekidel et al., 2018; Matoba & Zhang, 2018; L. Yang et al., 2022). Global chromatin accessibility patterns transition from a somatic to a zygotic configuration through the loss of donor cell-specific DNase I hypersensitive sites (DHSs) and the emergence of zygote-specific DHSs (Djekidel et al., 2018). Notably, this transformation occurs independently of DNA replication and likely involves a global TF network shift. Maternal histones rapidly replace donor cell histones resembling the replacement of protamines from sperm chromatin during natural fertilization (Matoba & Zhang, 2018). For instance, the replacement of histone H3 in the donor nucleus with maternal H3.3 is considered essential for successful reprogramming of somatic nuclei to pluripotency (Wen et al., 2014). The histone variant macroH2A associated with repressive chromatin is rapidly displaced from donor cell chromatin (Chang et al., 2010). Interestingly, chromatin remodelling, which has been addressed extensively via oocyte mediated reprogramming in frog (reviewed in M. S. Oak & Hörmanseder, 2022; Pasque, Jullien, et al., 2011), revealed that many pathways seem to be conserved, such as histone replacement, as well as the necessity for H3.3 incorporation (Jullien et al., 2012) and the displacement of macroH2A (Pasque, Halley-Stott, et al., 2011).

Successful chromatin reprogramming also involves changes in DNA methylation patterns, chromatin organization, and broader histone modification landscapes (Hörmanseder, 2021; Matoba & Zhang, 2018). DNA methylation undergoes extensive reprogramming through both active demethylation via maternal TET3 enzymes and passive dilution during replication (T.-P. Gu et al., 2011; Iqbal et al., 2011; Matoba et al., 2018; Wossidlo et al., 2011). Furthermore, chromatin architecture has been reported to be dynamically reorganized, with topologically associating domains (TADs) initially dissolving upon nuclear transfer before reestablishing in a pattern that often differs from fertilized embryos (M. Chen et al., 2020; K. Zhang et al., 2020; K. Zhao et al., 2021). Nucleosome positioning around transcription start sites is also reprogrammed, though a recent study has proposed this to occur with delayed kinetics compared to natural fertilization (L. Yang et al., 2022). While these mechanisms have been studied in the context of mouse SCNT reprogramming, the dynamics of DNA methylation, chromatin

architecture and nucleosome positioning remain to be addressed in amphibian reprogramming.

In mouse embryos, initial activation of the zygotic genome occurs at the middle of one-cell stage, known as minor ZGA, and major ZGA occurs at the mid-to-late 2-cell stage (AOKI, 2022; Aoki et al., 1997; Jukam et al., 2017). ZGA is characterized by degradation of maternally stored RNAs and, simultaneously, new RNA synthesis from the zygote. While not much is known about how ZGA in SCNT embryos differs from fertilized embryos (Matoba & Zhang, 2018), gene expression analyses of mouse 2-cell stage SCNT embryos have revealed that the transcriptome of somatic nuclei is reprogrammed to a large extent, with notable differences in the transcriptomes of SCNT and fertilized embryos (W. Liu et al., 2016; Y. Liu et al., 2018; Long et al., 2021; Matoba et al., 2014a). These differences mainly manifest in two categories: a group of embryonic genes fails to activate properly, while certain donor cell-specific transcripts remain inappropriately expressed, collectively pointing towards a transcriptional memory of the somatic donor cell (Hörmanseder, 2021; Matoba et al., 2014a; Matoba & Zhang, 2018). Importantly, these categories of misregulated genes in NT-embryos can be found across all species analyzed to date, including frog (Hörmanseder et al., 2017; Zikmund et al., 2025). The molecular details of such reprogramming resistance are discussed in detail in Section 3.5 below.

3.3. Cell-cell fusion

Cell-cell fusion was another key demonstration of nuclear reprogramming by Helen Blau and colleagues (Blau et al., 1983). By introducing human amniocytes into the cytoplasm of differentiated mouse muscle cells, multinucleated heterokaryons were generated in which the expression of four human-specific muscle proteins was detected. This demonstrated successful activation of previously silent genes from the human genome, suggesting that the mouse muscle cell can reprogram the human nucleus. Such a phenomenon can also be observed when forming heterokaryons from mouse muscle synctia and diverse cell types, including cells from all germ layers (endoderm, mesoderm and ectoderm), therefore demonstrating the plasticity of the differentiated state (Blau et al., 1985). From cell-cell fusion experiments, we have learned that the relative ratio of nuclei or gene dosage contributed by two cell types is crucial in determining the direction of reprogramming, as well as that the frequency and kinetics of reprogramming are variable for different cell types (Yamanaka & Blau, 2010). These experiments broke the persistent dogma of the time that the mammalian differentiated cell state is irreversible and fixed. Instead, Blau and Blakely showed that this state is rather subject to a continuously acting balance of regulators that stabilize it, and can be altered upon shifting that balance (Blau & Blakely, 1999).

Later studies expanded this approach by fusing somatic and embryonic stem cells (ESCs), resulting in hybrid cells that expressed pluripotency marker genes and exhibit ESC-like properties. Most notably, fused cells have been used to produce chimeric mice and for *in vitro* differentiation (Brown & Fisher, 2021; Yamanaka & Blau, 2010). These experiments revealed that ESCs contain dominant factors capable of reprogramming differentiated nuclei to a pluripotent state, for instance an abundance of pioneer transcription factors which can actively bind and reprogram the somatic chromatin to induce pluripotent gene expression programs (Brown & Fisher, 2021). In addition, during fusion to ESCs, somatic cells acquire the unique cell cycle characteristics of ESCs, such as high proportions of cells in S-phase and rapid cycling, which is considered a requirement for successful reprogramming (Brown & Fisher, 2021). This provides a window of opportunity to remodel chromatin and introduce changes in DNA methylation patterns (Brown & Fisher, 2021). Interestingly, a study using cohesin-depleted somatic cells as donors has revealed key mechanistic differences between cell fusion and nuclear transfer reprogramming (Lavagnolli et al., 2015). While cohesin-depleted somatic cells fail to reprogram in mammalian heterokaryon systems due to defective DNA replication, these cells are successfully reprogrammed when transferred to *Xenopus* oocytes. This suggested that while DNA replication is important for cell-fusion mediated reprogramming, it is not required for NT-induced reprogramming in *Xenopus* oocytes.

The fusion approach remains particularly valuable for studying the molecular mechanisms of reprogramming, as it allows tracking the changes in gene expression and chromatin states during the reprogramming process (Brown & Fisher, 2021). Moreover, this approach has been used as a screening method to identify novel reprogramming factors, such as Nkx3-1 (Mai et al., 2018) and Pou3f2 (W. T. Wong et al., 2017). While cell fusion has provided valuable mechanistic insight in the molecular events and agents in reprogramming, its potential for therapeutic applications is confounded by the presence of both nuclei in the resulting heterokaryons. Nowadays, cell-cell fusion is mainly used for mechanistic studies in induced pluripotency combined with imaging and single cell approaches (Brown & Fisher, 2021).

3.4. Transdifferentiation

The discovery of transcription factor (TF)-mediated cell fate alterations is a landmark achievement in developmental biology, fundamentally challenging Waddington's epigenetic landscape model and widening our understanding of cell differentiation (Waddington, 2014). The first compelling evidence that single TFs can alter cell fates came from *Drosophila melanogaster* studies in the 1980s, in which loss-of-function mutations of the Hox gene *Antennapedia (Antp)* resulted in converting the

second pair of legs into ectopic antennae, while gain-of-function mutations led to conversion of the antennae into ectopic legs (Schneuwly et al., 1987; Scott et al., 1983). Furthermore, the first example of a so-called “master regulator” TF, MyoD, was identified, whose ectopic expression in mouse fibroblasts was sufficient to convert them to myoblasts (Davis et al., 1987). This process, in which one somatic cell type is converted into another without going through a pluripotent or totipotent intermediate state is known as *transdifferentiation*. Interestingly, however, the overexpression of XMyoD in early *Xenopus* embryos in cells destined to become ectoderm, could activate muscle genes in this lineage, but did not result in differentiation to muscle (Hopwood & Gurdon, 1990).

Soon followed many other reports where TF-overexpression led to cell fate conversions. Examples of these are the GATA1-mediated conversion from myeloblasts to megakaryocyte and erythrocyte precursors (Kulessa et al., 1995), as well as the CCAAT/enhancer-binding protein-α CEBPα conversion of β B-lymphocytes to macrophages (H. Xie et al., 2004). Notably, the overexpression of *Ascl1*, *Brn2*, and *Myt1l* c convert fibroblasts into functional induced neurons (Vierbuchen et al., 2010). This discovery was soon followed by reports of direct lineage conversions in various other contexts. For example, it was found that overexpressing *Gata4*, *Mef2c*, and *Tbx5* can reprogram fibroblasts into cardiomyocytes (Ieda et al., 2010). By using *Hnf4α* and *FoxA* factors, fibroblasts were reprogrammed into induced hepatocytes (P. Huang et al., 2014), and the overexpression of Oct4 alone is sufficient to reprogram fibroblasts into blood progenitor cells (Szabo et al., 2010). A notable example with significant potential for therapeutic applications is the direct conversion achieved from astrocytes to neurons first *in vitro* (Berninger et al., 2007) and later *in vivo* (Guo et al., 2014).

These principles of transcription factor-mediated transdifferentiation have also been reported in amphibian models. For example, liver-to-pancreas cell conversion has been achieved using Pdx1 overexpression in *Xenopus* (Horb et al., 2003). Additionally, lens regeneration in *X. laevis* tadpoles can occur through transdifferentiation of central outer corneal cells following surgical lens removal, induced by a thus far unidentified vitreous factor and without evidence of return to a pluripotent state during the process (Day & Beck, 2011; Freeman, 1963). This process has been reported to include the re-expression of transcription factors such as Pax6, Prox1, Otx2, and Sox3, with Pax6, thought to confer competence to respond to the vitreous factor and enabling transdifferentiation (Beck et al., 2009).

Together, these studies across diverse model systems suggest that transcription factor-mediated cell-fate conversion is a conserved mechanism that can be harnessed for regenerative purposes.

3.5. Induced pluripotent stem cell (iPSC)-reprogramming

The reprogramming field was revolutionized by a seminal study from 2006 showing that viral transduction of four TFs, Oct4, Sox2, c-Myc and Klf4 (also referred to as OSKM-factors) into embryonic and adult mouse fibroblasts can induce pluripotency and give rise to so-called *induced pluripotent stem cells* (iPSC) (Takahashi & Yamanaka, 2006). The finding that a set of TFs can reprogram fibroblasts into iPSC was soon reproduced in human cells (Takahashi et al., 2007; Yu et al., 2007). The OSKM-factors initiate a cascade of molecular events that gradually erase the somatic cell identity and establish pluripotency. These events have been categorized into three stages: early (initiation), intermediate and late (maturation and stabilization) phase (Samavarchi-Tehrani et al., 2010), largely characterized by analyzing the transcriptional and epigenetic changes following OSKM-introduction at different time points and cell populations upon OSKM-overexpression (Buganim et al., 2013; Hansson et al., 2012; Polo et al., 2012; Buganim et al., 2012).

In order to adopt a stem cell-like chromatin signature, the epigenome of the somatic starting cell should be erased and reprogrammed (Apostolou & Hochedlinger, 2013; Buganim et al., 2013). The initial phase of reprogramming is thought to involve the binding of OSKM-factors to the genome. Oct4, Sox2, and Klf4 possess pioneer activity (Zaret & Carroll, 2011), which enables them to access and bind closed chromatin regions that are typically inaccessible to most transcription factors. This pioneering function would then allow OSK to facilitate subsequent c-Myc binding to these regions. Notably, c-Myc has been proposed to enhance OSK binding to chromatin, creating a positive feedback loop to amplify the reprogramming process (Soufi et al., 2015). As OSKM-factors bind their target sites, they were shown to be associated with a series of epigenetic modifications that progressively overcome the restrictive chromatin landscape of the somatic cell. For instance, this entails changes in the somatic cell-specific DNA methylation patterns and chromatin accessibility, ultimately enabling the activation of pluripotency-associated gene networks (Zaret & Carroll, 2011). Through concerted action, OSKM are thought to evict somatic cell-specific TFs from their respective enhancers early in reprogramming, followed by activation of pluripotency-specific enhancers at a later stage (Apostolou & Stadtfeld, 2018; J. Chen et al., 2016; Chronis et al., 2017). On a transcriptome level, the first stages of iPSC-reprogramming are marked by silencing of somatic transcripts and induction of the pluripotency gene expression program. This phase is also accompanied by metabolic changes, histone mark changes, as well as activation of DNA repair and RNA processing (Buganim et al., 2013). These are thought to be global changes which may be required for reprogramming, but do not

guarantee that these cells will be successfully reprogrammed (Samavarchi-Tehrani et al., 2010).

In the intermediate phase of inducing pluripotent stem cells, a heterogeneous population of both reprogramming-competent and reprogramming-refractory cells are thought to co-exist (Hanna et al., 2010). During this phase, pluripotency gene expression is stochastically activated, accompanied by transient upregulation of developmental regulators. Once nascent iPSC activate endogenous *Oct4, Sox2* and *Nanog* expression, a self-sustaining pluripotent state is acquired, which no longer requires exogenous TF expression (Apostolou & Hochedlinger, 2013; Hanna et al., 2010). From this point onward, the molecular events that accompany reprogramming are considered to occur in a deterministic or hierarchical fashion. This marks the entry into the maturation and stabilization phase, during which the OSKM-transgenes are silenced, the core pluripotency circuitry is activated, epigenetic resetting and chromatin reorganization occurs and gonad and gamete genes are activated, among other cellular events (Buganim et al., 2013). The resulting cells after this stage resemble ESCs in several aspects (Takahashi & Yamanaka, 2006), as determined by testing their developmental potency and molecular analyses of their gene expression and epigenetic patterns (Hanna et al., 2010). Importantly, the reprogramming events induced by OSKM-factors, culminating in the establishment of a pluripotent state can be maintained independently of further ectopic OSKM-overexpression (Papp & Plath, 2013).

3.5. Reprogramming barriers and epigenetic memory

Cell-fate reprogramming, either by OSKM-overexpression or via SCNT, has low efficiency as only a small fraction of donor cells become iPSC (Hanna et al., 2010; Takahashi & Yamanaka, 2006), and less than 10% of the NT embryos generated from differentiated cells reach adulthood (Gurdon, 1960b). Early work using NT In *Xenopus* showed that the success of NT procedures decreases with increased differentiation status of the donor nuclei (Gurdon, 1960b). This implies that as cells differentiate, they acquire specific properties that stabilize their differentiated cell identity and confer resistance to cell fate changes. For example, genes necessary for early development could be silenced in differentiated cells and fail to reactivate their expression in NT embryos, therefore accounting for the progressively lower efficiency of NT using differentiated donor nuclei (Gurdon, 2013; Hörmanseder, 2021). Conversely, genes expressed in the donor cell have been found to maintain their expression in the wrong cell type of the cloned embryo, despite undergoing multiple cell cycles in the absence of transcription in the early *Xenopus* embryo (Hörmanseder et al., 2017; Ng & Gurdon, 2005). Furthermore, a study using serial NT showed that donor cell-like gene expression continued in up to 50% of the second generation of NT embryos, indicating the stability of somatic gene expression

programs (Ng & Gurdon, 2008b). These observations pointed to the existence of *epigenetic memory,* where cells retain molecular signatures indicative of their previous identity even after reprogramming (Ng & Gurdon, 2008a). The term 'epigenetic' is used to describe changes in gene expression which do not involve changes in DNA sequence and are mitotically or meiotically heritable (Russo et al., 1996). Thus, epigenetic phenomena can manifest in stable gene expression patterns that maintain cell identity and stably propagate it onto the daughter cells. This resistance of genes to reprogramming can be observed in frog and mammalian NT embryos, as well as in cell fusions and iPSCs, and thus epigenetic memory is thought to pose a significant barrier to successful cell fate reprogramming across species and reprogramming systems (Hörmanseder, 2021).

Systematic analyses of gene expression in reprogrammed cells and cloned embryos have been beneficial in characterizing the patterns of resistance to reprogramming. Transcriptome analyses have identified two categories of genes that resist reprogramming: (1) genes that are silenced in the starting cell type and fail to be activated in the reprogrammed cell or NT embryo (memory of a repressive state) (Matoba et al., 2014a) and (2) genes that are actively expressed in specialized starting cell types and maintain their active expression even in the wrong cell lineage of the cloned embryo (memory of an active state) (Hörmanseder et al., 2017). It has been reported that reprogramming-resistant genes are marked by chromatin modifications in the starting cell type that stabilize their expression state and prevent it from changing upon exposure to reprogramming factors (Hörmanseder, 2021; Hörmanseder et al., 2017; Jullien et al., 2017; Matoba et al., 2014a; Onder et al., 2012; Pasque, Jullien, et al., 2011; Soufi et al., 2012). Closely linked to all DNA-templated processes in a cell, chromatin composition is thought to reflect cell identity and to contain epigenetic information that is propagated across cell divisions to maintain gene expression programs and cellular identities (Reinberg & Vales, 2018; Stewart-Morgan et al., 2020). Therefore, the question of epigenetic memory in reprogramming is centered around the chromatin states of the starting cell type and how they affect the cell-fate conversion to the target cell type.

Similar patterns of epigenetic memory have been observed in iPSC reprogramming systems. For example, a study in OSKM-reprogramming (Polo et al., 2010) has shown that iPSC derived from various genetically matched somatic cell types have distinct transcriptomes at early passages. Despite their ability to grow independently of OSKM overexpression and form teratomas, iPSC cell lines derived from different cells of origin showed a differentiation bias, preferentially enabling the iPSCs to differentiate into the cell lineage of origin. Interestingly, when analyzed at late passages, the transcriptome differences of the iPSCs were largely resolved, and the authors proposed a passive replication-dependent loss of the chromatin marks resembling the somatic cell

of origin. While culturing iPSCs for extended periods of time may seem like a feasible approach to remove epigenetic memory from these cells, caution has to be taken with respect to genomic instability that has been reported to occur in late-passage iPSC cultures (Yoshihara et al., 2017).

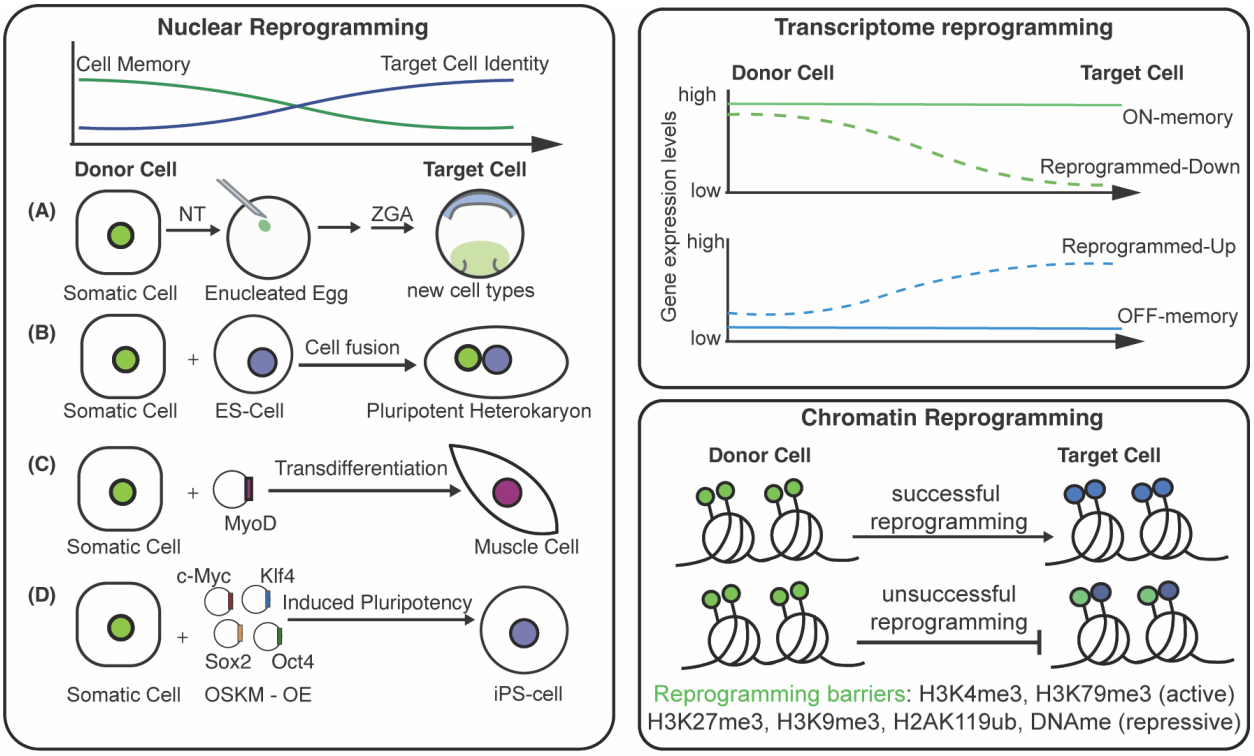

Figure 3: **Overview of nuclear reprogramming procedures and current model for transcriptome and chromatin reprogramming.** Boxes from left to right, clockwise: Schematic representation of nuclear reprogramming via (A) Somatic Cell Nuclear Transfer (NT), (B) Cell-cell fusion of a somatic cell and embryonic stem (ES) cell and heterokaryon generation, (C) Transdifferentiation via MyoD overexpression to reprogram somatic cells to muscle cells, (D) Induced pluripotency via c-Myc, Klf4, Sox2 and Oct4 overexpression to produce induced pluripotent stem cells (iPSC). During nuclear reprogramming the cell memory of the somatic cell is gradually lost, and the target cell identity is acquired. Transcriptome reprogramming: ON-memory genes are inefficiently repressed during reprogramming, while OFF-memory genes fail to reactivate in the target cell type. Reprogrammed-down and Reprogrammed-Up genes are correctly reprogrammed. Chromatin Reprogramming: Successful reprogramming requires extensive chromatin remodeling from the donor to the target cell type. Often, reprogramming fails due to incomplete chromatin reprogramming, mediated by active (H3K4me3, H3K79me3) and repressive chromatin (H3K73me3, H3K9me3, H2AK119ub, DNA-methylation) barriers. Based on Hörmanseder (2021).

Understanding the molecular basis of resistance to reprogramming is helped by experimental systems that can distinguish between the chromatin mechanisms that propagate memory of the starting cell type, and the chromatin mechanisms involved in establishing the new cell fate of the target cell type (Hörmanseder, 2021). A unique

feature of SCNT experiments is that donor cells can be perturbed to achieve lowered levels of chromatin marks and lower the epigenetic memory of the somatic donor cell fate, while leaving the chromatin-modifying activities in the recipient egg and the resulting cloned embryo unperturbed (Hörmanseder, 2021). This makes SCNT reprogramming systems particularly suitable to address questions related to epigenetic memory. In induced pluripotency and transdifferentiation experiments, perturbations of candidate epigenetic barriers coincide with ongoing transcription during the reprogramming process (Ebrahimi et al., 2019; Mikkelsen et al., 2008; Onder et al., 2012; Sridharan et al., 2013). Therefore, it is complicated to distinguish whether a chromatin mark plays a role in maintaining the expression patterns of the somatic cell or in the establishment of the new gene expression profiles of the target cell type. While the NT reprogramming system allows clear evaluation of the reprogramming success by quantifying the development of the cloned embryo, in TF-mediated reprogramming it is often difficult to address the success of cell fate conversion beyond transcriptome readouts or marker protein expression, as functional characterization of the reprogrammed cells is often not possible(Hörmanseder, 2021). This is an important aspect to consider when discussing findings on epigenetic memory in the context of reprogramming in these distinct reprogramming systems.

In the following sections of this chapter, the major reprogramming barriers, as well as players in epigenetic memory maintained from the donor to the target cell, identified in SCNT or iPSC-reprogramming will be described.

3.5.1. DNA methylation

The methylation of DNA at CpG islands has been associated with stable transcriptional repression (Greenberg & Bourc'his, 2019; Reik, 2007). During cellular differentiation, DNA methylation is progressively deposited on stem cell-related genes and accumulates at developmental genes that should be silenced in specific cell types (Meissner et al., 2008). This methylation pattern is thought to be established by the *de novo* methyltransferases Dnmt3a and Dnmt3b and maintained by Dnmt1. Indeed, ESCs lacking Dnmt3a and Dnmt3b fail to downregulate pluripotency factors and cannot differentiate properly (T. Chen et al., 2003; Jackson et al., 2004). Given this role in maintaining cell-type specific gene silencing, the erasure of DNA methylation upon reprogramming is considered a prerequisite for reactivating the expression of repressed genes. Global reversal of DNA methylation upon reprogramming has been observed in systems such as NT, cell fusion, and induced pluripotency (Apostolou & Hochedlinger, 2013; Brumbaugh et al., 2019). To date, the contribution of DNA methylation in amphibian NT reprogramming remains unclear.

In mammalian NT, DNA methylation has been associated with poor development of the resulting embryos in bovine embryos (Kang et al., 2001). Moreover, SCNT experiments using donor nuclei with a hypomorphic allele of DNA methyl-transferase-1 (Dnmt1) resulted in global hypomethylation of the genome and improved the efficiency in deriving embryonic stem (ES) cells (Blelloch et al., 2006). In mouse SCNT studies, it has been shown that DNA methylation is extensively reprogrammed through dual mechanisms (Matoba & Zhang, 2018). Active DNA demethylation has been shown by co-localization of oocyte-stored TET3 to the pseudo-pronucleus and induction of 5mC to 5hmC conversion (T.-P. Gu et al., 2011; Iqbal et al., 2011; Wossidlo et al., 2010, 2011) , but the contribution of this mechanism to the development of SCNT embryos has not been addressed fully (A. Inoue et al., 2015; Matoba & Zhang, 2018). Studies profiling the DNA methylome of early mouse SCNT embryo have revealed similar DNA methylation patterns between the SCNT embryo and the donor cells, with notable differences between SCNT and fertilized embryos (Chan et al., 2012; Gao et al., 2018; W. Liu et al., 2016; Matoba et al., 2018). Gao *et al.* combined genome-wide DNA methylation analyses with embryo biopsy of embryos arrested at different stages in development, and identified aberrant DNA re-methylation patterns in SCNT embryos, particularly affecting genes and retrotransposons critical for ZGA (Gao et al., 2018). These re-methylation defects were more pronounced in embryos that arrested at 2- or 4-cell stages compared to those that developed further and could be rescued by Dnmt3a+b knockdown in the recipient oocytes. Moreover, combining inhibition of DNA methyltransferases with histone demethylase overexpression synergistically reduced these aberrant methylation patterns and substantially improves cloning efficiency (Gao et al., 2018). A related study (Matoba et al., 2018) analyzed DNA methylation in mouse SCNT blastocysts, without discriminating between successfully developing and arrested embryos, and showed that the global DNA methylation levels in SCNT blastocysts became similar to those of fertilized embryos. This suggested passive dilution of DNA methylation though replication similar to normal development of mouse preimplantation embryos (Matoba & Zhang, 2018; Shen et al., 2014). Collectively, these studies demonstrate that proper DNA methylation reprogramming contributes to successful mammalian SCNT reprogramming.

In TF-induced reprogramming, the use of demethylating agents such as Ten-eleven Translocation (TET) family proteins or manipulations of Dnmt1 levels has resulted in improved reprogramming efficiencies and showed that DNA methylation is an important epigenetic barrier to achieving induced pluripotency (Brumbaugh et al., 2019). The inhibitory role of DNA methylation in reprogramming has been further exemplified by recent targeted approaches. Activation of the TF Sox1 by using dCas9-VP64 was shown to increase de-differentiation from neural progenitor cells to neural stem cells when accompanied by dCas9-Tet1 targeting to the Sox1 promoter (Baumann et al., 2019).

Additionally, studies investigating iPSC transcriptome differences indicative of cell-of-origin identity have attributed these patterns to incompletely reprogrammed DNA methylation signatures from donor somatic cells (Doi et al., 2009; Kim et al., 2010, 2011; Lister et al., 2011; Ohi et al., 2011).

Taken together, these examples from various experimental approaches support the role of DNA-methylation as an epigenetic roadblock to reprogramming.

3.5.2. Histone modifications

Histone proteins consist of a structured core domain, closely associated with DNA, and an unstructured N-terminal histone tail (Luger et al., 1997). A large number and variety of post-translational modifications (PTMs), such as acetylation, methylation, phosphorylation, and ubiquitination, has been identified on the N-terminus of histones (Bannister & Kouzarides, 2011). In brief, histone modifications can be deposited by enzymes termed ‘writers’ and can be removed by enzymes called ‘erasers’, commonly referred to as histone-modifying enzymes. ‘Readers’ are proteins or protein domains which recognize and bind histone marks, therefore allowing their recruitment to chromatin, which may be followed by recruiting or inhibiting the binding of further protein factors (T. Zhang et al., 2015). Besides, writers and erasers often contain reader domains, which facilitate their histone-modifying activity via positive feedback loops or inhibit their activity via recognition of other histone marks (Morgan & Shilatifard, 2020). Many post-translational modifications on histones have been correlated with active or repressive transcriptional states, and combinations of several marks are often interpreted as signatures of distinct chromatin states (Millán-Zambrano et al., 2022).

Given their association with gene regulation and stabilizing cell identity, repressive histone modifications in particular have emerged as key mediators of epigenetic memory during reprogramming. The persistence of histone marks from the donor nuclei can impede activation of pluripotency genes and the silencing of somatic genes, thereby creating barriers to efficient reprogramming. Therefore, successful reprogramming should include correct reprogramming of histone modifications from the donor cell to those of the target cell type (Hörmanseder, 2021; Matoba & Zhang, 2018). In the following sections, the active and repressive histone modifications identified as reprogramming barriers will be discussed.

3.5.2.1. Repressive histone modifications in reprogramming

Silent chromatin states, i.e. chromatin states not associated with active gene expression, are characterized by DNA methylation, H3K9me3, H3K27me3 and H2AK119ub-marked regions (T. Zhang et al., 2015). Mechanistic studies in the context of reprogramming showed that failing to activate the correct gene expression profiles of the target cell type may be caused by the persistence of repressive chromatin marks from the starting cell type (Jullien et al., 2014; Kim et al., 2010; Mansour et al., 2012; Mikkelsen et al., 2008; Soufi et al., 2012). In a study using mouse donor cells for NT to *Xenopus* oocytes, removal of DNA methylation and the repressive histone marks H3K9me3, H3K27me3 and H2AK119ub, individually or in combination, was reported to improve the activation of genes upon NT (Jullien et al., 2017). Repressive chromatin features have been proposed to contribute to epigenetic memory by suppressing aberrant gene expression and maintaining cell-type specific gene expression profiles (Reinberg & Vales, 2018). Such an epigenetic mechanism could inhibit the activation of lineage genes in the reprogrammed cell type and pose a barrier to successful cell fate conversion. Therefore, research on reprogramming barriers has focused on chromatin modifications that stabilize silent states and prevent gene activation during reprogramming (Hörmanseder, 2021; Lim et al., 2024; Matoba & Zhang, 2018).

Di- and trimethylation on histone H3K9 are considered repressive histone marks, which are found in large domains of constitutive heterochromatin and contribute to silencing of repetitive elements in the genome. The refractory role of H3K9me3 in reprogramming was first appreciated by a genome-wide study addressing the binding of OSKM (Soufi et al., 2012), which identified megabase-sized regions of the genome not bound by OSK, enriched in repetitive elements and marked by H3K9me3. Knockdown of SUV39H1 (an H3K9 methyltransferase) in fibroblasts improved iPSC-reprogramming efficiency (Onder et al., 2012). In mouse SCNT, *Kdm4a/d* overexpression and H3K9-demethylation (M. Chen et al., 2020; W. Liu et al., 2016; Matoba et al., 2014a) has been reported to improve the gene activation at ZGA. In studies addressing chromatin accessibility dynamics in mouse SCNT reprogramming, regions failing to switch from a closed to open configuration were enriched in H3K9me3, further implying the refractory role of this histone mark in reprogramming (Djekidel et al., 2018). In addition, aberrantly hypoacetylated regions around H3K9-trimethylated regions have been identified in a mouse SCNT study, which could be rescued with HDAC inhibition and Dux overexpression to correct the activation of transcripts at ZGA (G. Yang et al., 2021). Collectively, these studies point towards H3K9me3 on heterochromatin as a major epigenetic barrier to nuclear reprogramming.

H3K27me3 is a mark of facultative heterochromatin deposited by the Polycomb complex important for maintaining cell identities and silenced transcriptional states (Comet et al., 2016). The trimethylated state of H3K27 has been classified as a

reprogramming barrier in different species and reprogramming methods (Jullien et al., 2014; L. Yang et al., 2018). In donor nuclei, removal of H3K27me3 prior to reprogramming has been found beneficial in improving SCNT efficiency (B. Xie et al., 2016; C. Zhou et al., 2019), while in mammalian SCNT-experiments, developmental abnormalities of the cloned animals have been attributed the loss of H3K27me3-imprinted loci (K. Inoue et al., 2020; Matoba et al., 2018; L.-Y. Wang et al., 2020).

In iPSC-reprogramming, the inhibition of the Polycomb-subunits Eed, Ezh2 and Suz12 has been found to impair reprogramming, likely due to failure to silence the fibroblast transcriptional program in the absence of H3K27me3-depositing activities (Onder et al., 2012). A later mechanistic study suggested that the Ezh2-dependent trimethylation of H3K27 promotes the silencing of the somatic transcriptional program during the mesenchymal-to-epithelial transition in the early stages of reprogramming (R. A. Rao et al., 2015). However, studies addressing whether H3K27me3 contributes to epigenetic memory of a repressive chromatin state from the starting cell type to the reprogrammed cell in TF-mediated reprogramming are still lacking. To address this question, it would be necessary to transiently reduce H3K27me3 before introducing the reprogramming factors, and allowing unperturbed establishment of H3K27me3 during reprogramming (Hörmanseder, 2021).

Together, these studies demonstrate that repressed chromatin states in the starting cell type represent major barriers to be overcome in order to achieve successful reprogramming.

3.5.2.2. Active histone modifications in reprogramming

Currently, it is debated whether active histone marks also play a role in cellular memory and whether they can be classified as epigenetic (reviewed in (Hörmanseder, 2021; Reinberg & Vales, 2018). However, recent experiments in SCNT suggest that active chromatin states from the starting cell type could indeed stabilize and propagate the transcriptional program indicative of the donor cell into the reprogrammed cell, therefore preventing successful cell fate conversion. Specifically, in *Xenopus* SCNT experiments, it was reported that the active histone mark H3K4me3 acts as a reprogramming barrier (Hörmanseder et al., 2017). Using this experimental setup, it was found that cell lineage genes of endoderm donor cells are aberrantly expressed in ectoderm cells of the NT embryos. For comparison, these genes are not expressed or were expressed at significantly lower levels in ectoderm tissues of IVF embryos. Genes demonstrating such behavior were termed ‘ON-memory’ genes, in contrast to genes which were correctly downregulated in reprogramming, termed ‘reprogrammed-down’ genes (Figure 3). Indeed, the aberrant expression of endoderm ON-memory genes in epidermal tissues of *Xenopus* SCNT embryos was linked to differentiation defects and

increased apoptosis (Zikmund et al., 2025). Genome-wide analysis using ChIP-seq revealed that H3K4me3 signal on ON-memory gene promoters had higher intensity and domain breadth compared to reprogrammed genes. When overexpressing the histone H3K4-demethylase Kdm5b in donor nuclei, the aberrant expression of endoderm lineage genes in ectoderm tissues of the resulting NT embryos could be rescued. Importantly, the development of NT embryos generated from H3K4-demethylated donor nuclei was improved when compared to those produced from wildtype donor nuclei, with developmental rates indistinguishable from those obtained using pluripotent blastula nuclei as donors. This indicated that active chromatin states have the potential to act as epigenetic barriers to NT reprogramming. These findings have later been reproduced in several mammalian systems (Y. Huang et al., 2023; Z. Zhang et al., 2018; C. Zhou et al., 2020).

Interestingly, in iPSC reprogramming, the histone demethylase Kdm5b was classified as a barrier (Kidder et al., 2013), as reprogramming was improved in its absence. However, during iPSC reprogramming, transcription is continuously ongoing, unlike in the *Xenopus* NT setup, where the NT embryos undergo a transcriptionally silent window of 12 cell divisions until their zygotic genome is activated. Therefore, in iPSC reprogramming, Kdm5b-mediated demethylation could have prevented the activation of pluripotency transcripts.

Active chromatin marks, such as the histone modifications H3K27ac and H3K4me3, among others, may play distinct roles in SCNT reprogramming, depending on the time-window during the reprogramming process that is being studied. For instance, in the starting cell type, where active histone modifications are intertwined with active gene expression, or in the resulting SCNT embryo, in which the zygotic genome needs to be re-activated. Multiple reports from SCNT in various species have suggested that increased levels of histone acetylation play an important role in improving SCNT efficiency (G. Chen et al., 2020; Hou et al., 2014; Iager et al., 2008, 2008; Jin et al., 2017; Rybouchkin et al., 2006; J. Zhao et al., 2010). These findings were mostly derived by employing histone deacetylase (HDAC) inhibitors after NT, during the early stages of embryonic development. Inhibiting histone deacetylation after NT might support the already established role of H3K27ac in zygotic genome activation (ZGA) and activation of pluripotency transcripts (Sato et al., 2019; M. Wang et al., 2022; K. Wu et al., 2023). In the context of iPSC-reprogramming, the use of HDAC inhibitors has also been found to improve reprogramming outcomes (G. Chen et al., 2020; Huangfu, Maehr, et al., 2008; Huangfu, Osafune, et al., 2008; Kretsovali et al., 2012; Mali et al., 2010; Staszkiewicz et al., 2013), mainly by improving pluripotency transcript activation. Of note is a chemical screen performed in iPSC reprogramming, in which the p300/CBP bromodomain inhibitor CBP30 was found to improve reprogramming when applied in the first 7 days of reprogramming (Ebrahimi et al., 2019). A noteworthy finding of this study was that CBP30

treatment correlated with reduced fibroblast-specific gene expression, while pluripotency induction remained unperturbed.

DOT1L-mediated methylation on H3K79 has been found to impede transcriptional reprogramming in induced pluripotency (Onder et al., 2012). However, this discovery was achieved via an shRNA screen, in which shRNA knockdowns were begun five days before OSKM-overexpression, thus spanning the entire reprogramming process, including both the 'loss' of the somatic cell identity and the establishment of the induced pluripotent state. While this finding implicates DOT1L-mediates H3K79 methylation as a reprogramming barrier, it does not clarify if these modifications play a role in epigenetic memory or the acquisition of a new cell fate. In SCNT reprogramming, treatment of early porcine SCNT embryos with a DOT1L inhibitor improved their development (Tao et al., 2017).

In summary, active chromatin modifications seem to play dual roles in reprogramming, depending on the timing and context of their deposition or perturbation. Importantly, the discovery of H3K4 methylation as an 'active' chromatin barrier to reprogramming has pointed towards a new, underexplored axis of reprogramming resistance, exhibited as the memory of active transcriptional states from the donor to the reprogrammed cells.

3.5.3. Chromatin organization

Reprogramming via SCNT, as well as via OSKM-overexpression, requires extensive chromatin remodeling to reprogram the differentiated somatic nucleus to a totipotent or a pluripotent state, respectively (Apostolou & Hochedlinger, 2013; Ladstätter & Tachibana, 2018; Matoba & Zhang, 2018). Advanced genomic approaches like low-input Hi-C have provided insights into the temporal dynamics of 3D chromatin architecture during SCNT reprogramming in the mouse model (M. Chen et al., 2020; K. Zhang et al., 2020). This process was suggested to involve restructuring of multiple levels of chromatin organization, with successful reprogramming correlating with proper reconfiguration of nucleosome positioning, chromatin accessibility, and 3D genome architecture (M. Chen et al., 2020; L. Yang et al., 2022; K. Zhang et al., 2020; K. Zhao et al., 2021). Remarkably, some aspects of chromatin reorganization seem to occur rapidly. For instance, within 12 hours post SCNT, the chromatin accessibility landscape of donor cells is drastically reprogrammed to recapitulate that of fertilized zygotes via a replication-independent mechanism (Djekidel et al., 2018). However, SCNT embryos often demonstrate improper rewiring of other chromatin features, potentially contributing to their low developmental efficiency (M. Chen et al., 2020; Djekidel et al., 2018; K. Zhang et al., 2020). A recent study investigated genome-wide nucleosome positioning in mouse SCNT embryos,

revealing delayed nucleosome positioning dynamics, as indicated by the later establishment of nucleosome-depleted regions around the TSSs in SCNT embryos compared to fertilized counterparts (L. Yang et al., 2022). Interestingly, this study revealed a correlation between aberrant gene expression in SCNT embryos and promoter nucleosome-depleted regions in donor cells, suggesting that the memory of nucleosome occupancy in donor cells might be a barrier to SCNT reprogramming (L. Yang et al., 2022).

Furthermore, dynamic changes in topologically associating domains (TADs) were proposed to follow a complex pattern during SCNT reprogramming. Upon transfer into an enucleated oocyte, the donor chromatin undergoes rapid condensation, temporarily erasing preexisting 3D structures (K. Zhao et al., 2021). Following this initial dissolution, TADs and compartments begin to reestablish, though often imperfectly. For instance, TADs were shown to be stronger in SCNT 1-cell embryos at the PPN stage in contrast to fertilized zygotes (K. Zhang et al., 2020), which generally show weak insulation at these early stages and become progressively stronger over pre-implantation development (Bondarieva & Tachibana, 2024). Then, TADs in SCNT embryos appear to become weaker at the 2-cell stage before reconsolidating around the 8-cell stage. These dynamics seem to have functional consequences for development, as TAD boundaries resistant to reprogramming preferentially associate with misregulated genes in SCNT embryos and H3K9me3-enriched regions (M. Chen et al., 2020; K. Zhang et al., 2020). Furthermore, taking advantage of an auxin-inducible system to deplete a cohesin subunit in donor cells but not during SCNT, Zhang *et al.* showed that reducing cohesin levels in donor embryonic stem cells prior to reprogramming can weaken TAD boundaries, induces the expression of genes typically expressed in 2-cell embryos and improve the outcomes of the resulting NT-embryos. CTCF has also been reported to act as a barrier to cellular reprogramming, as CTCF depletion in embryonic stem cells was reported to lead to spontaneous conversion to a totipotent-like two-cell-like state in culture, characterized by the expression of genes typically found in 2-cell embryos and the reactivation of endogenous retroviral elements (Olbrich et al., 2021). It would be of interest to test in the future whether CTCF perturbation can also improve *in vivo* reprogramming via SCNT.

These findings collectively support a role of dynamic chromatin reorganization in successful nuclear reprogramming, yet investigation in the amphibian SCNT system remains subject of future studies.

3.6. Aim of this study

Reprogramming resistance in nuclear transfer systems has previously been attributed to the failure of the reprogrammed cells to activate correct gene expression patters in the cloned embryo (Hörmanseder, 2021; Matoba et al., 2014b; Matoba & Zhang, 2018). Thus, this has been implicated as a key reason for the developmental failure of SCNT embryos. However, an understudied, yet equally important, mechanism hindering successful nuclear reprogramming is the persisting gene expression indicative of the cell type of origin in the wrong cell type of the cloned embryos (Hörmanseder et al., 2017; Zikmund et al., 2025). A previous study using endoderm donor cells for NT to *Xenopus* eggs revealed that ectoderm cells of the resulting NT embryos continue to express genes characteristic of the endoderm donor cell fate. This phenomenon can be conceived as a molecular memory of an active transcriptional state, termed ON-memory. Importantly, the promoter regions of genes exhibiting such aberrant expression patterns were strongly enriched in H3K4me3, and its removal via overexpression of a histone demethylase, could correct the transcriptome and improve the developmental outcome of cloned embryos (Hörmanseder et al., 2017). A later study showed that the aberrant expression of endoderm genes in the wrong lineage of NT embryos can lead to differentiation failure, cell death and abnormal body patterning (Zikmund et al., 2025). By reducing the expression of candidate ON-memory genes, differentiation defects in NT embryos could be improved. These studies highlighted that ON-memory is an important epigenetic mechanism of reprogramming resistance warranting further investigation and molecular characterization.

While histone demethylase overexpression could correct the transcriptome of NT-embryos and significantly improve their development, a subset of ON-memory genes remained reprogramming-resistant despite reduced H3K4me3 levels on their promoters (Hörmanseder et al., 2017). Thus, the possibility that other chromatin modifications could act in parallel to H3K4me3 or together with H3K4me3 arose. Moreover, it could also be possible that distinct subsets of memory genes are marked by distinct chromatin modifications or regulated by distinct mechanisms in the donor cell type. Therefore, an exciting question emerges: do genes which exhibit transcriptional memory in reprogramming carry an ‘epigenetic barcode’ in the starting cell type that stabilizes gene expression patterns in differentiated cells and prevents reprogramming-induced cell fate changes? If so, could such an ‘epigenetic barcode’ be predictive of the memory status of genes in reprogramming?

To address this question, our group previously generated large-scale gene expression and histone modification datasets in different donor cell types and NT embryos. Leveraging these datasets, our group developed a machine learning model capable of predicting reprogramming outcomes on a transcriptome level, as well as identifying novel epigenetic barriers to reprogramming (Janeva et al., 2025). The present study follows up

on the machine learning modeling approach by selecting candidate histone modifications to test their role as putative reprogramming barriers *in vivo* and investigate their mechanistic contributions to reprogramming resistance. Specifically, this study focuses on H3K27ac and aims to test its contribution to maintaining an 'active chromatin state' from the donor cell to the reprogrammed cell via NT in *Xenopus laevis.* Therefore, the specific aims of the present study are presented below.

The first aim of the project is to select a candidate histone modification to be tested *in vivo* as a putative novel player in ON-memory. This is achieved by evaluating the results of the computational model described above, under the following criteria: the mark should be a strong predictor of ON-memory status and an experimental approach to perturb the selected histone mark is available and feasible in *Xenopus* donor embryos. Thus, H3K27ac was selected as the candidate of interest.

The second aim of this project is to generate donor cells for nuclear transfer with perturbed histone acetylation levels, including phenotypic and biochemical assessment of the perturbed cells.

The third aim of this project is to evaluate the reprogramming outcomes of NT embryos generated using donor nuclei with perturbed histone acetylation levels. This aim is addressed on a transcriptome level by analyzing the extent to which genes are aberrantly expressed in NT embryos from control and perturbed donor nuclei, as well as by analyzing the developmental outcome of the cloned embryos.

The fourth aim of this project is to evaluate the contribution of H3K27ac and other histone modifications on genomic cis-regulatory elements in mediating reprogramming resistance. This is achieved by employing genome-wide profiling of histone modifications in donor nuclei with perturbed histone acetylation to integrate the chromatin profiles in the donor cells and transcriptome phenotypes observed in NT embryos.

By addressing the aims outlined above, this project addresses a gap in our current understanding of (i) the contributions of chromatin modifications to active transcriptional memory in reprogramming and (ii) the role of histone acetylation in transcriptional regulation upon challenge to the cell identity via nuclear transfer.

4. Results

4.1. Previous results and project background

The results of this chapter were generated by Dr. Eva Hörmanseder (transcriptome data and chromatin profiling) and Dr. Christopher Penfold (developing Digital Reprogramming)

A key barrier to successful reprogramming via SCNT is the memory of the previous cell identity which can be detected in reprogrammed cells (Hörmanseder, 2021), as observed by the aberrant transcriptome patterns in NT embryos which correlate with specific chromatin modifications in donor nuclei (Hörmanseder et al. 2017, Matoba et al. 2014). However, due to the complex molecular mechanisms that underlie on one hand, epigenetic memory, and on the other hand, the reprogramming process itself, it has thus far been challenging to comprehensively understand the factors that maintain or erase epigenetic memory *in vivo.* While key players in transcriptional memory have been identified, such as for instance H3K9me3 in maintaining OFF-memory (Matoba *et al.*, 2014), and H3K4me3 in maintaining ON-memory (Hörmanseder *et al.,* 2017), other molecular features that contribute to these phenomena have remained understudied.

In particular, it is unknown how ON-memory is maintained from donor cells to NT embryos on a molecular level. For instance, an important question is whether other 'active' or 'repressive' chromatin marks work in parallel or in concert with H3K4me3 to stabilize gene expression states indicative of the donor cell fate, which may act as a barrier to reprogramming. Furthermore, it is unclear whether specific combinations of chromatin modifications in the donor cell can be used to predict reprogramming outcomes on a transcriptome level.

As a first step towards addressing these questions, my colleagues (Dr. Christopher Penfold and Dr. Eva Hörmanseder) constructed a large-scale chromatin and transcriptome datasets in NT reprogramming (
Figure *4*) (Janeva et al., 2025). These datasets allowed them to define memory genes in different cell types of *Xenopus laevis* embryos obtained by NT, as well as to profile a set of active and repressive histone modifications in two different donor cell types. Then, these datasets were leveraged to train and develop a machine learning model capable of identifying novel reprogramming barriers and predicting reprogramming outcomes on a transcriptome level (Janeva et al., 2025) (
Figure *4*).

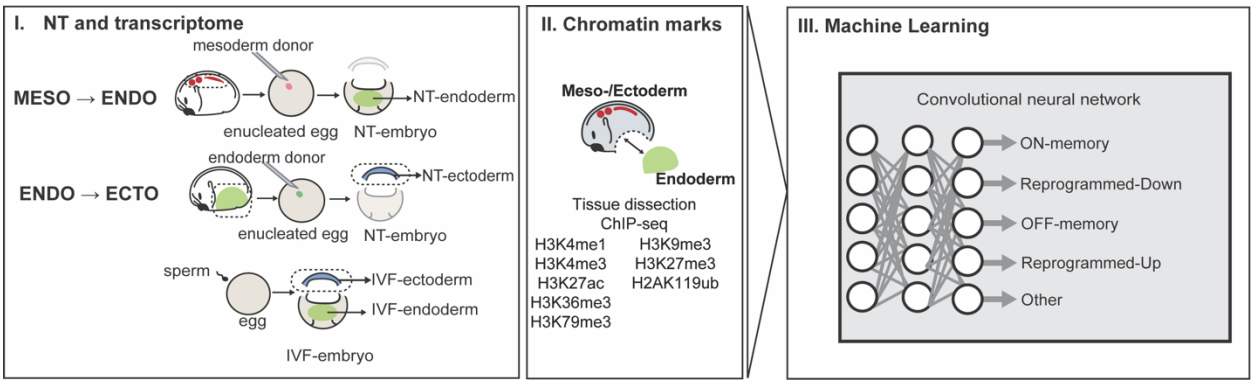

Figure 4: Schematic overview outlining the experimental setup and analysis to develop Digital Reprogramming. Panel I: Experimental setup for NT-induced reprogramming from mesoderm to endoderm, and endoderm to ectoderm, as well as producing *in vitro* fertilized control tissues. Panel II: Profiling active and repressive chromatin marks in mesoderm and endoderm donor tissues. Part III: Schematic representation of convolutional neural network used as a basis for the machine learning model, classifying genes as ON-memory, reprogrammed-down, OFF-memory, reprogrammed-up or Other in the respective reprogramming setup.

4.1.1. Constructing a large-scale chromatin and transcriptome dataset for Digital Reprogramming

To identify memory genes, mesoderm donor nuclei were transplanted to enucleated eggs and the endoderm tissues of the resulting NT embryos were analyzed (Figure 5A, D). As a control for wildtype gene expression, eggs were *in vitro* fertilized (IVF) and their endoderm tissues were collected. To analyze the transcriptome, NT- and IVF-endoderm samples, alongside mesoderm donor samples, were subjected to RNA-seq and differential gene expression analyses were performed. Comparing the NT-endoderm, and the IVF-endoderm tissues resulted in 9890 differentially expressed genes (DEGs). To define a set of ON-memory genes, genes which were expressed in donor nuclei and remained significantly upregulated in NT-endoderm compared to IVF-endoderm were filtered, resulting in a set of 1737 ON-memory genes (Figure 5B,C). To identify genes correctly downregulated in reprogramming, genes expressed in donor cells were filtered for those that were downregulated to comparable levels in NT and IVF, revealing 3071 reprogrammed-down (RD) genes. Vice versa, to define a set of OFF-memory genes, genes were selected which were expressed at lower levels in donor mesoderm compared to IVF-endoderm and were also expressed at lower levels in NT-endoderm compared to IVF-endoderm. Of note is that this class of genes also includes a group of genes that were not expressed (or were below the detection threshold) in donor nuclei or in NT embryos. Thus, 2013 mesoderm OFF-memory genes were identified (Figure 5B,C). Correspondingly, to obtain a set of genes correctly upregulated during reprogramming, genes expressed at lower levels in donor mesoderm than in IVF-

endoderm were filtered for genes that are expressed at similar levels in NT-endoderm and in IVF-endoderm, resulting in a set of 3068 reprogrammed-up genes.

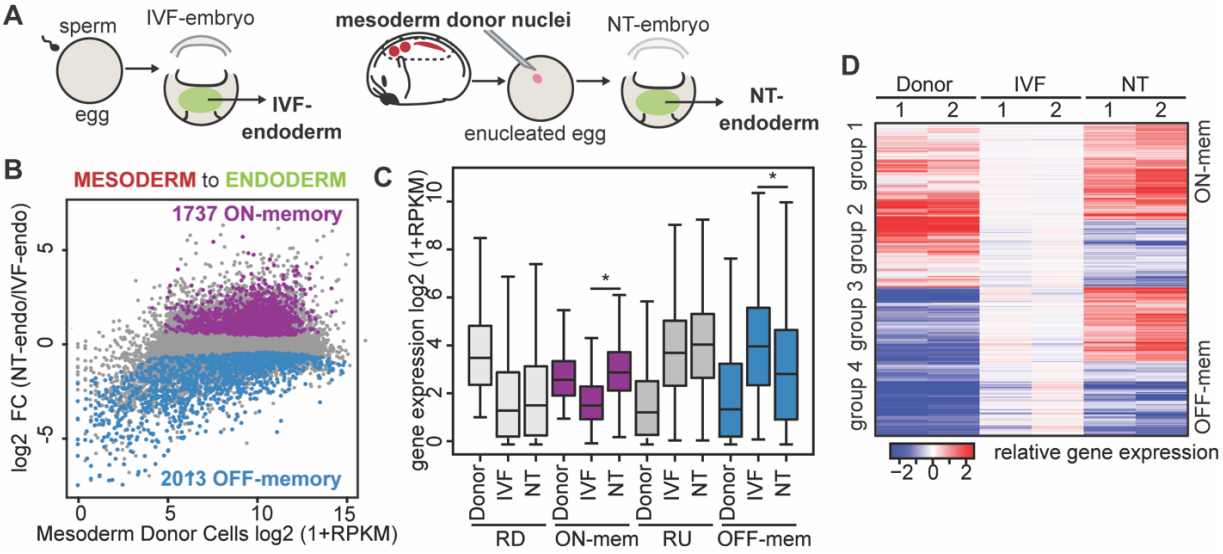

Figure 5: **Memory genes resist mesoderm-to-endoderm reprogramming via NT.** (A) Memory genes were identified in stage 11 endoderm following nuclear transfer (NT) with mesoderm donor nuclei compared to IVF endoderm. (B) MA-plot comparing gene expression between endoderm samples in NT vs. IVF embryos. The mean log2-fold change (log2FC) gene expression in NT embryos over IVF is plotted on the y-axis, while the mean log2(RPKM+1) gene expression in mesoderm donor nuclei is plotted on the x-axis. NT reprogramming from mesoderm to endoderm revealed 1737 ON-memory genes (purple) and 2013 OFF-memory genes (blue). (C) Boxplots showing log2(RPKM+1) mean expression levels of Reprogrammed-Down (RD; light gray), ON-memory (ON-mem; purple), Reprogrammed-Up (RU; dark gray), and OFF-memory (OFF-mem; blue) genes in mesoderm donor samples and endoderm IVF and NT samples. P-values for pairwise comparisons were calculated using Wilcoxon rank-sum test. * indicates $p<0.001$ (D) Heatmap showing relative gene expression (z-score) of DEGs obtained by pairwise comparisons between mesoderm donor and IVF-endoderm, and between NT-endoderm and IVF-endoderm samples. Rows: log2FC in expression levels over mean expression levels in IVF. Hierarchical clustering of rows classified these genes into four groups, note group 1 (ON-memory genes) and group 4 (OFF-memory genes).

In addition, previously published endoderm-to-ectoderm reprogramming datasets were re-analyzed in a corresponding manner (Hörmanseder et al., 2017) (Figure 6A). This revealed 1382 endoderm ON-memory genes and 1372 endoderm OFF-memory genes in endoderm-derived NT ectoderm cells (Figure 6B,C). Mesoderm ON-memory genes, compared to reprogrammed-down genes, maintained aberrantly high expression levels in the endoderm of NT embryos when compared to the endoderm of IVF embryos (Figure 5C). Similarly, endoderm ON-memory genes, in contrast to reprogrammed-down genes, maintained high expression levels in the ectoderm of NT embryos compared to

the ectoderm of IVF embryos (Figure 6C). It was further observed that the number of identified genes with ON- and OFF-memory status differed depending on the donor and target tissue used. Together, these results revealed that ON- and OFF-memory gene expression is a persistent feature of nuclear reprogramming using NT.

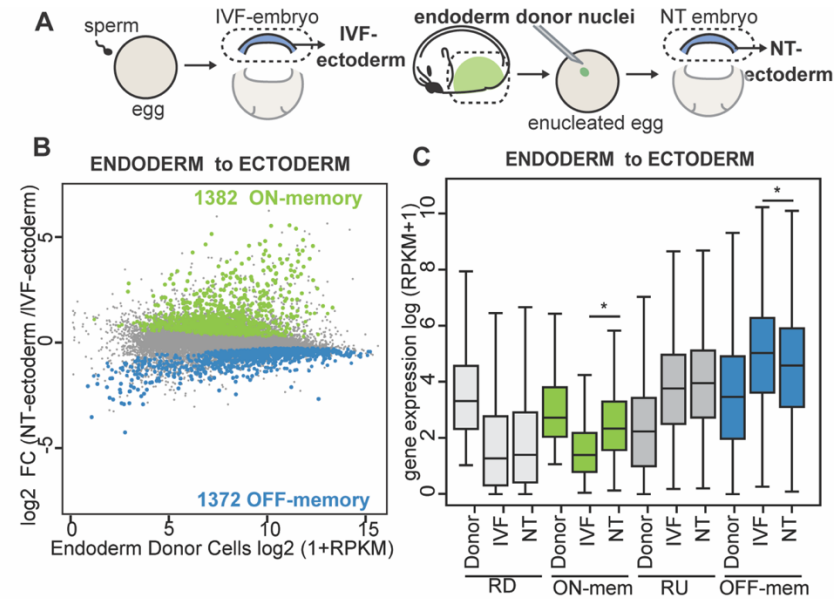

Figure 6: Memory genes resist endoderm-to-ectoderm reprogramming via NT. (A) Memory genes were identified in stage 11 ectoderm following NT with endoderm donor nuclei compared to IVF ectoderm. (B) MA-plot comparing gene expression between ectoderm samples in NT versus IVFs. The mean log2-fold change gene expression in NT embryos over IVF is plotted on the y-axis, while the mean log2(RPKM+1) gene expression in endoderm donor nuclei is plotted on the x-axis. NT reprogramming from endoderm to ectoderm revealed 1382 ON-memory genes (green) and 1372 OFF-memory genes (blue). (C) Boxplots showing log2(RPKM+1) mean expression levels of Reprogrammed-Down (RD; light gray), ON-memory (ON-mem; green), Reprogrammed-Up (RU; dark gray) and OFF-memory (OFF-mem; blue) genes in endoderm donor samples and ectoderm IVF and NT samples. p-values for pairwise comparisons were calculated using Wilcoxon rank-sum test. * $p<0.001$

To investigate if histone modifications apart from the previously reported H3K4me3 act as reprogramming barriers by stabilizing ON-memory *in vivo*, ChIP-seq was performed to profile a variety of histone modifications using ChIP-seq across meso-/ectoderm and endoderm donor tissues (

Figure 7). This included histone modifications associated with gene repression (Bannister & Kouzarides, 2011; Millán-Zambrano et al., 2022; T. Zhang et al., 2015): H3K9me3, H3K27me3 and H2AK119ub, marks associated with active gene expression

(Bannister & Kouzarides, 2011; Millán-Zambrano et al., 2022; T. Zhang et al., 2015): H3K4me3, H3K27ac, H3K36me3 and H3K79me3, marks associated with active enhancers (Creyghton et al., 2010; Heintzman et al., 2007, 2009; Rada-Iglesias et al., 2011): H3K27ac and H3K4me1, and the histone variant H2A.xf1 (Shechter et al., 2009) with a less well-documented role.

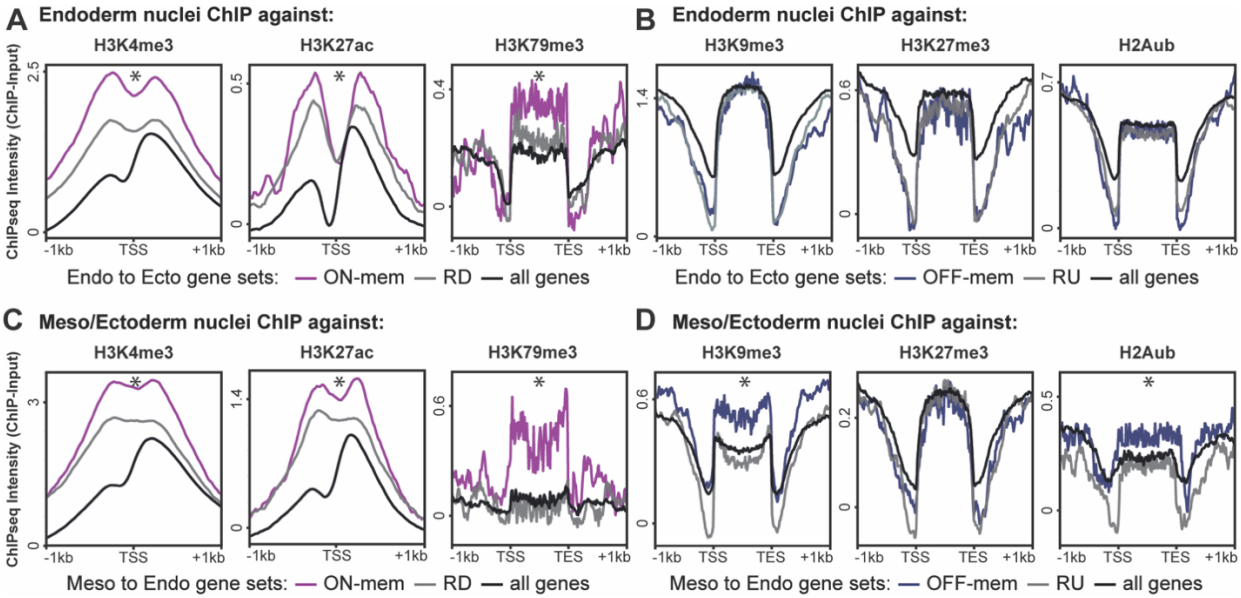

Figure 7: Genome-wide profiling of histone modifications (H3K4me1/me3, H3K9me3, H3K27ac/me3, H3K36me3, H3K79me3, H2AK119ub, H2A.X-f) in *Xenopus laevis* neurula-stage embryonic tissues. (A, C) Identification of histone modifications enriched around the TSS or gene bodies on ON-memory or (B, D) OFF-memory genes in endoderm donor tissue or (H-I) meso-/ectoderm tissue. P-value in (F) and (G) * indicates a p-value <0.001, Kolmogorov-Smirnov-test.

To address the role of these histone marks on genomic regions of reprogramming-resistant or reprogramming-permissive genes, the enrichment levels of each histone mark were compared between ON- or OFF-memory genes and reprogrammed-down and reprogrammed-down genes, respectively, in each donor cell type (

Figure 7). In the context of endoderm-to-ectoderm reprogramming, H3K4me3 levels were significantly enriched on the promoters of ON-memory genes compared to reprogrammed-down genes, as reported previously (Figure 7A) (Hörmanseder et al., 2017). In addition, the active mark H3K27ac was also enriched on the promoters of ON-memory versus reprogrammed-down genes, as well as H3K79me3 in the gene bodies (Figure 7A). When analyzing repressive histone marks H3K9me3 and H3K27me3 in endoderm donor cells and comparing OFF-memory versus reprogrammed-up genes, no significant differences were found (Figure 7B).

Furthermore, comparing histone PTM levels in meso-/ectoderm donor cells around the promoters or gene bodies revealed significant enrichment of H3K4me3, H3K27ac, and H3K79me3 for mesoderm ON-memory genes compared to reprogrammed-down genes, similar to the results from endoderm cells (

Figure *7* A,C). Interestingly, analysis of repressive histone marks revealed that OFF-memory genes were significantly enriched in H3K9me3 and H2AK119ub on their gene bodies in contrast to reprogrammed-up genes (

Figure *7* B,D). While a wider range of histone modifications was analyzed, they did not reveal any significant differences around promoters or gene bodies of ON- and OFF-memory genes compared to correctly reprogrammed gene sets. Together, these analyses revealed that ON-memory correlates with specific histone modifications in the somatic cell donor nucleus and that this is consistent across the tested cell types.

4.1.2. Digital Reprogramming accurately predicts reprogramming outcomes on a transcriptome level

Next, the question was addressed which histone modifications, or combinations thereof, around the promoter regions of genes in the donor nuclei, are predictive of their memory class status after reprogramming in NT embryos. In an initial attempt to reveal potential patterns in our combined chromatin and transcriptome profiling, reduced dimensionality representations such as PCA and UMAP were applied, which were unable to separate correctly reprogrammed genes from memory genes. Therefore, two possible scenarios emerged: (1) gene memory status may exist on a continuum that cannot be unambiguously separated into discrete groups, or (2) it may be distinct combinations of histone modifications that confer an identifiable memory status.

To identify such potential complex and hidden patterns in our data sets, convolutional neural network (CNN) algorithms were used to predict the reprogramming outcome of genes (Figure 8). Therefore, it was tested if CNN models are capable of inferring memory-class status based on a combination of gene expression and chromatin modifications around the promoter. To this end, chromatin modification data was first represented as a 1D array with 22 channels in wild-type somatic donor cell types, i.e., a one-dimension position along the TSS with each histone modification representing an individual channel (Figure 8A). A window 5 kb up- and downstream of the TSS was selected, so that potential instructive epigenetic information residing around promoter regions, proximal enhancer regions, and gene body were included (Figure 8A). These channels were then combined in a “Chromatin Modification Module” (CMM). Information on gene expression in the wild-type somatic donor cell type as well as on the wild-type

counterpart of the target cell type was combined in a “Gene Expression Module” (GEM). As output, the memory-class status of genes was used (ON- or OFF memory; reprogrammed-up or -down genes).
CNNs were used to jointly integrate the so-represented histone modification data around the TSS and gene expression data. The input data was divided into three parts: one to train the model, one for making predictions, and one for determining significance. Using this processed input data, three different CNN models were built to predict memory class status in the reprogrammed cell, each with increasing complexity to test how much information input is needed for successful prediction: (1) chromatin modification module (CMM-CNN), (2) CMM and gene expression data in the wild-type target somatic cell types (“CMM+target-CNN”), (3) complete chromatin modification module and gene expression module in the donor and target cell type (FULL-CNN). To provide a baseline for the predictive performance of CNNs, a random forest classification algorithm corresponding to the FULL-CNN using chromatin modification and gene expression in the donor and target cell type was used (FULL-RF) (Figure 8 B-E).

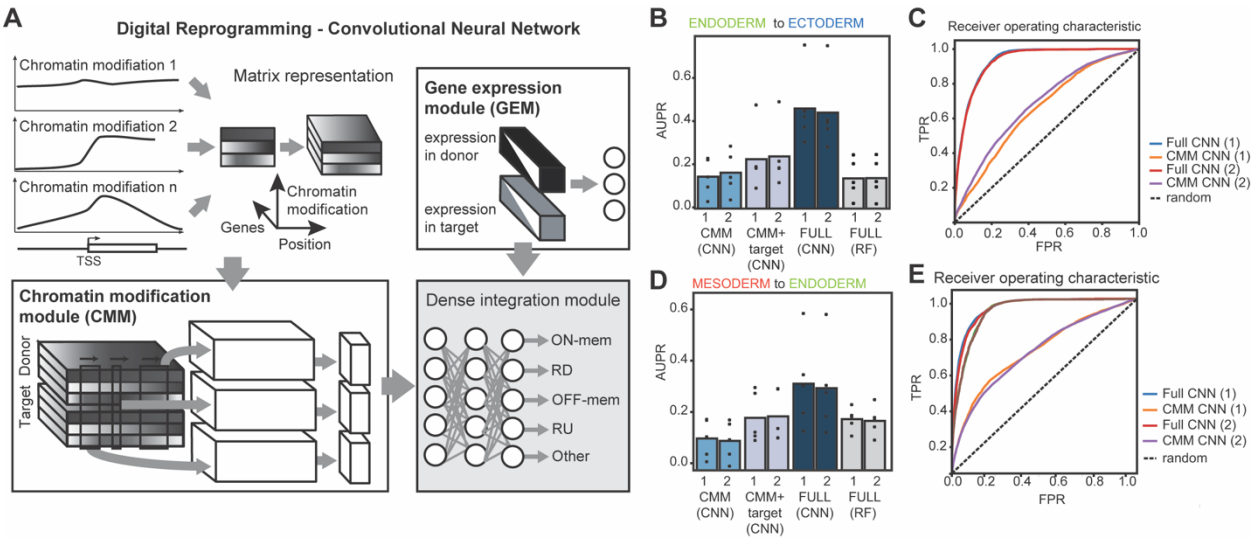

Figure 8: Developing Digital Reprogramming. (A) Schematic of Convolutional Neural Networks (CNNs) used to infer memory status. (B) Average area under Precision-Recall (AUPR) scores in endoderm to ectoderm reprogramming using different CNN and random forest (RF) models as indicated. (C) Receiver operating characteristic (ROC) curve for (d) endoderm to ectoderm reprogramming models as indicated, seed 1 and 2 (D) Average AUPR scores for somite to endoderm reprogramming. (E) ROC curve for (E) mesoderm to endoderm reprogramming models as indicated, seed 1 and 2

Then, the prediction accuracy of each model was quantified using the Area Under Precision-Recall (AUPR) or Receiver Operating Characteristics (ROC) on a one-vs-all basis (Figure 8 B-E). All three CNNs could infer the memory status of a gene with accuracy comparable to or better than random forest classifiers, with both performing substantially better than expected by random classification (Figure 8 B-E). Including both histone modification and gene expression information (FULL-CNN) in predictive models

showed the greatest accuracy, with reduced models i.e., using donor tissue histone modification and target tissue expression (CMM+target CNN), still retaining accuracy. Using histone modification alone provided the lowest classification accuracy, albeit also higher than random, with CNNs performing better than the corresponding RFs. This suggests that chromatin features around genes can predict their reprogramming outcomes, with additional predictive power gained from gene expression data in donor and target cell types. In summary, the models' predictive accuracy suggested that CNNs could identify useful predictive features from the provided data.

To test if the models were learning useful histone modification combinations, transfer learning approaches were used to make predictions in NT reprogramming using alternative cell types. Specifically, the full TSS model trained on ectoderm-derived endoderm was used to make predictions about memory status in mesoderm-derived endoderm (Figure 9A). This was termed naïve transfer learning (nTL), as CNNs were directly applied to new datasets with no additional parameter optimization. A second form of transfer learning was also applied, in which the network architecture and parameters were transferred, but with the parameters in the final dense layers of the network optimized using a subset of data (full transfer learning; TL). It was noted that whilst the nTL showed a slight drop in performance compared to a fully tuned CNN, its performance remained better than random forest and tuning of the densely connected layers showed performance comparable to that of a fully optimized network (Figure 9 B,C). The observation that features in the CNNs could be transferred between cell types and still retain predictive performance suggests that useful representations of the features were indeed being learned in the upper layers of the network. Furthermore, it suggested that CNNs trained with one cell type can be used to predict the transcriptome reprogramming of any other cell type of interest.

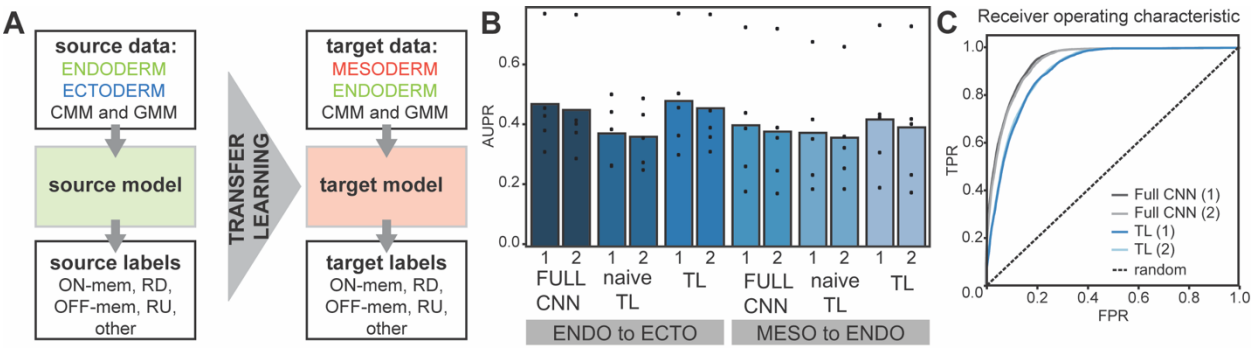

Figure 9: Digital Reprogramming Transfer Learning. (A) Schematic for transfer learning used to gauge the effectiveness of learned features (B) Average PR scores in TL schemes. (C) ROC curves for (B).

4.1.3. Selecting candidate marks to test as novel barriers to reprogramming

An equally important objective of the 'Digital Reprogramming' model was to identify possible classes of ON-memory genes regulated by different histone modifications or combinations thereof. To identify which of the histone modification features are predictive of memory status, the activations of the here-used genomic regions using DeepExplain were calculated (Ancona & Gross, 2017; Melis & Jaakkola, 2018). Specifically, for the region 5 kb up- and downstream flanking the TSS of a given gene, the attributions of a specific histone mark to a specific classifier could be calculated (Figure 10A-B). To look for individual classes of memory status genes, the overall attribution for each histone modification to ON-memory status was calculated, and hierarchical clustering was performed. The genes were clustered based on the similarity of the calculated activation contributions to individual subclasses and H3K4me3, H3K4me1, and H3K27ac were identified as important contributors to ON-memory status.

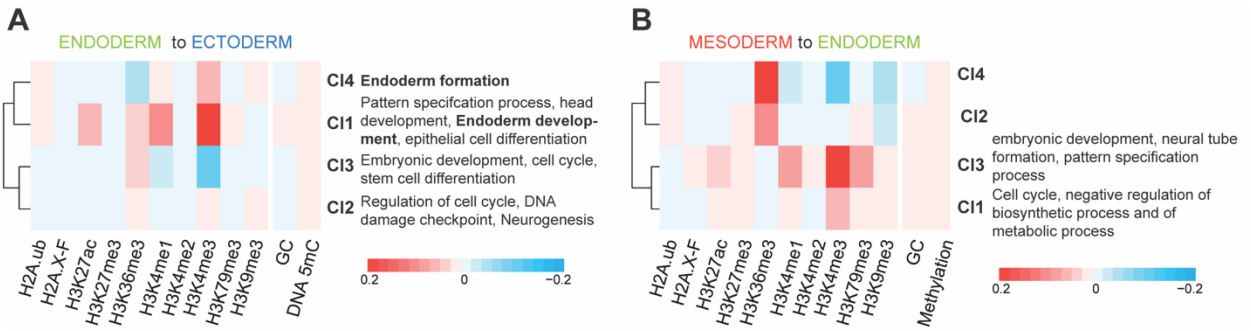

Figure 10: H3K4me3, H3K27ac and H3K4me1 were identified as novel contributors to the ON-memory status of genes. (A and B) Average activations of ON-memory genes over true positive genes were subclustered to identify different classes of ON-memory genes in (A) endoderm to ectoderm and (B) mesoderm to endoderm reprogramming. Colors indicate the sum over the cluster average activation of the 5kb TSS-flanking region, with higher scores indicating a greater contribution of that histone modification to predicted memory status.

Of the four subclusters formed by the endoderm ON-memory gene set, cluster 1 showed the strongest influence by H3K4me3, with cluster 4 and cluster 2 also showing some influence by H3K4me3 (Figure 10A). In addition to H3K4me3, cluster 1 also appeared to be influenced more strongly by H3K4me1 and H3K27ac than by other chromatin modifications, such as H3K36me3 (Figure 10A). Clusters 1, 2, and 4 were also influenced by DNA methylation and the GC content of the investigated gene region. Gene ontology (GO) enrichment analyses revealed that genes in clusters 1 and 4 were enriched for terms related to endoderm and other developmental signaling, indicating that this could be relevant chromatin modifications of genes important for donor cell identity. Cluster 3 was enriched for ontologies relating to the cell cycle, development and

differentiation. Cluster 2, with no clear signature, was enriched for terms related to the cell cycle and DNA damage checkpoint.

A similar sub-clustering based on the activations of individual histone marks was performed for mesoderm ON-memory genes (Figure 10B). H3K4me3 was identified as an important contributor to ON-memory status, as previously reported (Hörmanseder et al., 2017). Clusters 1 and 3 were influenced by H3K4me3, with cluster 3 being additionally influenced by H3K4me1, H3K27ac and H3K79me3 (Figure 10B). Cluster 2 and 4 were mainly influenced by H3K36me3. GO enrichment analyses revealed that genes in cluster 3 were associated with terms relating to development and pattern specification processes, and cluster 1 with cell cycle and metabolic processes. Cluster 2 and 4 showed no significant enrichment.

Together, this suggested that clusters marked in both donor cell types by H3K4me3, H3K4me1 and H3K27ac were enriched for cell lineage genes (Figure 10). Such lineage genes have previously been determined to be ON-memory genes, whose correct reprogramming is essential for successful cell fate conversion in NT embryos (Zikmund et al., 2025). Therefore, H3K4me1, H3K4me3, and H3K27ac may represent an important combination of histone modifications stabilizing cell lineage genes and master ON-memory genes. In summary, Digital Reprogramming approach accurately predicted transcriptional reprogramming outcomes by classifying genes as memory class genes or reprogrammed genes. Furthermore, Digital Reprogramming identified candidate reprogramming barriers linked to the inheritance of ON-memory, which were consistent between two donor cell types, endoderm and mesoderm. Finally, the model confirmed H3K4me3 as a key chromatin feature of ON-memory genes overall and identified H3K4me1 and H3K27ac as novel features.

4.2. Generation of donor cells with reduced H3K27ac levels

Based on our Digital Reprogramming analysis, we hypothesized that H3K27ac enrichment around promoters of ON-memory genes in donor cells contributes to transcriptional memory in NT embryos, thus hindering NT-mediated reprogramming. To test this hypothesis, I aimed to globally perturb H3K27ac levels in endoderm donor cell nuclei and assess whether this improves nuclear reprogramming efficiency following transplantation to enucleated eggs.

To reduce H3K27ac levels in donor nuclei before NT-reprogramming, I evaluated several strategies to achieve this. First, our group previously attempted to perturb H3K27ac levels by overexpressing histone deacetylase (HDAC) proteins which collectively describe a class of enzymes that remove acetyl groups from lysine residues on histones and non-histones (Seto & Yoshida, 2014) (unpublished results by Huiwen Li reproduced in my independent experiments). This approach was unsuitable, as H3K27ac levels could not be reduced in donor embryos, in contrast to previous reports in *Xenopus* embryos (A. Rao & LaBonne, 2018). An alternative to this approach would be the use of a dominant-negative mutant histone alike H3.3 K4M which binds and inhibits the SET domain of H3K4-specific methyltransferase enzymes as used before to produce H3K4me3-perturbed donor nuclei (Hörmanseder et al., 2017). To my knowledge, such a dominant-negative mutant that could inhibit the deposition of acetylation marks has not been identified thus far, rendering this strategy not feasible.

Second, I considered genetic manipulation of chromatin factors, for instance through mutating key residues for catalytic activity of acetylation 'writer' enzymes. The candidate for such perturbation would be p300/CBP, the writer enzyme of histone acetylation (Bannister & Kouzarides, 1996; Ogryzko et al., 1996). However, genetic perturbations in the *Xenopus laevis* model are challenging considering the allotetraploid genome, requiring targeting of multiple alleles simultaneously. In addition, the 1-2 years required for *Xenopus laevis* frogs to reach sexual maturity and allow for use of genetically manipulated donor embryos pose a significant challenge.

Thus, I selected a pharmacological p300/CBP perturbation approach, which decreases histone acetylation levels by inhibiting the deposition of these modifications by p300/CBP (Ebrahimi et al., 2019; Lasko et al., 2017; Raisner et al., 2018). p300 (also termed KAT3B) and the CREB binding protein (CBP) are paralogous acetyltransferases of histone and non-histone proteins, as well as transcriptional co-activators (Dancy & Cole, 2015). Due to the high sequence homology observed between p300 and CBP, these two proteins are collectively referred to as p300/CBP, and this terminology will also be used in this study.

p300/CBP has a central acetyltransferase domain (also termed HAT), which catalyzes the transfer of the acetyl group from acetyl-CoA to a lysine residue of a protein. The HAT domain may also be referred to as the ‘writer’ domain of p300/CBP. Adjacent to the 'writer’ is the bromodomain, or the ‘reader’ domain, which recognizes acetylated lysine residues on histones (Dhalluin et al., 1999; Park et al., 2017). Bromodomains also facilitate HAT-mediated acetylation (Zaware & Zhou, 2019), both by engaging in intra- and/or intermolecular reactions with the auto-inhibitory loop of p300/CBP (Ortega et al., 2018), and by binding acetylated lysine (Dhalluin et al., 1999) and aiding substrate recruitment. In particular, the p300/CBP bromodomain has been reported to selectively regulate acetylation on H3K27ac (Raisner et al., 2018), thus highlighting it as a suitable target for chemical inhibition to achieve depleted H3K27ac levels in our system. As an orthogonal approach allowing us to discern the contribution of the bromodomain to the architectural role of p300/CBP (J. Chen et al., 2010; Manning et al., 2001), I also used a catalytic inhibition approach, previously reported to target H3K27ac and other acetylation on other histone residues (Lasko et al., 2017; Weinert et al., 2018).

In the following sections, I present two manipulation approaches aiming at depleting H3K27ac in donor nuclei suitable for use in NT-induced reprogramming (i) p300/CBP bromodomain inhibition using the small molecule SGC-CBP30 and (ii) p300/CBP catalytic domain inhibition using the small molecule A-485. For both strategies, I treated *Xenopus laevis* embryos starting at late gastrula until the neurula-stage to ensure embryonic viability. I then characterized the effects of such manipulations phenotypically by monitoring the development of the treated and control embryos, as well as biochemically by using Western Blot and histone mass-spectrometry analysis to analyze the levels of H3K27ac and other histone modifications. Subsequently, we injected the perturbed donor nuclei into enucleated eggs with unperturbed p300/CBP activities to obtain reprogrammed cells for transcriptome assays and for scoring the developmental outcome of the cloned embryos. Therefore, I devised an experimental approach allowing us to address whether perturbing p300/CBP activities and histone acetylation in donor nuclei can correct the ON-memory phenotype in NT embryos.

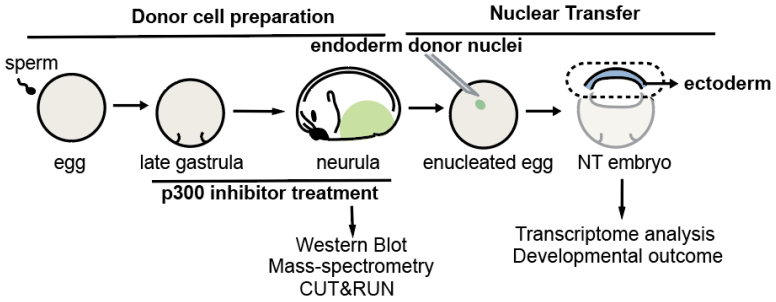

Figure 11: Schematic overview of the experimental approach used to perturb histone acetylation in donor nuclei for subsequent nuclear transfer

4.2.1. p300/CBP bromodomain inhibition reduces H3K27ac levels in *X. laevis* donor embryos

The mass-spectrometry results presented here were obtained by Dr. Ignasi Forne at the ZfP at BMC, LMU who performed the data acquisition and processing.

To obtain H3K27ac-perturbed donor nuclei, I aimed to establish a p300/CBP inhibitor setup that efficiently depletes H3K27ac levels while preserving the viability of the donor embryos until the neurula stage (Nieuwkoop-Faber stage 18; NF-stage) (Nieuwkoop, 2020). We selected endoderm cells as donors for several reasons: endoderm cells are large, therefore convenient to manipulate under the microscope for NT (Elsdale et al., 1960; Gurdon, 1960a; Gurdon & Uehlinger, 1966), these cells are still ongoing cell divisions and are thought to exhibit homogenous gene expression profiles which would help limit the cell-to-cell variability when selecting a single donor cell. Moreover, at the neurula stage, when we isolate the endoderm cells for use as donor nuclei (Hörmanseder et al., 2017), endoderm cell fate is established but not yet terminally differentiated (Horb & Slack, 2001), therefore being suitable for reprogramming assays (Gurdon, 1960a).

In order to obtain donor cells with perturbed H3K27ac levels, I first tested two different treatment protocols in which the embryos were exposed to a p300/CBP inhibitor either at the 2-cell-stage or during late gastrulation (NF-stage 12). In both cases, the embryos were incubated in an inhibitor-containing medium and allowed to develop. Treatments at the 2-cell stage, preceding ZGA in *Xenopus*, led to gastrulation arrest and death (Figure 12). Thus, this approach was unsuitable for collecting endoderm donor nuclei for NT (Figure 12A), as the donor embryos did not develop until the neurula stage. Instead, I chose a starting point of the inhibitor treatment from the late gastrula stage (NF-stage 12) when major developmental milestones such as ZGA and germ layer commitment have already taken place. Thus, I treated the donor embryos with CBP30 from NF-stage 12 until the neurula stage (NF-stage 18). Upon treatment with 40 µM SGC-CBP30 at stage 12, I observed delayed neural fold closure by approximately one hour compared to DMSO controls, but otherwise, the CBP30-treated embryos were otherwise morphologically indistinct from control embryos.

Therefore, I deemed this delay in development acceptable and pursued further experiments using the treatment starting at NF-stage 12. Importantly, in order to ensure that the developmental stages of CBP30-treated embryos match the DMSO controls, CBP30-treated embryos were collected at the time point of neural fold closure (Figure 12B).

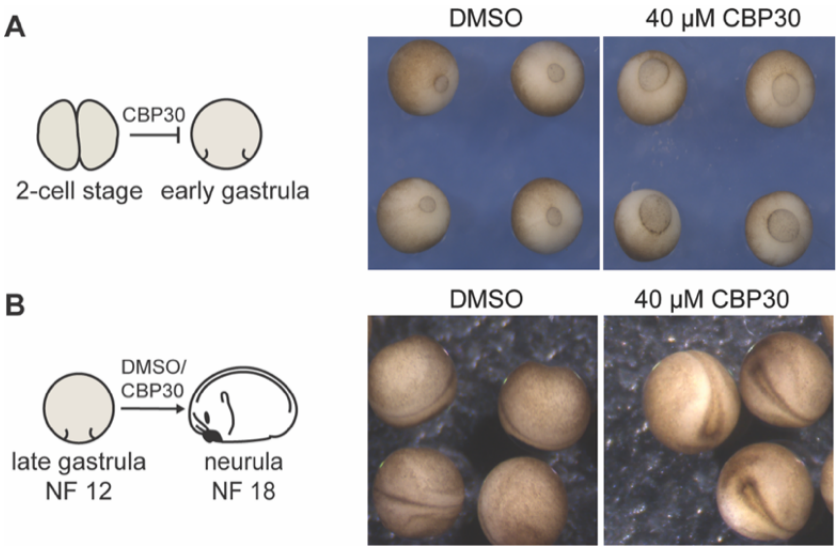

Figure 12: CBP30 treatment setup in wildtype embryos to produce H3K27ac-perturbed donor nuclei for NT. (A) Schematic depiction of the treatment protocol with CBP30 or DMSO-control, starting from the 2-cell-stage until developmental arrest was visible at the early gastrula stage. Representative images of embryos treated with DMSO or CBP30, n=3. (B) Schematic depiction of the treatment protocol with CBP30 or DMSO-control, starting from the late gastrula until the neurula stage. Representative images of embryos treated with DMSO or CBP30 depicting the delayed neural fold closure phenotype, n=3.

Next, I addressed if this above established CBP30 treatment, which targets the p300/CBP bromodomain specifically perturbs H3K27ac histone acetylation levels in donor embryos. I first assessed this via Western Blot for a set of candidate histone acetylation marks and then evaluated additional effects of this treatment on histone tail PTMs globally via mass spec analyses.

Whole embryo chromatin lysates were analyzed using Western Blot against several acetylated lysine residues on histone H3. Semi-quantitative immunoblotting revealed significantly reduced H3K27ac levels in CBP30 treated samples (Figure 13A,B), but not H3K18ac and pan-H3 lysine acetylation levels, consistent with previous reports from cell culture systems (Ebrahimi et al., 2019; Raisner et al., 2018). Moreover, I detected a mild reduction in H3K9ac levels upon CBP30 treatment, potentially as a secondary effect of H3K27ac perturbation. This indicates that CBP30 treatment successfully reduces global H3K27ac levels in donor embryos, with a mild decrease in H3K9ac levels suggesting potential off-target or secondary effects of this perturbation.

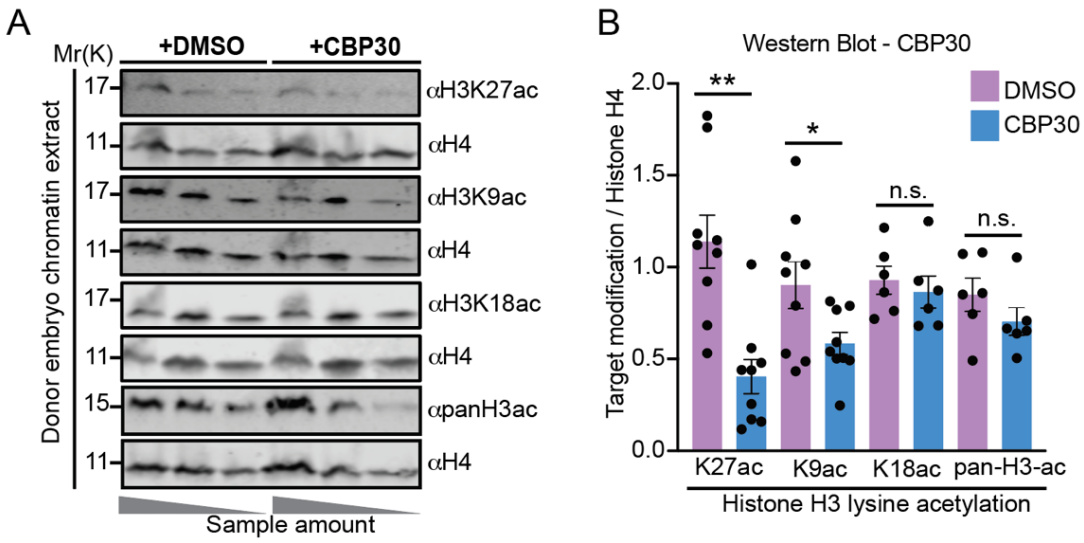

Figure 13: **Western Blot analysis of acetylated lysine residues on histone H3.** (A) Immunoblots depicting H3K27ac, H3K9ac, H3K18ac and pan-H3-acetylation (acetyl K9+K14+K18+K23+K27) levels, alongside histone H4 as loading control, for chromatin extracted from whole embryo lysates in DMSO and CBP30-treated embryos. Samples were loaded as a dilution series in 2-fold steps, from the highest to the lowest concentration. (B) Band density quantification of Western Blot results for H3K27ac (n=3), H3K9ac (n=3), H3K18ac (n=2) and pan-H3-acetylation (n=2). Error bars represent the mean+/- SEM, and stars indicate p-values calculated using a paired t-test. (n.s.: $p > 0.05$, *: $p \leq 0.05$, **: $p \leq 0.01$, ***: $p \leq 0.001$). Purple bars: DMSO-control, blue bars: CBP30-treated.

Considering the promiscuous nature of p300/CBP, its various histone lysine substrates in the nucleus or any potential secondary effects upon p300/CBP inhibition (Dancy & Cole, 2015; Shvedunova & Akhtar, 2022; Weinert et al., 2018), I wondered if CBP30 treatment affected other histone modifications apart from H3K27ac in our treatment setup. Therefore, to address the effects of CBP30 treatment on histone post-translational modifications (PTMs), we collaborated with Dr. Ignasi Forne and applied a liquid chromatography coupled to tandem mass spectrometry (LC-MS/MS; hereinafter MS for brevity) approach detecting lysine modifications on the N-terminal tail of histones H3 and H4 (Figure 14). This approach allowed us to quantify histone modification levels in an antibody-independent and high-throughput manner, both for single and combinations of modified lysine residues on the corresponding tryptic peptides.

Our MS analysis revealed a mean 1.7-fold reduction of H3K27ac levels upon CBP30 treatment compared to DMSO controls, while H3K18ac levels remained unaltered, consistent with our Western Blot results shown above (Figure 14A,C, Table 1, N=3). Unfortunately, the liquid chromatography preceding MS/MS could not separate H3K9ac and H3K14ac levels on the H3 K9-K17 tryptic peptide. Instead, we could only quantify this peptide when carrying an acetylation mark on one of the lysine residues or when both

were acetylated. In both cases, we did not detect changes between DMSO control and CBP30-treated samples (Figure 14A). A similar limitation of our method applies to acetylation modifications on histone H4 (Figure 14B).

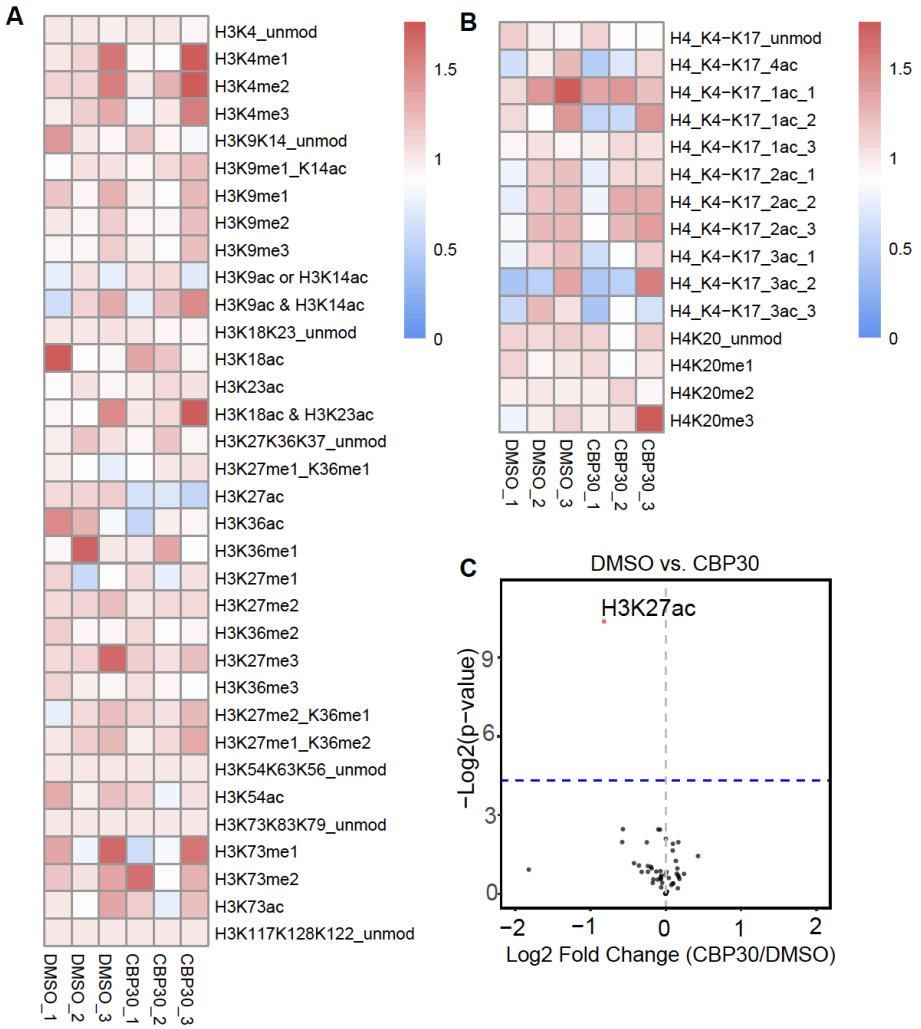

Figure 14: **Histone mass-spectrometry on CBP30 treated neurula-stage whole embryos** (A-B) Heatmaps depicting the relative abundance of post-translational modifications on histone lysine residues, normalized over the abundance of histone PTM levels in untreated samples on (A) histone H3 and (B) histone H4. N=3. (C) Volcano plot comparing histone mark levels quantified via mass-spectrometry in CBP30 compared to DMSO samples. y-axis shows the p-value calculated using an unpaired student's t-test, x-axis shows the log2 fold-change of histone mark levels in CBP30 versus DMSO samples.

Considering the role of p300/CBP as a transcriptional co-activator, I wondered if perturbing p300/CBP activities using CBP30 could perturb methylation marks associated with active chromatin states, such as H3K4me3 (Santos-Rosa et al., 2002) or H3K36me3

(Morris et al., 2005). Moreover, I asked if depleting H3K27ac could lead to a global increase in the antagonistic repressive mark H3K27me3 as described in other species (Pasini et al., 2010; Tie et al., 2009). I did not detect changes in the levels of any of the methylation marks measured in our MS assay (Figure 14A), suggesting that p300/CBP bromodomain inhibition mainly affected H3K27ac levels. Together, our immunoblot and histone mass-spectrometry analyses (Figure 13, Figure 14) revealed that CBP30-induced inhibition of the p300/CBP-bromodomain leads to globally reduced H3K27ac and H3K9ac levels.

In summary, I deemed the p300/CBP bromodomain inhibition approach at embryonic stage 12 suitable for generating endoderm donor nuclei with reduced histone acetylation levels for subsequent nuclear transfer.

4.2.2. p300/CBP HAT domain inhibition reduces H3K27ac, among other marks, in donor nuclei

The mass-spectrometry results presented here were obtained by Dr. Ignasi Forne at the ZfP at BMC, LMU who performed the data acquisition and processing

Having observed that treating donor embryos with CBP30, a p300/CBP bromodomain inhibitor can reduce H3K27ac levels globally, I next aimed at employing an alternative perturbation strategy. I reasoned that inhibiting the p300/CBP bromodomain may also perturb the architectural role of p300/CBP by perturbing histone binding or chromatin association (Zaware & Zhou, 2019). Therefore, a strategy was needed that would allow us to distinguish between the potential perturbation of the architectural role of p300/CBP by inhibiting the bromodomain and the loss of histone acetylation. Therefore, I employed a complementary approach to perturb histone acetylation levels in donor nuclei before nuclear reprogramming.

To this end, I used the small molecule A-485, targeting the p300/CBP HAT domain by acting a competitive inhibitor of acetyl-CoA and preventing lysine acetylation on histones (Lasko et al., 2017). I treated IVF-derived donor embryos with A-485 and A-486 (an inactive control compound for A-485 (Lasko et al., 2017)) from the late gastrula until the neurula stage as described for CBP30 (Figure 15A). Similar to the phenotypes observed using the bromodomain antagonist approach, I observed delayed closure of the neural fold in embryos treated with both the catalytic inhibitor A-485 and the inactive control A-486 compared to DMSO-controls (Figure 15B). Therefore, to ensure comparable developmental stages with the DMSO-controls for downstream biochemical assessment of histone modifications, small molecule-treated embryos were collected at the point of neural fold closure.

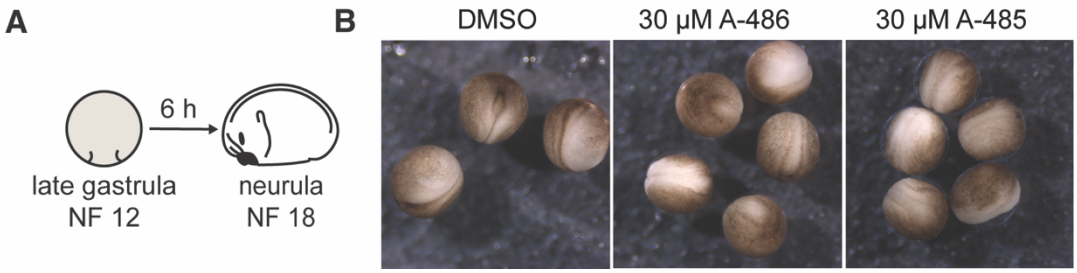

Figure 15: **A-485 treatment setup in wildtype embryos to produce H3K27ac-perturbed donor nuclei for NT.** (A) Schematic depiction of the treatment protocol with CBP30 or DMSO-control, starting from the late gastrula until the neurula stage. (B) Representative images of embryos treated with DMSO, A-485 or A-486 depicting the delayed neural fold closure phenotype, n=3.

As described for CBP30, this delay was deemed acceptable and a treatment setup using the HAT inhibitor A-485 was established allowing us to proceed with further experiments.

To quantitatively test the effects of p300/CBP HAT domain inhibition on donor embryos before NT, we performed histone mass spectrometry as described above for CBP30. We observed that the inactive control compound A-486 (gift from the Structural Genomics Consortium) reduced the global levels of H3K27ac and other histone PTMs to a similar extent as the inhibitor A-485, likely due to the high concentration and duration of the treatment in the *X. laevis* embryos, which exceeded the concentration and duration reported previously (Lasko et al., 2017). Considering that the A-486 control compound also caused a developmental delay in the treated embryos, along with the perturbed histone mark levels (Figure 21), I selected DMSO as an adequate control for the A-485 treatments. Compared to DMSO, A-485 treatment in donor embryos led to a 1.8-fold reduction in global H3K27ac levels, but also affected H3K18ac and H3K23ac levels, as well as several other acetylated lysine residues on the histone H4 N-terminal tail, indicating broad reduction of histone acetylation levels upon p300/CBP HAT inhibition (Figure 16 A-B).

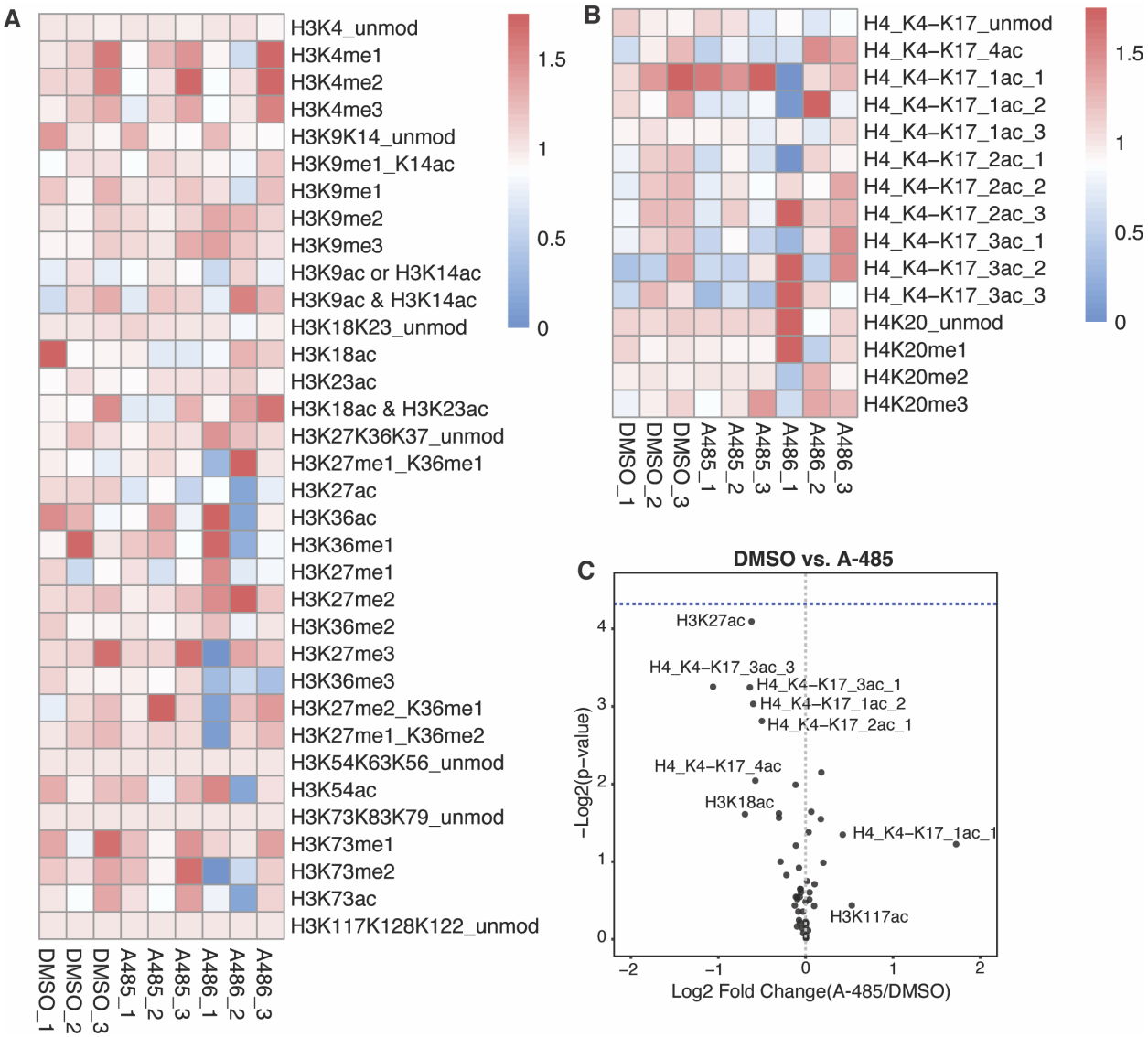

Figure 16: **Histone mass-spectrometry on histones isolated from DMSO, A-485 or A-486 treated neurula-stage whole embryos** (A-B) Heatmaps depicting the relative abundance of post-translational modifications on histone lysine residues, normalized over the abundance of histone PTM levels in untreated samples on (A) histone H3 and (B) histone H4. N=3. (C) Volcano plot comparing histone mark levels quantified via mass-spectrometry in A-485 compared to DMSO samples. y-axis shows the p-value calculated using an unpaired student's t-test, x-axis shows the log2 fold-change of histone mark levels in A-485 versus DMSO samples.

Western Blot analysis targeting H3K27ac and H3K18ac in chromatin extracts from A-485 and DMSO-control treated embryos revealed similar results as the histone mass-spectrometry (Figure 17 A-B). In addition, I also detected a reduction in pan-H3-acetylation levels by using an antibody that can recognize acetylated K9, K14, K18, K23

and K27 residues on the histone H3 N-terminus. This result is in line with the MS results presented above.

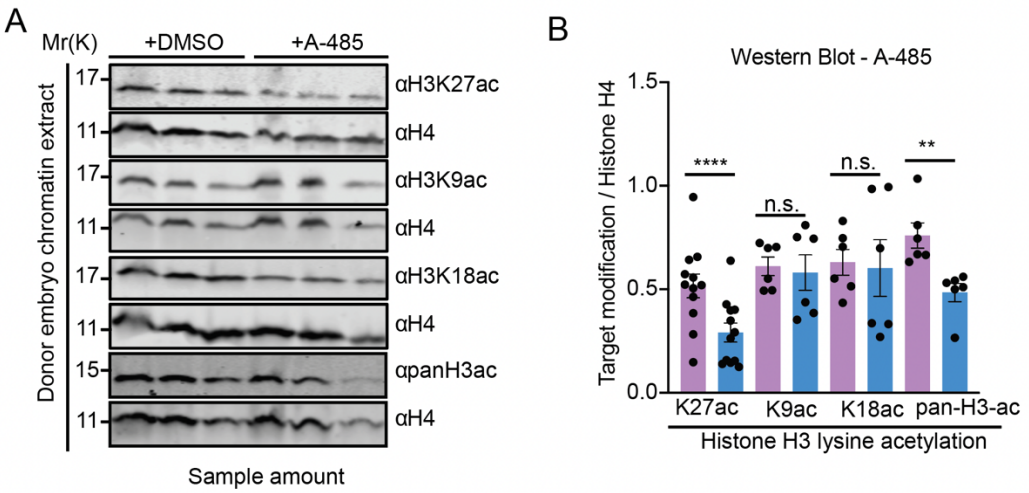

Figure 17: **Western Blot analysis of acetylated lysine residues on histone H3.** (A) Immunoblots depicting H3K27ac, H3K9ac, H3K18ac and pan-H3-acetylation (acetyl K9+K14+K18+K23+K27) levels, alongside histone H4 as loading control, for chromatin extracted from whole embryo lysates in DMSO and A-485-treated embryos. Samples were loaded as a dilution series in 2-fold steps, from the highest to the lowest concentration. (B) Band density quantification of Western Blot results for H3K27ac (n=4), H3K9ac (n=2), H3K18ac (n=2) and pan-H3-acetylation (n=2). Error bars represent the mean+/- SEM, and stars indicate p-values calculated using a paired t-test. (n.s.: $p > 0.05$, *: $p \leq 0.05$, **: $p \leq 0.01$, ***: $p \leq 0.001$, ****: $p < 0.0001$). Purple bars: DMSO-control, blue bars: A-485-treated.

In summary, the A-485 treatment broadly affected histone H3 and H4 lysine acetylation in donor nuclei, while the CBP30 treatment depleted H3K27ac and H3K9ac specifically, thus allowing us to compare the different contributions of global histone acetylation versus H3K27ac/H3K9ac to transcriptional memory during nuclear reprogramming.

4.3. Assessing the reprogramming outcome of NT embryos generated using donor nuclei with reduced histone acetylation levels

Having established a p300/CBP inhibition setup in donor embryos, allowing us to obtain donor nuclei for NT with reduced histone acetylation levels, I next sought to address whether such perturbation of histone acetylation levels in donor nuclei can improve reprogramming via NT. In particular, it was of key importance to address whether

perturbing H3K27ac in donor nuclei can reduce the aberrant expression of genes indicative of the donor cell type in NT embryos, termed ON-memory. Next, I aimed to determine whether perturbing H3K27ac by p300/CBP inhibition in donor nuclei can improve the developmental outcome of NT-embryos.

To address the effects of p300/CBP inhibition on a transcriptome level in the context of NT reprogramming, we performed RNA-seq experiments to profile the transcriptome of endoderm donor cells from control and inhibitor-treated conditions, as well as ectoderm tissues from NT-embryos derived from the so-generated donor nuclei (as described in Hörmanseder et al., 2017). As a control for the wildtype transcriptome of ectoderm tissues at this stage, we *in vitro* fertilized eggs and collected their ectoderm tissues. Such a comparison of the transcriptomes of donor, NT and IVF samples allowed us to measure whether inhibiting p300/CBP in donor nuclei correlates with changes in the expression of genes indicative of the cell type of origin, i.e. endoderm cells, in the wrong cell type of the cloned embryos, i.e. ectoderm. Moreover, we assessed the developmental outcome of NT embryos generated from p300/CBP inhibitor-treated donor nuclei to assess whether this manipulation of the donor nuclei correlates with improved reprogramming on a functional level.

Together, these experiments allow us to test the hypothesis that H3K27ac could be an epigenetic barrier to reprogramming by maintaining transcriptional memory of an active chromatin state from the donor to the reprogrammed cell. Moreover, these experiments will reveal whether perturbing this putative reprogramming barrier can improve the efficiency of NT-induced cell-fate reprogramming.

4.3.1. p300/CBP bromodomain inhibition in donor nuclei correlates with a moderate ON-memory decrease in NT embryos

In the following section, Nuclear Transfer injections were performed by Dr. Tomas Zikmund; bioinformatic analyses were supported by Dr. Tobias Straub.

Previous work from our group has shown that NT embryos display aberrant expression of a transcriptional program indicative of the endoderm donor cell type in the ectoderm of NT-embryos, termed ON-memory (Hörmanseder et al., 2017; Zikmund et al., 2025). Therefore, I tested if reducing H3K27ac levels in the endoderm donor cells can improve transcriptional reprogramming by reducing ON-memory in the newly generated ectoderm cells in NT embryos.

To achieve this, I treated the donor embryos with the CBP30 as described above. We then used the CBP30-treated embryos and DMSO-control (vehicle control to account

for any effects by this solvent) neurula-stage endoderm cells as donors to generate NT(CBP30) and NT(DMSO) embryos, respectively (Figure 18). As a control for wildtype embryonic transcriptome of the cell type we aim to obtain by reprogramming, I generated IVF embryos. To analyze the transcriptome of the reprogrammed cells, I collected the ectoderm (also termed animal cap in *Xenopus* embryos) of NT and IVF embryos at the gastrula stage. This stage was selected because at this point ectoderm and endoderm lineages are established in the frog embryo, but it precedes the developmental defects usually observed in NT embryos (Hörmanseder et al., 2017). Therefore, it was key to ensure that only properly cleaved embryos are collected, to allow comparison of memory gene expression between the transcriptomes of NT and IVF embryos while minimizing the confounding factors on the transcriptome arising from abnormal development. In summary, I collected the animal cap from NT(DMSO), NT(CBP30) and IVF embryos, alongside donor(DMSO) and donor(CBP30) endoderm, and subjected these tissues to bulk RNA-seq, as summarized in Figure 18.

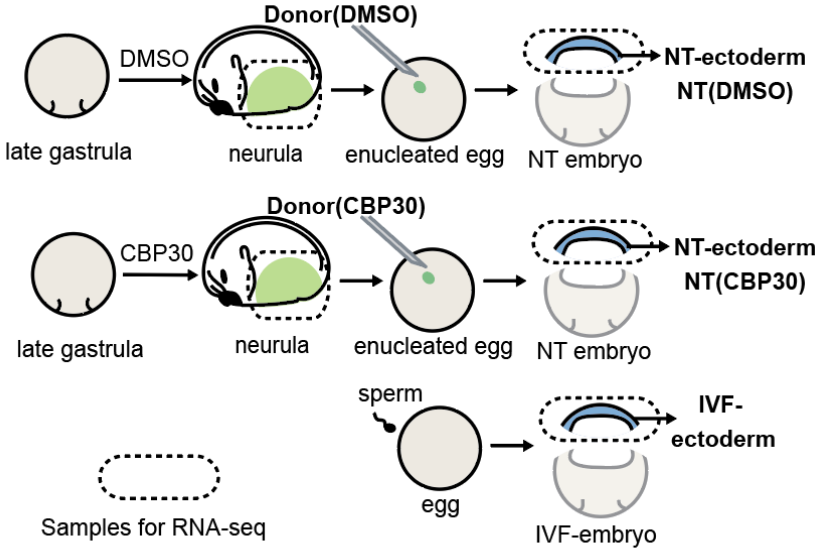

Figure 18: Schematic overview of NT-experiments performed to test the transcriptome reprogramming of endoderm-donor cells treated with p300/CBP bromodomain inhibitor to ectoderm via NT

First, I compared the global transcriptomes of donor, NT and IVF samples using principal component analysis (PCA) (Figure 19). Donor(DMSO) and donor(CBP30) endoderm samples clustered together and separated from all ectoderm samples along principal component (PC) 1. Importantly, the transcriptomes clustered by cell type and not by experimental batch. I then wondered if NT(CBP30) ectoderm samples showed greater similarity to IVF ectoderm samples compared to NT(DMSO), but did not observe a closer grouping of NT(CBP30) with IVF samples in PC space compared to NT(DMSO) and IVF samples. This suggested that CBP30 treatment in donor nuclei did not globally improve

the transcriptome of NT(CBP30) embryos but might rather have effects on distinct groups of genes.

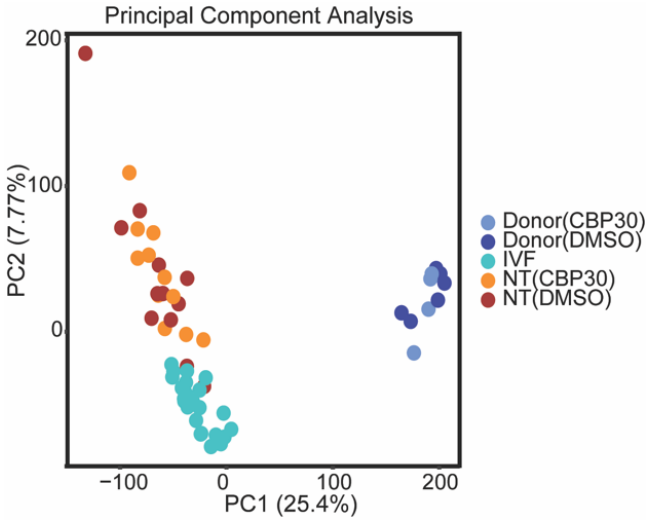

Figure 19: Principal Component Analysis (PCA) comparing the global transcriptome of donor(DMSO), Donor(CBP30), IVF, NT(DMSO) and NT(CBP30) samples. The x-axis shows Principal Component 1 (PC1) explaining 25,4% of the variance, and the y-axis shows Principal Component 2 (PC2) explaining 7,77%.

Therefore, I next addressed the effects of p300/CBP bromodomain inhibition on the expression levels of individual genes in endoderm donor cells by performing differential gene expression analysis. Thus, this analysis revealed 3282 differentially expressed transcripts between CBP30-treated and DMSO-control donor cells, with most of the genes being downregulated (2538 downregulated *vs*. 744 upregulated genes upon CBP30 treatment) (Table 3), consistent with the role of p300/CBP as a transcriptional co-activator. Therefore, while the transcriptomes of CBP30- and DMSO-treated donor cells co-clustered in PCA (Figure 20), suggesting no global differences, a number of genes was significantly misregulated upon inhibitor treatment.

Next, I tested if CBP30 treatment of the donor cells results in a loss of ON-memory gene expression in the NT embryos generated from these treated donor nuclei, when compared to NT embryos generated from control donor nuclei. To address this question, I first compared the transcriptome of control donor(DMSO) cells, the ectoderm of IVF embryos, and the ectoderm of control NT(DMSO) embryos and identified 5238 genes that were significantly differentially expressed (p-adj<0.05) between these three groups of samples. To identify ON-memory genes that maintain an active state of gene expression from donor cells to NT-embryos, I then filtered this gene set based on gene expression in the donor(DMSO) samples (TPM>1) and identified 1360 ON-memory genes in NT(DMSO) embryos (Figure 21A). For comparison, I performed differential gene expression analysis following the same filtering strategy under CBP30 conditions, i.e.,

comparing donor(CBP30) vs. IVF and NT(CBP30) vs. IVF samples. This resulted in a set of 1071 ON-memory genes (Figure 21B), indicating that fewer genes could be classified as ON-memory genes in NT embryos derived from donor embryos treated with CBP30. Intersection analysis revealed 771 ON-memory genes that could be identified in both the set of ON-memory(DMSO) and ON-memory(CBP30) groups, while 589 genes were unique to the DMSO group and 300 genes were unique to the CBP30 group (Figure 21C). The strong overlap of the genes classified as ON-memory genes in DMSO or CBP30 samples suggests that the CBP30 effect on transcriptome reprogramming could be moderate.

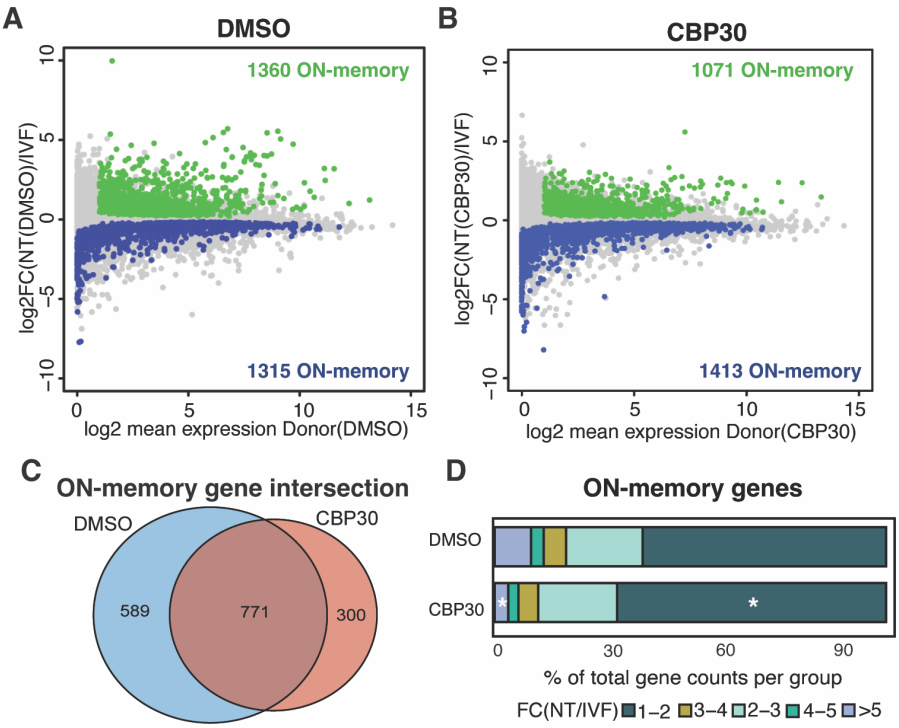

Figure 21: Memory gene expression in NT embryos derived from CBP30 treated donor nuclei. (A-B) MA-plots comparing gene expression between (A) NT(DMSO) and IVF, (B) NT(CBP30) and IVF. Mean log2FC in NT over IVF ectoderm expression levels is plotted on the y-axis, and the mean log2(TPM+1) expression in endoderm (A) donor(DMSO) and (B) donor(CBP30) nuclei is plotted on the x-axis. Gray: all transcripts. Green: ON-memory genes. Blue: OFF-memory genes. (C) Venn Diagram comparing the overlap of genes classified as ON-memory genes in DMSO samples and CBP30 samples. (D) Percentage of ON-memory genes defined under DMSO (n=1360) and CBP30 (n=1071) conditions, partitioned based on their fold change in NT/IVF samples. two-sided Fisher's test, * p-value < 0.0001

While intersection analysis revealed substantial overlap between ON-memory genes defined under both DMSO and CBP30 conditions, this approach only identified the

presence or absence of memory genes in each gene set without considering quantitative differences in their expression levels. To better assess the extent of transcriptional memory, I compared the fold-changes in gene expression between NT and IVF samples across conditions (Figure 21D). My reasoning was that if CBP30 treatment effectively reduced ON-memory, genes in NT(CBP30) embryos should exhibit expression patterns more similar to IVF embryos than those in NT(DMSO) embryos. I therefore stratified ON-memory genes in 5 groups based on their fold-change in expression between NT and IVF samples under both conditions. This analysis revealed that the proportion of ON-memory genes with higher expression in NT(CBP30) *versus* IVF was significantly decreased compared to NT(DMSO) *versus* IVF. Conversely, the proportion of ON-memory genes with lower fold-change between NT(CBP30) *vs.* IVF significantly increased compared to NT(DMSO) *vs.* IVF. This indicates that CBP30-treatment in donor nuclei not only decreased the number of ON-memory genes but also decreased the extent to which ON-memory genes are abnormally expressed in NT(CBP30) compared to IVF embryos.

Furthermore, I asked if CBP30 treatment in donor nuclei led to changes in gene expression levels of ON-memory genes in NT(CBP30) embryos. To address this, I compared the mean expression levels of ON-memory genes defined under DMSO conditions in donor(DMSO) *vs.* donor(CBP30), as well as NT(DMSO) *vs.* NT(CBP30) samples. In both cases, I found that the mean ON-memory gene expression levels were moderately decreased (Figure 22). To distinguish whether this is a phenotype specific to the ON-memory gene set, I compared the mean expression levels of a control gene set termed reprogrammed-down genes in the different embryonic tissues (Figure 22). This group describes a set of genes expressed at similar levels as ON-memory genes in donor cells, but was correctly downregulated in reprogramming, i.e., gene expression levels were similar in IVF and NT samples (Hörmanseder et al., 2017). In this case, I observed that the mean expression levels of reprogrammed-down genes were slightly but non-significantly decreased in donor(CBP30) compared to donor(DMSO) endoderm samples and remained unaltered in NT(CBP30) compared to NT(DMSO) ectoderm samples. Therefore, this analysis revealed that CBP30 treatment in donor nuclei results in decreased ON-memory but not reprogrammed-down gene expression in NT(CBP30) embryos.

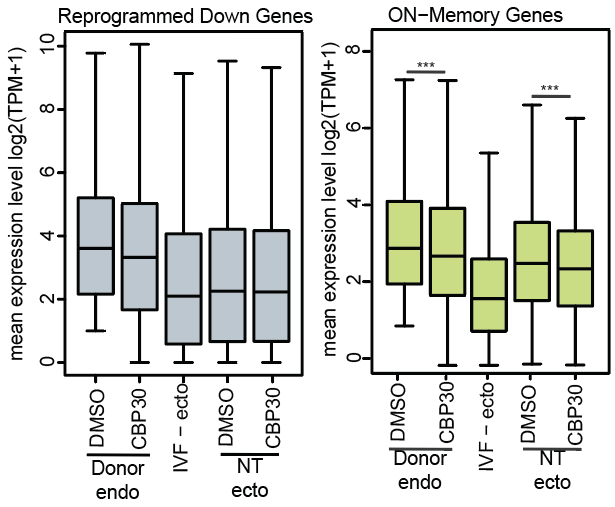

Figure 22: CBP30 treatment in endoderm donor nuclei moderately decreases ON-memory gene expression in NT ectoderm. Boxplots comparing mean expression levels of reprogrammed-down and ON-memory transcripts in endoderm donor cells, IVF ectoderm, and NT ectoderm samples. Boxplots depict the median and the interquartile range (IQR). p-values for pairwise comparisons calculated using a two-sided Wilcoxon rank-sum test.

I next asked if CBP30 treatment in donor nuclei affected the transcriptional memory of OFF-memory genes, describing a set of genes expressed at aberrantly lower levels in NT embryos compared to IVF embryos, indicating failure to upregulate its expression levels correctly from the donor to the reprogrammed cell. This filtering strategy resulted in 1315 OFF-memory genes in NT(DMSO)-ectoderm samples, and 1413 OFF-memory genes in NT(CBP30)-ectoderm samples, thus suggesting an increase in the number of genes classified as OFF-memory genes (Figure 21 A-B). Comparing the mean expression levels of OFF-memory genes in donor samples revealed a mild decrease in donor(CBP30) samples *vs.* donor(DMSO) samples (Figure 23). When comparing NT(DMSO) and NT(CBP30) samples, I did not detect any changes in OFF-memory gene expression. Of note, the mean expression levels of reprogrammed-up genes, i.e. genes that demonstrated correctly upregulated gene expression upon nuclear reprogramming, remained unaltered upon CBP30 treatment in donor samples, as well as in NT samples (Figure 23).

In summary, the transcriptome assay described in this section suggests that CBP30 treatment in donor nuclei can moderately improve ON-memory in NT embryos, but not OFF-memory.

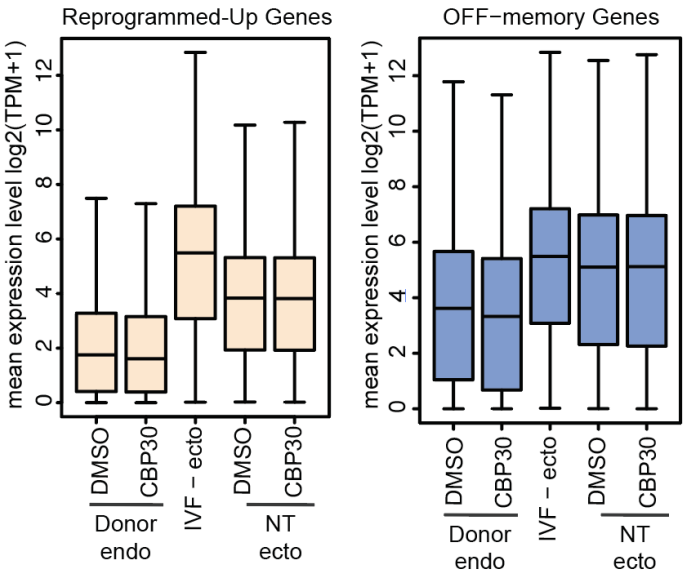

Figure 23: CBP30 treatment in endoderm donor nuclei left Reprogrammed-Up and OFF-memory gene expression levels unperturbed in NT ectoderm cells. Boxplots comparing mean expression levels of reprogrammed-up and OFF-memory transcripts in endoderm donor cells, IVF ectoderm, and NT ectoderm samples. Boxplots depict the median and the interquartile range (IQR). p-values for pairwise comparisons calculated using a two-sided Wilcoxon rank-sum test.

4.3.2. p300/CBP catalytic inhibition in donor nuclei moderately improves ON-memory in NT-embryos

In the following sections, Nuclear Transfer injections were performed by Dr. Eva Hörmanseder; bioinformatic analyses were supported by Dr. Tobias Straub

The results presented in chapters 4.2. and 4.3.1. indicated that p300/CBP bromodomain inhibition in donor nuclei reduced global H3K27ac levels and moderately improved ON-memory. However, bromodomain inhibition may also perturb p300/CBP chromatin association in addition to perturbing histone acetylation, due to its binding to acetylated lysine residues on histones (Dhalluin et al., 1999; Zaware & Zhou, 2019; Zeng & Zhou, 2002). Therefore, I asked if inhibition of p300/CBP catalytic activity and reducing histone acetylation levels, while leaving the architectural role of p300/CBP unperturbed, would result in comparable effects in reprogramming on the transcriptome level. To address this question, I treated IVF-derived donor embryos with A-485 as described above and injected them to enucleated eggs to produce NT(A-485) embryos, which I then subjected to RNA-seq analysis along with IVF-control embryos.

First, I tested the effects of p300/CBP HAT domain inhibition on the transcriptome in endoderm donor cells and detected 5493 DEGs between donor(DMSO) and donor(A-485) samples, of which 3259 were downregulated upon A-485 treatment in endoderm donor samples, and 2234 were upregulated (Table 3). While the higher number of downregulated genes upon A-485 treatment in donor cells is consistent with the role of p300/CBP as a transcriptional co-activator, the relatively high number of upregulated genes suggests an overall misregulation of the transcriptome.

To assess the effects of p300/CBP HAT inhibitor treatment in donor nuclei on reprogramming, I evaluated the transcriptome of NT ectoderm tissue derived from A-485 treated donor nuclei compared to NT(DMSO) controls. The transcriptome response in NT(A-485) embryos elicited by catalytic p300/CBP inhibition in donor cells closely followed the observations presented in chapter 4.3.1. using the bromodomain inhibitor CBP30. For instance, comparing the global transcriptomes using PCA showed clear separation along PC1 for the donor endoderm and NT and IVF ectoderm samples, yet the IVF, NT(DMSO) and NT(A-485) grouped together (Figure 24). This indicated that A-485 treatment in donor nuclei did not globally improve the transcriptome of NT(A-485) embryos but may have affected distinct gene sets, similarly to the CBP30 treatment.

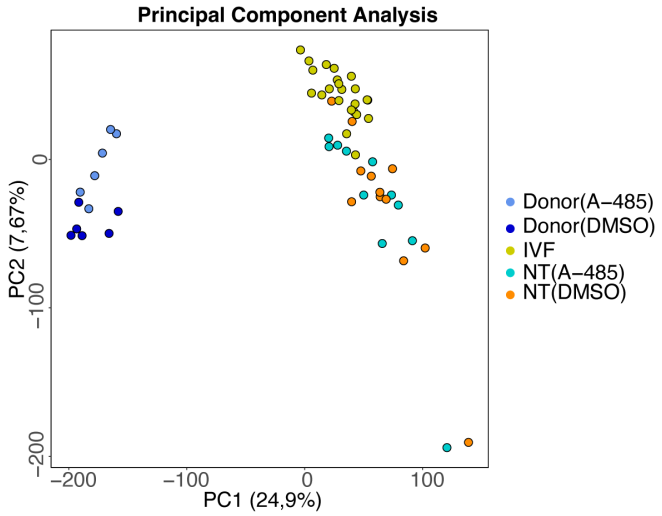

Figure 24*:* Principal Component Analysis (PCA) comparing the global transcriptome of donor(DMSO), Donor(A-485), IVF, NT(DMSO) and NT(A-485) samples. The x-axis shows Principal Component 1 (PC1) explaining 24,9% of the variance, and the y-axis shows Principal Component 2 (PC2) explaining 7,67%.

Thus, I performed gene set filtering to identify reprogrammed and memory class genes as described in chapter 4.3.1. and in the *Materials and Methods* section. This revealed 1253 ON-memory genes in A-485-derived samples and 1525 OFF-memory genes (Figure 25A-B), indicating a modest reduction in the number of ON-memory genes and a modest increase in the number of OFF-memory genes compare to DMSO. I then asked if the genes classified as ON-memory genes under DMSO or under A-485 conditions are similar and performed intersection analysis. Such comparison of the ON-memory gene sets defined under DMSO and A-485 conditions revealed a substantial overlap between the two lists, indicating a moderate effect on ON-memory upon A-485 treatment in donor nuclei (Figure 25C). Given that this analysis does not account for differences in expression *levels* of ON-memory genes between DMSO and A-485 samples, I addressed whether the expression of ON-memory genes in NT-A485 embryos became more similar to IVF embryos and performed similar stratification and proportion testing as described in Figure 21. I observed that indeed the proportion of genes with the highest fold-changes between NT and IVF ectoderm samples was significantly lower in NT(A-485) embryos compared to NT(DMSO) embryos (Figure 25D). Therefore, these results point towards a modest improvement in the ON-memory phenotype upon A-485 treatment in donor endoderm nuclei.

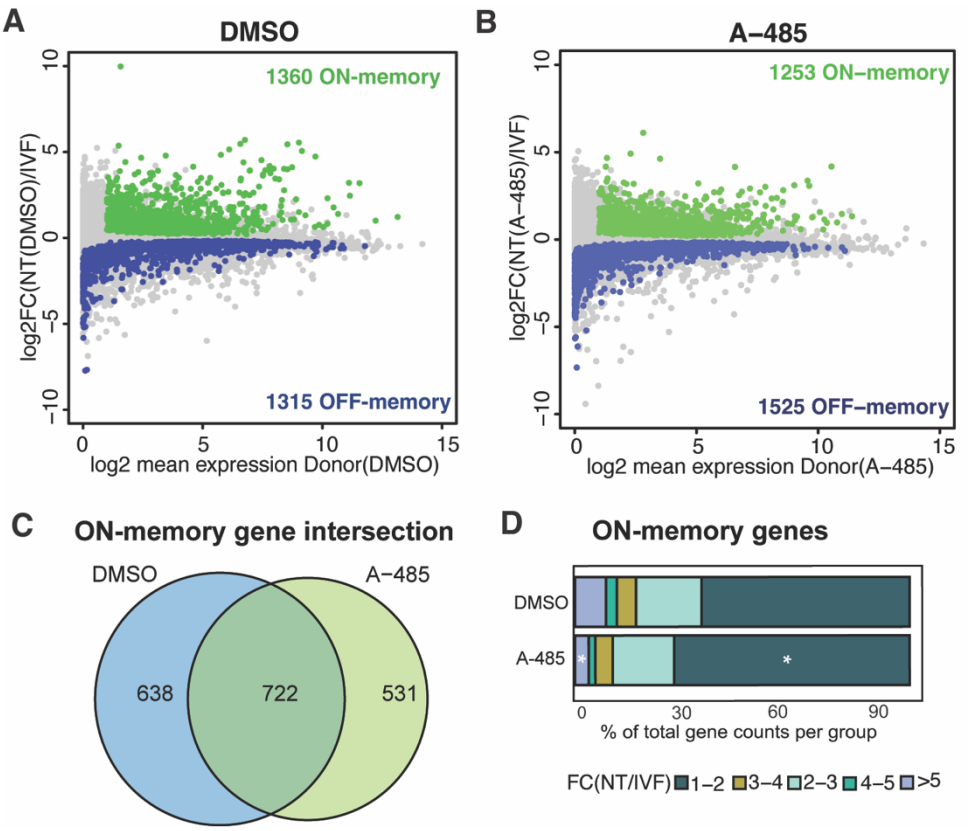

Figure 25: Memory gene expression in NT embryos derived from A-485 treated donor nuclei. (A-B) MA-plots comparing gene expression between (A) NT(DMSO) and IVF, (B) NT(A-485) and IVF. Mean log2FC in NT over IVF ectoderm expression levels is plotted on the y-axis, and the mean log2(TPM+1) expression in endoderm (A) donor(DMSO) and (B) donor(A-485) nuclei is plotted on the x-axis. Gray: all transcripts. Green: ON-memory genes. Blue: OFF-memory genes. (C) Venn Diagram comparing the overlap of genes classified as ON-memory genes in DMSO samples and A-485 samples. (D) Percentage of ON-memory genes defined under DMSO (n=1360) and A-485 (n=1253) conditions, partitioned based on their fold change in NT/IVF samples. two-sided Fisher's test, * p-value < 0.0001

I next compared the mean expression levels of ON-memory genes in NT embryos derived from A-485 treated donor nuclei, and observed a modest decrease compared to NT(DMSO) samples (Figure 26). On the other hand, reprogrammed-down genes demonstrated similar mean expression levels in NT(DMSO) and NT(A-485) samples, albeit showing decreased expression levels in donor(A-485) endoderm samples (Figure 26). This suggests that while A-485 treatment in endoderm donor nuclei correlates with a moderate improvement in ON-memory in NT ectoderm, reprogrammed-down genes seem unaffected in NT(A-485) embryos.

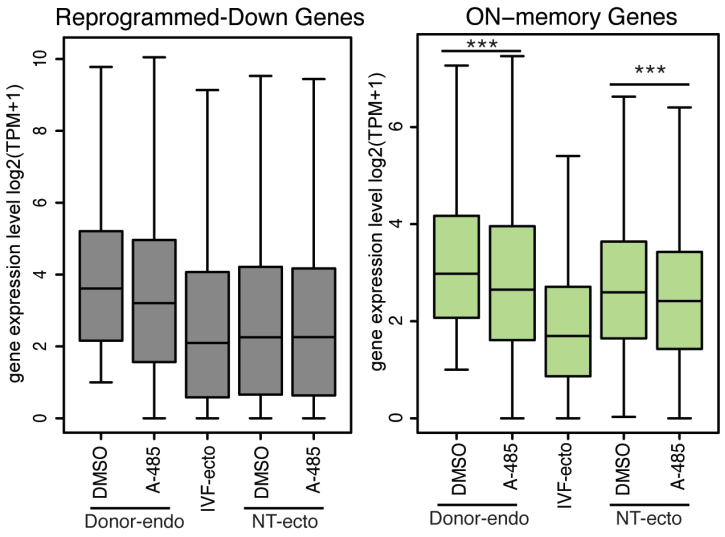

Figure 26: A-485 treatment in endoderm donor nuclei moderately decreases ON-memory gene expression in NT ectoderm. Boxplots comparing mean expression levels of reprogrammed-down and ON-memory transcripts in endoderm donor cells, IVF ectoderm, and NT ectoderm samples. Boxplots depict the median and the interquartile range (IQR). p-values for pairwise comparisons calculated using a two-sided Wilcoxon rank-sum test.

Furthermore, I checked the impact of p300/CBP HAT inhibition in donor nuclei on OFF-memory gene expression in donor nuclei. To this end, I compared the mean expression levels of OFF-memory genes in DMSO and A-485 samples, which revealed unaltered mean transcript levels for donor(DMSO) and donor(A-485) samples, as well as for NT(DMSO) and NT(A-485) samples (Figure 27). The corresponding control gene set, reprogrammed-up genes, which are expressed at similar levels as OFF-memory genes in donor nuclei but correctly upregulate their expression in NT embryos, also did not reveal any differences in mean transcript levels in the A-485 samples.

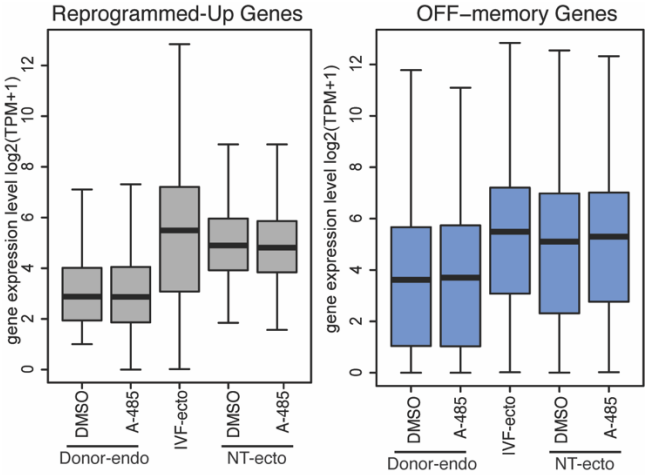

Figure 27: A-485 treatment in endoderm donor nuclei left Reprogrammed-Up and OFF-memory gene expression levels unperturbed in NT ectoderm cells. Boxplots comparing mean expression levels of reprogrammed-up and OFF-memory transcripts in endoderm donor cells, IVF ectoderm, and NT ectoderm samples. Boxplots depict the median and the interquartile range (IQR). p-values for pairwise comparisons calculated using a two-sided Wilcoxon rank-sum test.

The initial analysis of mean expression levels showed no significant overall changes in OFF-memory genes upon A-485 treatment in both donor nuclei and NT embryos. However, I wondered if individual OFF-memory genes might be differentially expressed in NT(A-485) embryos compared to NT(DMSO) embryos (Figure 28). Therefore, I filtered the OFF-memory transcripts based on statistical significance (p-adj < 0.05) between NT(DMSO) and NT(A-485) samples and identified 178 'A-485-sensitive' OFF-memory genes (Figure 28A). This subset of OFF-memory genes was expressed at low levels in donor(DMSO) nuclei and revealed a mild increase in donor(A-485) samples (Figure *28*B). Interestingly, I found that this subset of OFF-memory genes was correctly upregulated in NT(A-485) embryos compared to its aberrantly low expression levels in NT(DMSO) and reached expression levels comparable to those of IVF embryos. For comparison, when filtering the OFF-memory transcripts based on significant differential expression between NT(DMSO) *vs.* NT(CBP30), this resulted in only 4 genes, suggesting that A-485 treatment in donor nuclei improved the expression of a subset on OFF-memory gene expression in NT embryo, while CBP30 did not.

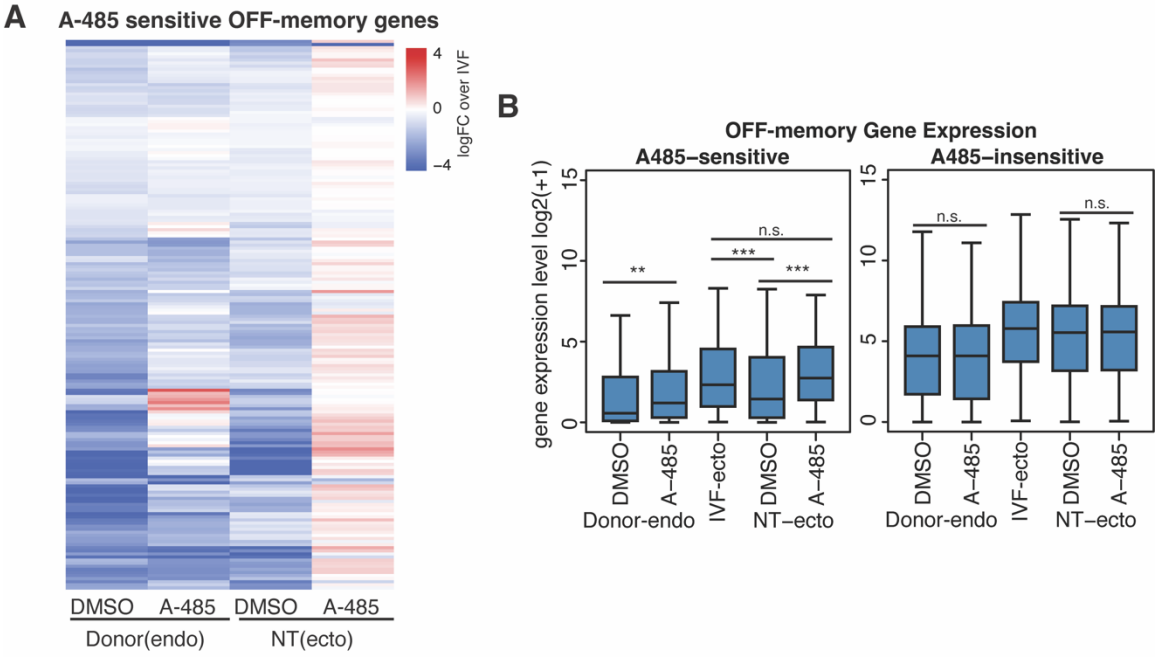

Figure 28**:** A-485 treatment in endoderm donor nuclei increases the expression levels of a subset of OFF-memory genes in NT(A-485) ectoderm. (A) Heatmap depicts ON-memory genes significantly differentially expressed between NT(DMSO) and NT(A-485) p-adj < 0.05 n=178

genes. Color key indicates log_2 fold-change over IVF ectoderm samples. (B) Comparison of gene expression levels of the subsets of A-485-sensitive (n=178) and A-485 insensitive (n=1137) OFF-memory genes. Boxplots depict the median and the interquartile range (IQR). P-values were calculated using Wilcoxon rank-sum test, two-sided.

In summary, this transcriptome analysis of A-485 perturbed endoderm donor nuclei and ectoderm nuclei of NT embryos derived from donor(A-485) revealed that p300/CBP HAT inhibition moderately decreased ON-memory expression and increased gene expression of a subset of OFF-memory genes. Therefore, we observed that using both a p300/CBP bromodomain and a HAT domain inhibitor similarly improved ON-memory expression, albeit modestly.

4.3.3. p300/CBP inhibition in donor nuclei corrects the aberrant expression of endoderm marker genes in NT ectoderm

Previous studies by our group have shown that endoderm master regulators are memorized from endoderm donors to NT ectoderm cells (Hörmanseder et al., 2017) and that such aberrant expression causes differentiation defects in NT ectoderm (Zikmund et al., 2025). Therefore, I asked if p300/CBP inhibitor treatment in donor nuclei could reduce the ON-memory expression of endoderm marker genes in NT ectoderm.

To this end, I filtered the set of ON-memory genes based on significantly downregulated expression in NT ectoderm from p300/CBP-inhibitor treated donors compared to NT(DMSO) controls (p-adj < 0.05, log2FC < 0). Differential expression analysis between NT(DMSO) and NT(A-485) ectoderm samples identified 118 genes expressed at significantly lower levels in NT(A-485). In contrast, comparison between NT(DMSO) and NT(CBP30) revealed a smaller gene set of 36 significantly downregulated ON-memory genes in NT(CBP30). In the further text, the ON-memory genes significantly downregulated in either NT(CBP30) or NT(A-485) samples compared to NT(DMSO) will be referred to as ‘sensitive’, while the remaining ON-memory genes will be referred to as ‘insensitive’ genes.

To compare the genes sensitive to each type of treatment, I intersected the genes obtained by comparing NT(DMSO) *vs*. NT(CBP30) and NT(DMSO) *vs*. NT(A-485) ectoderm. This analysis resulted in a list of 30 genes, including several key endoderm cell fate markers such as *sox17a*, *sox17b*, *gata6*, *darmin, foxa1, foxa2* and others (Figure 29A-B) (Mukherjee et al., 2020; Sinner et al., 2006), suggesting that both treatments in the donor cells could reduce the expression of key endoderm ON-memory genes in the ectoderm of NT embryos. I next compared the magnitude of differential expression in

NT(CBP30) *vs.* NT(DMSO) and NT(A-485) *vs.* NT(DMSO) samples by comparing the mean expression levels of the respective sensitive and insensitive ON-memory gene subsets. Interestingly, I found that the 'CBP30-sensitive' ON-memory gene subset demonstrated a stronger decrease in mean expression levels in NT(CBP30) *vs.* NT(DMSO), in contrast to the decrease observed for the subset of 'A-485 sensitive' genes in NT(A-485) *vs.* NT(DMSO) samples (Figure 29C). Notably, the sets of treatment-sensitive genes maintained expression levels in the inhibitor-treated donor samples comparable to DMSO-control samples, suggesting effects on the maintenance of ON-memory rather than general transcriptional repression. Thus, it appears that the set of CBP30-sensitive genes, although it consist of fewer genes compared to the A-485 sensitive gene set, demonstrates a stronger reduction in ON-memory expression compared to the set of A-485 sensitive genes.

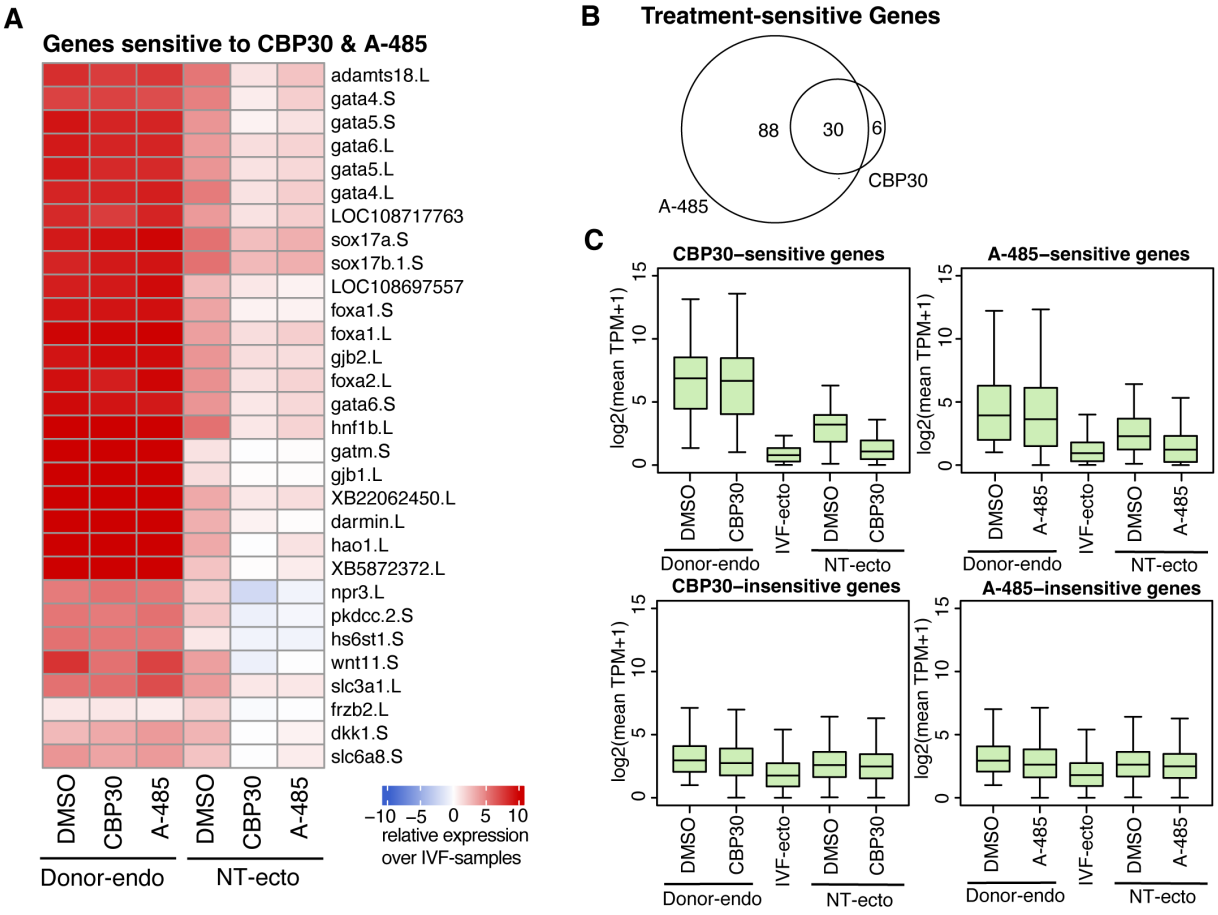

Figure 29: Key endoderm genes are sensitive to p300/CBP-inhibitor treatment in donor nuclei upon NT-reprogramming. (A) Heatmap depicts ON-memory genes significantly differentially expressed between NT(DMSO) and NT(CBP30) p-adj < 0.05 and NT(DMSO) and NT(A-485), n=30 genes. Color key indicates $\log_2$ fold-change over IVF ectoderm samples. (B) Euler Diagram showing the overlap between CBP30-sensitive and A-485-sensitive genes. (C) Comparison of gene expression levels of the subsets of CBP30-sensitive (n=36), CBP30-insensitive (n=1324),

as well as A-485-sensitive (n=118) and A-485 insensitive (n=1242) genes. Boxplots depict the median and the interquartile range (IQR).

In summary, our transcriptome experiments revealed that treating donor nuclei with p300/CBP inhibitors could render a key set of ON-memory genes permissive to reprogramming via nuclear transfer.

4.3.4. p300/CBP bromodomain inhibition in donor nuclei moderately improves the developmental outcome of NT-embryos

Nuclear Transfer injections were performed by Dr. Eva Hörmanseder

We next asked if perturbing p300/CBP-mediated histone acetylation, and thus reducing ON-memory in NT embryos, is sufficient to improve the developmental outcome of NT embryos. Given that the CBP30 treatment only revealed a decrease in ON-memory gene expression, but not an increase in OFF-memory expression, as well as a stronger decrease in the expression of CBP30-sensitive genes compared to the set of A-485 sensitive genes, we selected CBP30 as the more suitable treatment approach for generating donor nuclei prior to NT experiments aiming to evaluate the role of perturbing H3K27ac on the developmental outcome of NT embryos.

Thus, we generated NT-embryos using either DMSO or CBP30-treated donor nuclei, alongside IVF-embryos. We selected experiments where >80% of IVF embryos succeeded in development past gastrula stage, to ensure that the quality of a given batch of eggs was sufficient for NT. Then, we evaluated the embryos at the blastula stage and selected those that did not show any visible cleavage abnormalities and obvious cell death. At this point, the experiment was double blinded before further monitoring and quantifying the development of the NT embryos.

We found that both sets of NT embryos demonstrated similar developmental rates during the blastula and early gastrula stage, but we observed healthier morphology in NT(CBP30) embryos, which reflected higher rates of successful development compared to NT(DMSO) embryos past the neurula stage (Figure 30A-C). We followed embryonic development through tadpole stage, at which point embryos have completed major organogenesis milestones including heart formation and circulation, functional kidney development, and central nervous system patterning (Zahn et al., 2022). At this stage, tadpoles exhibit coordinated swimming behavior and have transitioned to free-swimming larvae, providing a robust assessment of successful reprogramming and normal developmental progression. While NT(CBP30) embryos reached the tadpole stage at slightly higher numbers than NT(DMSO) embryos, this difference was statistically not

significant. This could be due to selection pressure, which would have resulted in only the most robust embryos of each condition to reach this stage, therefore diminishing the observable difference between the two groups.

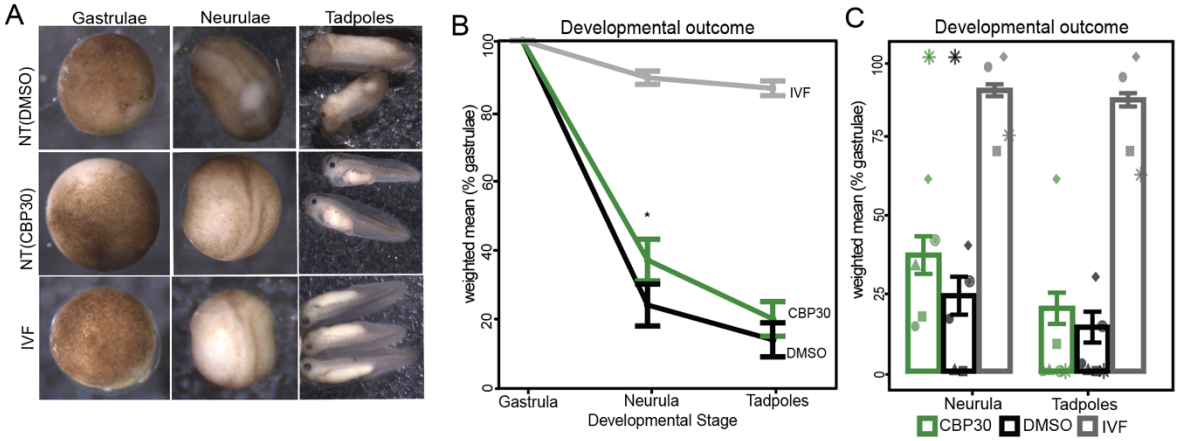

Figure 30: p300/CBP bromodomain inhibition in donor nuclei improves the developmental outcome of NT(CBP30) embryos. (A) NT(DMSO), NT(CBP30) and IVF embryos at gastrula and neurula stage. (B-C) The development of NT(DMSO), NT(CBP30) and IVF gastrulae (st.10.5) was monitored until the tadpole stage. y-axis represents the weighted mean percentage of gastrulating embryos reaching neurula and tadpole stages.

In summary, we observe that p300/CBP inhibition moderately improves the development of NT embryos. This suggests that H3K27ac represents a barrier to reprogramming, as its reduction correlated with decreased ON-memory expression in NT ectoderm, and with a mild increase in cloning efficiency.

4.4. Linking H3K27ac and related histone marks on *cis*-regulatory elements with reprogramming resistance

In chapter 4.3. I described that chemically perturbing p300/CBP correlated with globally decreased histone acetylation levels in endoderm donor nuclei and partial loss of ON-memory in the ectoderm of NT embryos. Furthermore, p300/CBP bromodomain inhibition in donor nuclei correlated with moderately improved development of NT embryos. In the scope of our Digital Reprogramming analysis (Figure 7), it was also identified that H3K27ac is strongly enriched on the promoters of ON-memory genes compared to a set of genes correctly downregulated in reprogramming. Importantly, our p300/CBP inhibition experiments revealed that while some ON-memory genes became permissive to reprogramming (treatment-sensitive), others remained resistant (treatment-insensitive). Thus, this finding raised two possibilities: (i) p300/CBP inhibitor treatment may not have targeted the promoters of treatment-sensitive and treatment-insensitive genes to the same extent (ii) additional H3K27ac-marked regulatory elements such as enhancers might play a role in maintaining ON-memory.

To address the first possibility, I employed a candidate-based approach using ChIP-qPCR analyzing changes in H3K27ac levels around the promoter elements of several candidate treatment-sensitive and insensitive ON-memory genes.

To address the second possibility that H3K27ac on additional regulatory elements could play a role in ON-memory, I sought to investigate a putative link between enhancers and transcriptional ON-memory. Specifically, we first performed computational identification of putative enhancers in endoderm donor nuclei aiming to compare the enhancer features of ON-memory *versus* correctly reprogrammed genes. Finally, I analyzed the H3K27ac levels on genomic regulatory elements genome-wide in control and p300/CBP inhibitor-treated donor nuclei via CUT&RUN, aiming to assess the changes in H3K27ac levels on regulatory elements linked to reprogramming-resistant and reprogramming-permissive genes. To address the potential effects on other histone modifications upon p300/CBP inhibition genome-wide in endoderm-donor nuclei, I also performed CUT&RUN experiments targeting H3K4me3 and H3K4me1, identified as potential barriers by Digital Reprogramming, along with H3K9ac, which showed mild global decrease in Western Blot assays upon p300/CBP inhibition in donor embryos.

Taken together, this chapter aims to dissect the distribution of H3K27ac and related histone modifications on genomic regulatory elements and the persistence of transcriptional ON-memory during nuclear reprogramming.

4.4.1. H3K27ac levels are decreased around the promoters of treatment-sensitive and insensitive genes

Using the p300/CBP inhibition approach, I observed that while the number of ON-memory genes and their mean expression levels were reduced with both drugs, not all ON-memory genes became permissive to reprogramming upon such manipulation of the donor nuclei. Therefore, I hypothesized that inhibiting p300/CBP in donor nuclei may not have targeted all ON-memory genes evenly, for instance if H3K27ac levels were only reduced around the promoters of treatment-sensitive but not on treatment-insensitive genes, which would explain the different behavior upon nuclear reprogramming.

To test whether reduced H3K27ac levels could explain the differential sensitivity of ON-memory genes to CBP30 treatment, I examined the H3K27ac levels at candidate gene promoters using ChIP-qPCR. For this purpose, I selected candidate treatment-sensitive genes (*sox17a.L, gata5.L, hao1.L*) and treatment-insensitive genes (*a2m.S, foxa4.L*) identified in our differential expression analysis between NT(DMSO) and NT(CBP30) ectoderm. Surprisingly, I found that both sensitive and insensitive ON-memory genes displayed reduced H3K27ac levels around their promoters (Figure 31), suggesting that reduced H3K27ac around the promoter region may not be sufficient to correct the ON-memory status of some genes.

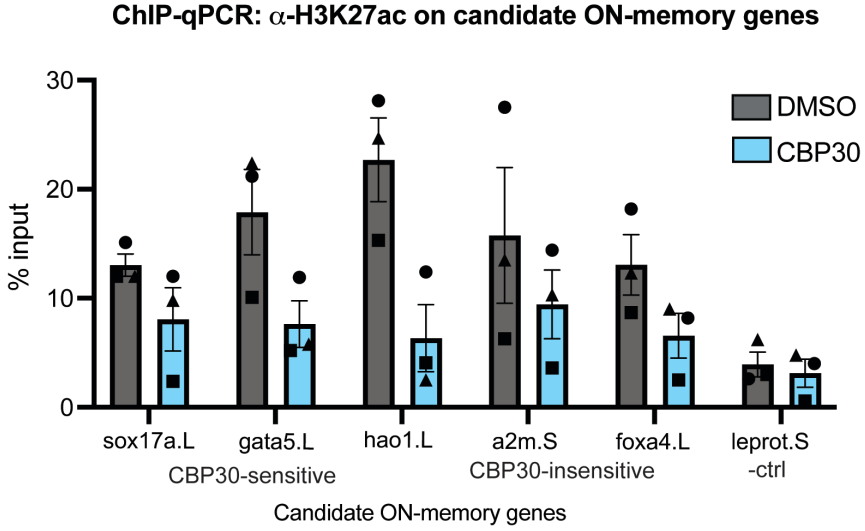

Figure 31: **ChIP-qPCR analysis of H3K27ac levels on candidate promoters of ON-memory genes in endoderm in endoderm of donor embryos.** y-axis represents the percent input. Gray bars indicate DMSO control samples, blue bars indicate CBP30 treated samples. Each data point represents an independent biological replicate, in total n=3. Each biological replicate is represented as a different shape.

Together, this led me to hypothesize, that H3K27ac on other cis-regulatory elements in the genome apart from promoters, may also be at play in mediating transcriptional ON-memory during reprogramming. Thus, I wondered if altered H3K27ac levels on other genomic sites apart from promoters may explain the findings of our transcriptome analyses under p300/CBP perturbed conditions.

4.4.2. H3K27ac-marked putative enhancers distinguish ON-memory genes from correctly reprogrammed genes

The computational identification of enhancers in this section was performed in collaboration with Dr. Sara Llorente-Armijo from the Vaquerizas group at the MRC, London.

Having observed that reduced H3K27ac levels on promoters alone did not correlate with the treatment-sensitive or treatment-insensitive status of candidate ON-memory genes, we turned our attention to enhancers as potential additional mediators of transcriptional memory. Besides its enrichment on actively transcribing promoters, H3K27ac is also considered a mark of active enhancers (Calo & Wysocka, 2013; Creyghton et al., 2010; Heinz et al., 2015; Rada-Iglesias et al., 2011; X. Wu et al., 2023). A previous study employing a bromodomain inhibitor similar to CBP30 suggested that p300/CBP bromodomain-dependent H3K27 acetylation is required for enhancer activity in a cell culture system (Raisner et al., 2018). Thus, we reasoned that the decrease in ON-memory expression may be due to CBP30-linked reduction of H3K27ac on enhancers. To test this hypothesis, we first performed bioinformatical prediction of putative enhancers in the *Xenopus laevis* genome to identify whether this correlates with ON-memory.

As there is no publicly available *Xenopus laevis* genome annotation that includes enhancers, we collaborated with Sara Llorente-Armijo from the Vaquerizas group to curate a list of predicted enhancers in neurula-stage endoderm. To achieve this goal, we integrated several datasets: a publicly available p300 ChIP-seq dataset in neurula-stage foregut and hindgut samples, i.e., endoderm (Stevens et al., 2017), H3K27ac and H3K4me1 ChIP-seq datasets from our group, as well as RNA-seq datasets in wild-type untreated endoderm samples from our group (Hörmanseder et al., 2017). As a starting point, we used p300-peaks and classified them into promoter and non-promoter peaks (at least 500 bp away from the promoter), which we considered putative enhancers (Figure 32). Furthermore, this classification was supported by the presence of transcripts from the promoter sequences and a lack of it from non-promoter sequences, as well as the presence of a detectable H3K4me1 signal on non-promoter p300-sites. To define a subset of putative *active* enhancers, we intersected the p300 non-promoter peak set with

a set of non-promoter H3K27ac broad peaks, resulting in a set of 1306 predicted active enhancers.

To assign the predicted active enhancers to their putative target genes, we used a proximity-based approach following a previously published workflow (Ing-Simmons, 2021), with the following criteria: (i) the potential target gene is actively expressed in neurula-stage endoderm (TPM >1), (ii) enhancers overlapping a gene body were assigned to that gene, (iii) enhancers overlapping more than one gene or not overlapping any genes were assigned to the nearest promoter. Therefore, putative active enhancers were paired with 1066 target genes.

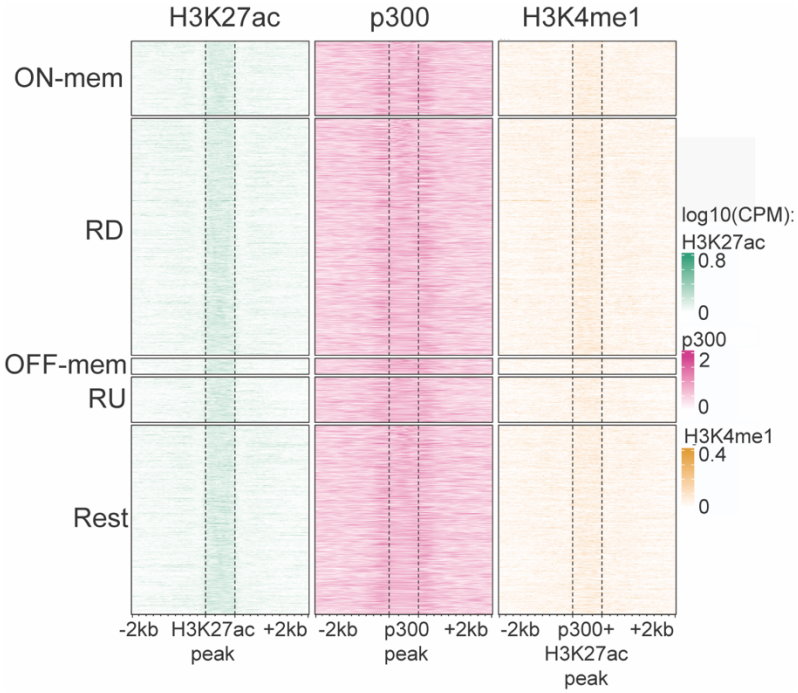

Figure 32: Heatmap showing H3K27ac, p300 and H3K4me1 signal on predicted enhancers, clustered for ON-memory, OFF-memory, reprogrammed-down and reprogrammed-up genes. Color keys indicate log2 counts per million (CPM).

I described earlier that ON-memory genes demonstrate elevated H3K27ac levels around their TSS compared to reprogrammed-down genes (Figure 7 A,C). Therefore, I wondered if H3K27ac on predicted enhancers, or active enhancers, can also distinguish ON-memory from reprogrammed-down genes. Using the set of putative enhancers defined by p300-peaks outside of promoters, I found significantly higher H3K27ac levels for such enhancers paired to ON-memory genes compared to reprogrammed-down genes (Figure 33 A). Furthermore, using the set of active enhancers defined by the presence of both p300 and H3K27ac peaks, I observed stronger enrichment of H3K27ac levels on enhancers proximal to ON-memory genes compared to reprogrammed-down

genes (Figure 33B). Thus, this hinted that H3K27ac on enhancers may also be involved in mediating transcriptional ON-memory.

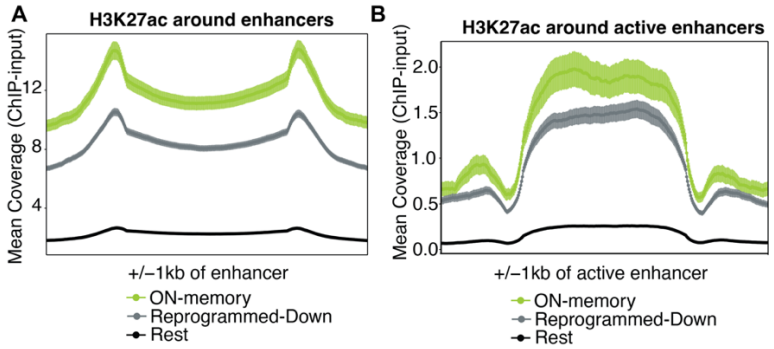

Figure 33: H3K27ac ChIP-seq data generated from wildtype neurula-stage endoderm donor nuclei depicted as coverage around predicted enhancers. (A) Meta plot of H3K27ac around p300-peaks outside of promoters, i.e. predicted enhancers, depicting log2-transformed mean intensities of H3K27ac ChIP minus input spanning 1 kb upstream and 1 kb downstream of the p300-peak. (B) Meta plot of H3K27ac around p300 peaks overlapping with broad H3K27ac peaks outside of promoters, i.e. predicted *active* enhancers, depicting log2-transformed mean intensities of H3K27ac ChIP minus input spanning 1 kb upstream and 1 kb downstream of the p300/H3K27ac-peak. (A-B) Enhancers were divided in groups based on gene sets they were paired to: ON-memory (green), Reprogrammed-Down (gray), Rest (black).

Next, I asked if memory genes and reprogrammed genes are enriched for genes proximal to enhancers, defined based on p300-peaks outside of promoters when compared to all genes detected in endoderm tissues from neurula-stage *Xenopus* embryos. Using enrichment analysis, I found that both memory-class and reprogrammed genes were significantly enriched in enhancer-gene pairs, including OFF-memory and reprogrammed-up genes, which also include genes that are lowly or not expressed in endoderm donor tissues (Figure 34A). However, the highest odds ratios were calculated for ON-memory genes and reprogrammed-down genes, indicating that these gene sets were most frequently found to be proximal to a p300-peak outside of their promoters. This finding is expected given their active expression in endoderm donor samples, potentially regulated by an enhancer.

As p300 alone is not an optimal predictor of enhancers in the genome (Holmqvist & Mannervik, 2013), I further analyzed the set of predicted *active* enhancers and tested if memory class and reprogrammed genes show enrichment for enhancer-proximal genes compared to all genes. Interestingly, I found that both ON-memory and reprogrammed-down genes were enriched for enhancer-gene pairs, in line with the active expression of these gene sets in the donor nucleus (Figure 34A). The groups of OFF-memory and reprogrammed-up genes, which also contain lowly expressed or not expressed in the donor cells, were not enriched in enhancer-gene pairs. Comparing reprogrammed-down

and ON-memory genes, I observed that ON-memory genes had a higher proportion of enhancer-paired genes compared to reprogrammed-down genes (Figure 34B), hinting that the proximity to an active enhancer could be a feature of ON-memory genes.

I then asked if the ON-memory genes that became permissive to reprogramming upon p300/CBP inhibition in donor nuclei, so-called 'treatment-sensitive' genes, were enriched for enhancer-proximal genes (Figure 34B). I performed such analysis using the sets of genes rendered permissive to reprogramming by either CBP30, i.e. CBP30-sensitive genes, or A-485, i.e. A-485-sensitive genes. Interestingly, I found that a third of the CBP30-sensitive genes were proximal to an active enhancer, while this was true for less than 10% of the A-485-sensitive genes (Figure 34B). This suggested that the genes sensitive to CBP30 treatment were more frequently proximal to an enhancer, which could suggest that the p300/CBP bromodomain inhibitor targeted H3K27ac on enhancers as suggested by previous studies (Raisner et al., 2018). This prompted me to hypothesize that, while both treatments resulted in similar transcriptome phenotypes, they may have perturbed H3K27ac on distinct genomic regions, warranting further genome-wide survey of H3K27ac occupancy under p300/CBP perturbed conditions. The experimental approach and results aiming to address this hypothesis are presented in Section 5.4.3. below.

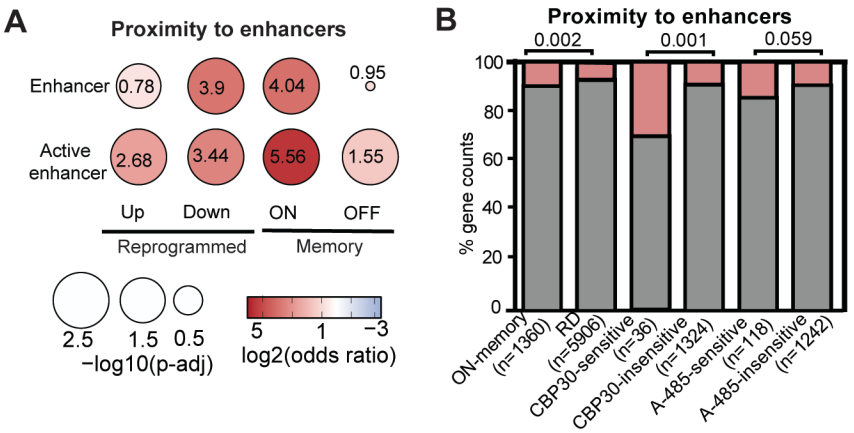

Figure 34: **CBP30-sensitive ON-memory genes are enriched for enhancer-proximal genes.** (A) Balloon plot comparing enrichment of enhancer-proximal reprogramming genes vs. all genes in endoderm nuclei. Balloon sizes represent p-adj; colors represent the log2 odds ratio. Balloons are labeled with the raw odds ratio of each comparison. (B) Proportions of ON-memory and RD genes proximal (pink) or not proximal (gray) to an active enhancer, as well as between CBP30-sensitive (n=36 genes) and CBP30-insensitive genes (n=1324 genes), and A485-sensitive (n=118 genes) and A485-insensitive genes (n=1242 genes). (A-B) Enrichment testing was performed using two-sided Fisher's text and p-values were corrected for multiple comparisons using the Benjamini-Hochberg method.

4.4.3. Genome-wide analysis of candidate histone modifications in p300/CBP bromodomain inhibitor-treated endoderm cells

In the previous chapter, I described that H3K27ac levels are enriched on putative enhancer sequences proximal to ON-memory genes compared to reprogrammed-down genes. Furthermore, I observed that CBP30-sensitive genes, i.e. genes that became permissive to reprogramming upon CBP30 treatment in donor nuclei, were significantly enriched for enhancer-proximal genes compared to genes that remained reprogramming-resistant upon CBP30 treatment. With this in mind, and my ChIP-qPCR results indicating that H3K27ac levels were decreased on the promoters of both CBP30-sensitive and insensitive genes, I wondered if the loss of ON-memory status of genes could be explained by perturbed H3K27ac levels on enhancers upon p300/CBP bromodomain inhibition.

To address this question, I performed CUT&RUN against H3K27ac in endoderm donor nuclei treated with DMSO or CBP30 (Figure 35A). As a reference peak set for sampling H3K27ac reads for each condition and performing subsequent differential peak analysis, we used the p300-peak set described above (Stevens et al., 2017), including promoter and non-promoter p300-peaks. Pairwise comparison between DMSO and CBP30 samples revealed 1291 p300-peaks (p-value<0.05), for which H3K27ac levels were decreased upon CBP30-treatment, and 871 peaks for which H3K27ac levels were increased (Figure 35B). Most of the differentially abundant p300-peaks were outside promoters (Figure 35C). Interestingly, when I divided the differentially abundant p300-peaks into peaks with decreased H3K27ac or increased H3K27ac levels upon CBP30-treatment, I observed that the vast majority (94,3%) of the p300-peaks with decreased H3K27ac levels were located on putative enhancers defined by non-promoter p300-peaks, while 40,6% of the p300-peaks with increased H3K27ac levels were located around promoters. This result suggests that CBP30 treatment mostly reduced H3K27ac on enhancers.

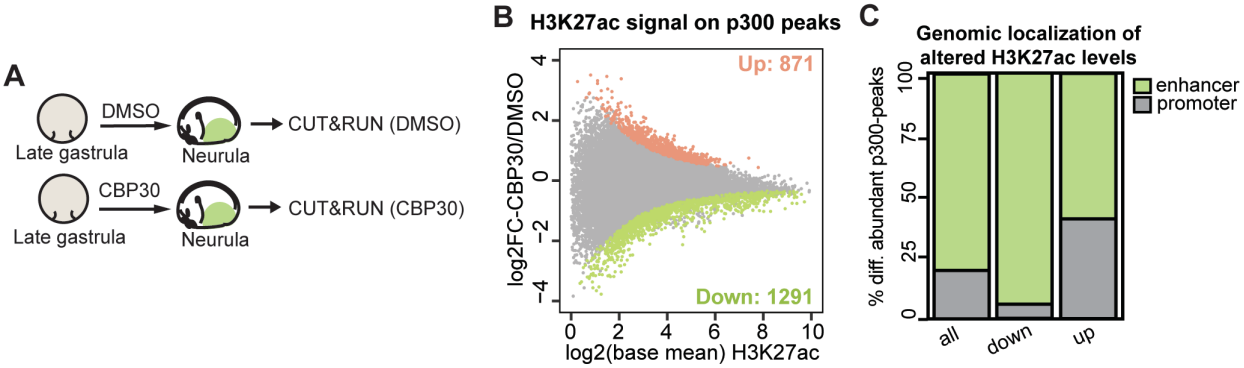

Figure 35: Genome-wide analysis of H3K27ac changes upon CBP30 treatment in endoderm donor nuclei. (A) CUT&RUN in donor embryos treated with DMSO or CBP30. Endoderm tissues (green) were isolated for CUT&RUN against H3K27ac. (B) MA-plot comparing H3K27ac levels in donor(CBP30) vs. donor(DMSO) endoderm on p300-peaks. Y-axis: mean log2FC (CBP30/DMSO); x-axis: base mean H3K27ac. Gray: all p300-peaks; green: p300-peaks with decreased H3K27ac levels (p-value <0.05), orange: p300-peaks with increased H3K27ac levels (p-value <0.05). (C) Genomic distribution of 2162 differentially abundant (DA) p300-peaks with H3K27ac, of which 1291 DA p300-peaks with decreased and 871 p300-peaks with increased H3K27ac levels on enhancers (green) or promoters (gray).

To further investigate the correlation between changes in H3K27ac changes in donor nuclei and the reduced ON-memory expression in NT embryos, I focused my analysis on p300-marked *cis*-regulatory elements around ON-memory genes. Thus, I performed correlation analyses comparing the ON-memory gene expression changes between NT(CBP30) and NT(DMSO) and the changes in H3K27ac levels between donor(CBP30) and donor(DMSO). Under CBP30 conditions, changes in H3K27ac levels on promoters in donor cells did not correlate with ON-memory gene expression changes in NT(CBP30) *vs.* NT(DMSO) (

Figure 36A). On the other hand, I detected a positive correlation between CBP30-induced H3K27ac reduction on active enhancers and reduced ON-memory expression in NT(CBP30) expression (

Figure 36A). In contrast, changes in H3K27ac levels on either promoters or enhancers did not reveal any significant correlation with gene expression changes in donor(CBP30) nuclei (

Figure 36A). As a control, I performed the same correlation analysis, but using the set of reprogrammed-down genes, for which we did not detect any correlation between changes in H3K27ac in donor nuclei and gene expression in NT embryos (

Figure 36B). Thus, I observed that perturbing H3K27ac levels in donor nuclei does not correlate with ON-memory gene expression changes in donor(CBP30) cells but rather correlates with gene expression changes upon reprogramming, as detected in NT(CBP30) embryos.

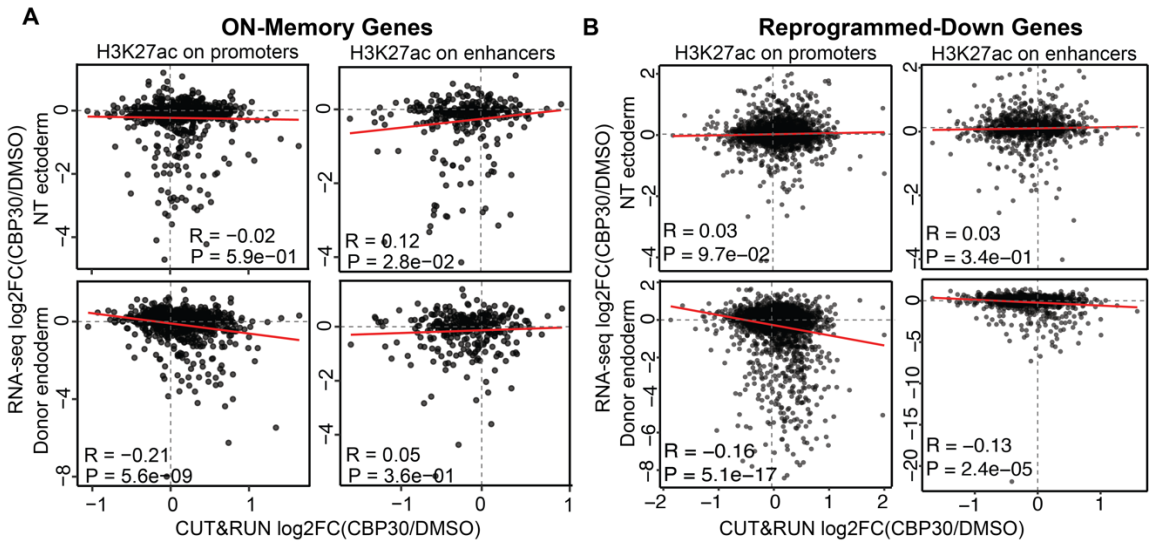

Figure 36: Changes in H3K27ac levels on enhancers upon CBP30 treatment in endoderm donor nuclei correlate with ON-memory, but not Reprogrammed-Down gene expression changes in the ectoderm of NT(CBP30) embryos. (A-B) Scatter plots comparing the log2FC in (A) ON-memory or (B) Reprogrammed-Down gene expression for NT(CBP30/DMSO) or donor(CBP30/DMSO), against log2FC in H3K27ac signal for donor(CBP30/DMSO) on promoters and active enhancers. Pearson's correlation coefficients and p-values are shown within each box.

Having observed a correlation between CBP30-mediated H3K27ac changes on enhancers and ON-memory gene expression changes in NT(CBP30) embryos, I asked if distinct subsets of ON-memory genes displayed distinct changes in H3K27ac levels. Thus, we classified ON-memory genes based on their gene expression changes in NT(CBP30) vs. NT(DMSO) embryos and donor(CBP30) vs. donor(DMSO) embryos. Enrichment analysis revealed a significant overrepresentation of enhancers with decreased H3K27ac levels within the ON-memory gene set that was downregulated in NT(CBP30) *vs.* NT(DMSO) embryos (log2FC < -1) (Figure 37A). I then performed these enrichment analyses comparing enhancers with reduced H3K27ac levels to differentially expressed genes in donor samples (CBP30 *vs*. DMSO). I did not detect any significant enrichment, suggesting that, upon CBP30 treatment, changes in H3K27ac levels around enhancers of genes in donor cells are not indicative of changes in their expression levels before reprogramming (Figure 37A). Instead, the CBP30-induced decrease in H3K27ac levels around enhancers is indicative of gene expression changes in their target genes only after reprogramming in NT embryos. When we focused on the set of 'CBP30-sensitive' genes (NT(CBP30) *vs.* NT(DMSO) p-adj<0.05), I found the strongest enrichment for genes paired to enhancers with reduced H3K27ac levels upon CBP30-treatment in donor nuclei (Figure 37A). This hinted that the reduction of H3K27ac levels on putative enhancers via p300/CBP bromodomain inhibition could underlie the loss of ON-memory status in nuclear reprogramming.

Next, I compared the H3K27ac levels on gene regulatory elements around CBP30-sensitive and insensitive genes in DMSO and CBP30-treated samples, focusing on putative enhancers and promoters (Figure 37B-E). I observed significantly reduced H3K27ac signal in CBP30 samples on enhancers associated with 'CBP30-sensitive' ON-memory genes (Figure 37 B). While H3K27ac levels were also moderately decreased on enhancers associated with 'CBP30-insensitive' genes, this difference was non-significant (Figure 37 B). I also observed a mild decrease in H3K27ac levels on enhancers associated with reprogrammed-down genes or other genes, yet to a lower extent than for the set of peaks proximal to 'CBP30-sensitive' genes (Figure 37 B). On promoters, I observed a mild increase in H3K27ac for CBP30-insensitive, reprogrammed-down and rest genes, which was non-significant, while the average H3K27ac signal on the promoters of CBP30-sensitive genes remained unaltered (Figure 37 C). Together, this suggests that CBP30 treatment reduces H3K27ac levels around putative enhancers of a set of ON-memory genes and renders them permissive to reprogramming.

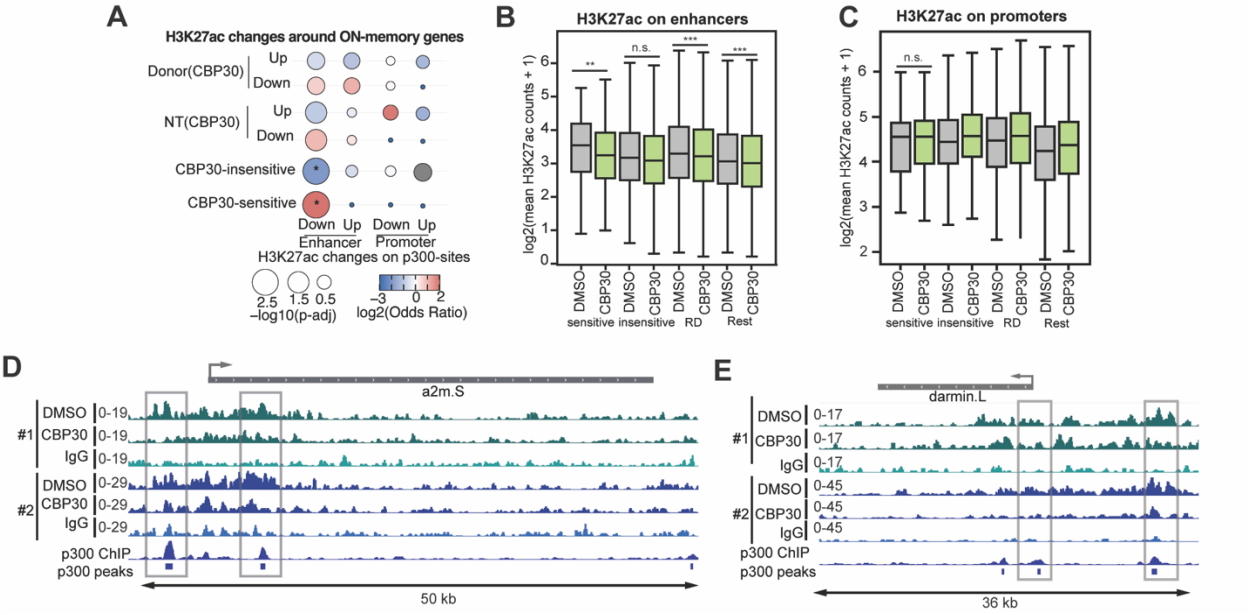

Figure 37: CBP30 treatment in endoderm donor nuclei correlates with decreased H3K27ac levels on enhancers (A) Balloon plot comparing subsets of ON-memory genes based on gene expression changes in donor(CBP30/DMSO), or in NT(CBP30/DMSO), against changes in H3K27ac levels on promoters or enhancers. Balloon sizes: -log10 p-adj; colors: log2 odds ratio. (B) Boxplot comparing H3K27ac levels in donor(DMSO) and donor(CBP30) on enhancers proximal to treatment-sensitive ON-memory genes (n=157 peaks, p-value = 0.03), treatment-insensitive ON-memory genes (n=4647, p-value = 10^{-5}), RD genes (n=14841, p-value =1.09×10^{-9}), and Rest (n=33256, p-value = 3.74×10^{-16}). Wilcoxon rank-sum test. (C) Boxplot comparing H3K27ac levels between donor(DMSO) and donor(CBP30) on promoters proximal to treatment-sensitive ON-memory genes (n= 23 peaks, p-value = n.s.), treatment-insensitive ON-memory genes (n= 741, p-value = 0.001), RD genes (n= 2654, p-value = 8.32×10-6), and Rest (n= 8993, p-value = 1.67×10-20). (D-E) Genome browser snapshots for the ON-memory genes *a2m.S* and *darmin.L*.

Furthermore, I tested if CBP30 treatment affected the genomic distribution of other candidate histone modifications in endoderm donor nuclei. To this end, I performed CUT&RUN as described for H3K27ac and profiled H3K4me3, which was previously reported to be an ON-memory mark (Hörmanseder et al., 2017), H3K4me1 which was predicted as a mark of a subset of ON-memory genes by our Digital Reprogramming analysis (Janeva et al., 2025), as well as H3K9ac for which I detected decreased levels in CBP30-treated samples via Western Blot (Figure 13).

To address the histone modification changes in endoderm donor nuclei, I used the reference peak set based on p300-peaks as described above and compared the histone modification levels on peaks associated with CBP30-sensitive, CBP30-insensitive, reprogrammed-down and other genes. When comparing H3K4me3 levels around the promoters of these gene sets, I did not find any significant difference between p300-marked promoters of CBP30-sensitive genes in DMSO versus CBP30-treated donor nuclei (Figure 38). When comparing the H3K4me3 levels on promoters for CBP30-insensitive, reprogrammed-down and Rest genes, I found moderately increased H3K4me3 levels on the promoters (Figure 38A). Interestingly, I observed that CBP30-insensitive genes had significantly higher levels of H3K4me3 on their promoters compared to CBP30-sensitive genes (Figure 38A). The latter group of genes demonstrated a significantly lower H3K4me3 signal on promoters compared to reprogrammed-down genes, suggesting that elevated H3K4me3 levels on promoters of ON-memory genes mark a subset of genes that remains reprogramming-resistant upon CBP30-treatment in donor nuclei.

I further analyzed the correlation between changes in H3K4me3 levels in CBP30-treated vs. DMSO-control donor nuclei and gene expression changes in donor(CBP30 vs. DMSO), as well as NT(CBP30 vs. DMSO) samples (Figure 38B). H3K4me3 changes in donor nuclei showed no correlation with gene expression changes upon CBP30 treatment in donor nuclei. Interestingly, I found that the log2-fold change in H3K4me3 signal positively, albeit weakly, correlated with gene expression changes in NT(CBP30 vs. DMSO) samples (Figure 38B). These findings, together with Hörmanseder et al. 2017, imply that H3K4me3 could be the primary chromatin modification on promoters which participates in ON-memory maintenance, while H3K27ac on enhancers plays an additional role.

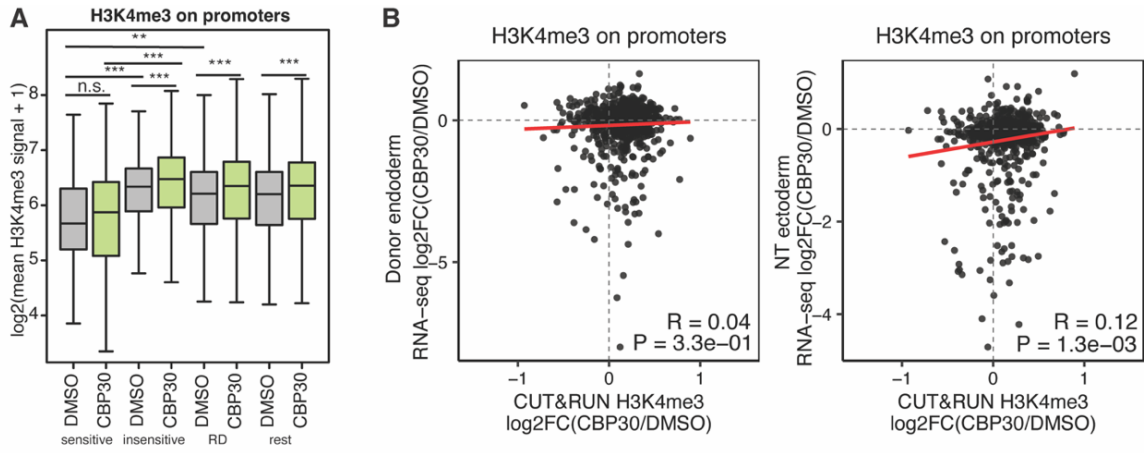

Figure 38: H3K4me3 modification on promoters correlates with gene expression changes during nuclear reprogramming. (A) Boxplot comparing H3K4me3 levels on promoters of CBP30-sensitive, CBP30-insensitive, reprogrammed-down (RD), and rest genes in DMSO and CBP30-treated donor nuclei. Note the significantly higher H3K4me3 levels on promoters of CBP30-insensitive genes compared to CBP30-sensitive genes (***p < 0.001). (B) Correlation analysis between log2FC of H3K4me3 signal in donor nuclei (CBP30/DMSO) and log2FC of gene expression in donor endoderm (left) or NT ectoderm (right). H3K4me3 changes show a weak but significant positive correlation (R = 0.12, p = 1.3e-03) with gene expression changes in NT embryos but not in donor cells.

I further compared H3K4me1 levels in DMSO and CBP30-treated donor endoderm nuclei, focusing on p300-sites outside of promoters, and did not detect any significant differences when comparing putative enhancer sites associated with CBP30-sensitive or CBP30-insensitive genes (Figure 39A-B).

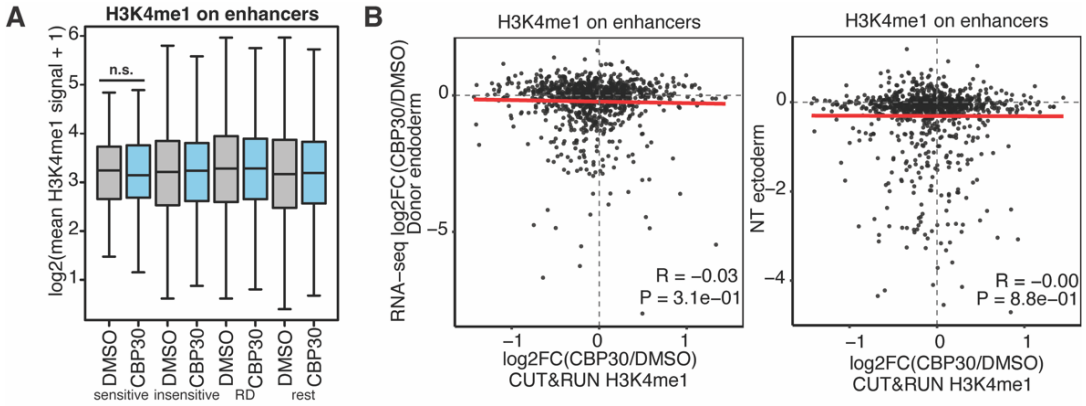

Figure 39: H3K4me1 levels on enhancers remain unchanged upon CBP30 treatment. (A) Boxplot comparing H3K4me1 levels on putative enhancers (p300-sites outside promoters) associated with CBP30-sensitive, CBP30-insensitive, reprogrammed-down (RD), and rest genes in DMSO and CBP30-treated donor nuclei. No significant differences were observed between any of the analyzed groups. (B) Correlation analysis between log2FC of H3K4me1 signal on enhancers

(CBP30/DMSO) and log2FC of gene expression in donor endoderm (left) or NT ectoderm (right). No significant correlations were detected between H3K4me1 changes and gene expression changes in either donor or NT samples.

Finally, I compared H3K9ac levels on promoter and non-promoter p300-sites in DMSO and CBP30-samples. When comparing H3K9ac levels on the promoters of CBP30-sensitive ON-memory genes in DMSO *vs.* CBP30, I found decreased H3K9ac levels, albeit statistically non-significant (Figure 40A). I detected a similar trend for CBP30-insensitive, reprogrammed-down and rest genes (Figure 40A). Interestingly, the promoters of CBP30-insensitive genes demonstrated elevated H3K9ac levels on their promoters compared to CBP30-sensitive genes, but similar levels compared to reprogrammed-down genes (Figure 40A). When comparing H3K9ac levels on enhancers, I found a mild increase across enhancers proximal to all analyzed gene sets, albeit non-significant (Figure 40B). When analyzing the correlation between changes in H3K9ac levels and gene expression changes in donor and NT samples, I only detected a correlation between changes in H3K9ac on putative enhancers and gene expression changes in donor nuclei, but not in NT(CBP30) samples (Figure 40C), which could suggest that changes in H3K9ac might contribute to changes in steady-state gene expression, but not in ON-memory in reprogramming.

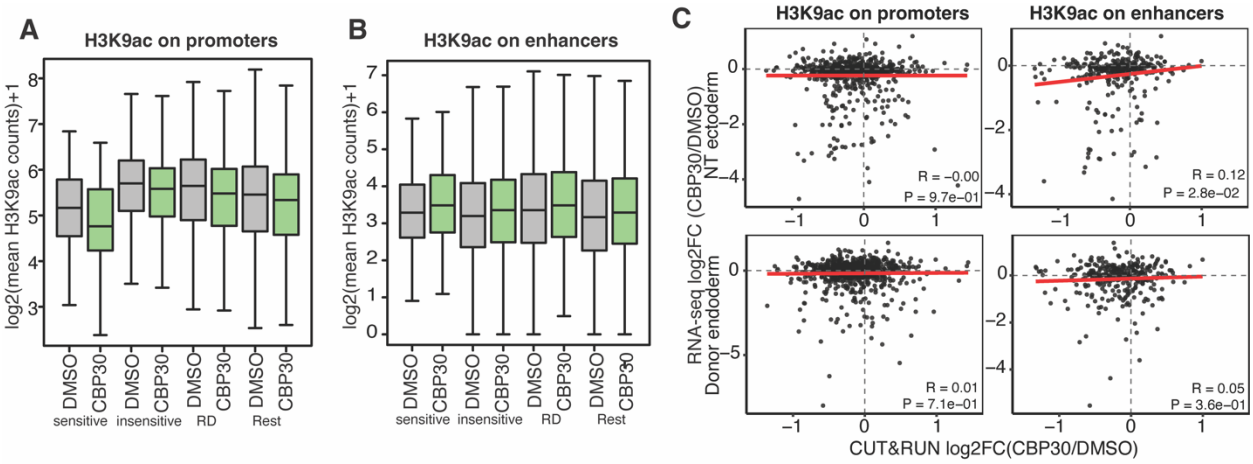

Figure 40: H3K9ac changes correlate with gene expression in donor nuclei but not in NT embryos. (A) Boxplot comparing H3K9ac levels on promoters of different gene sets in DMSO and CBP30-treated donor nuclei. (B) Boxplot comparing H3K9ac levels on putative enhancers CBP30-sensitive, CBP30-insensitive, reprogrammed-down (RD), and rest genes in DMSO and CBP30-treated donor nuclei. (C) Correlation analysis between log2FC of H3K9ac signal (CBP30/DMSO) and log2FC of gene expression in NT ectoderm (top) or donor endoderm (bottom) for promoters (left) and enhancers (right). A weak correlation was observed between H3K9ac changes on enhancers and gene expression changes in donor nuclei (R = 0.12, p = 2.8e-02) but not in NT samples.

In summary, the above-described analyses demonstrate that p300/CBP bromodomain inhibition leads to reduced H3K27ac levels at enhancers near ON-memory genes in donor nuclei, and these chromatin changes correlate with decreased ON-memory gene expression after nuclear transfer. This data further reveals that H3K4me3 levels at promoters remain relatively stable upon CBP30 treatment yet show a weak but significant correlation with gene expression changes in NT embryos. In contrast, H3K4me1 modifications at enhancers showed no significant changes upon CBP30 treatment, while H3K9ac changes correlated only with donor cell gene expression but not with ON-memory in NT embryos (

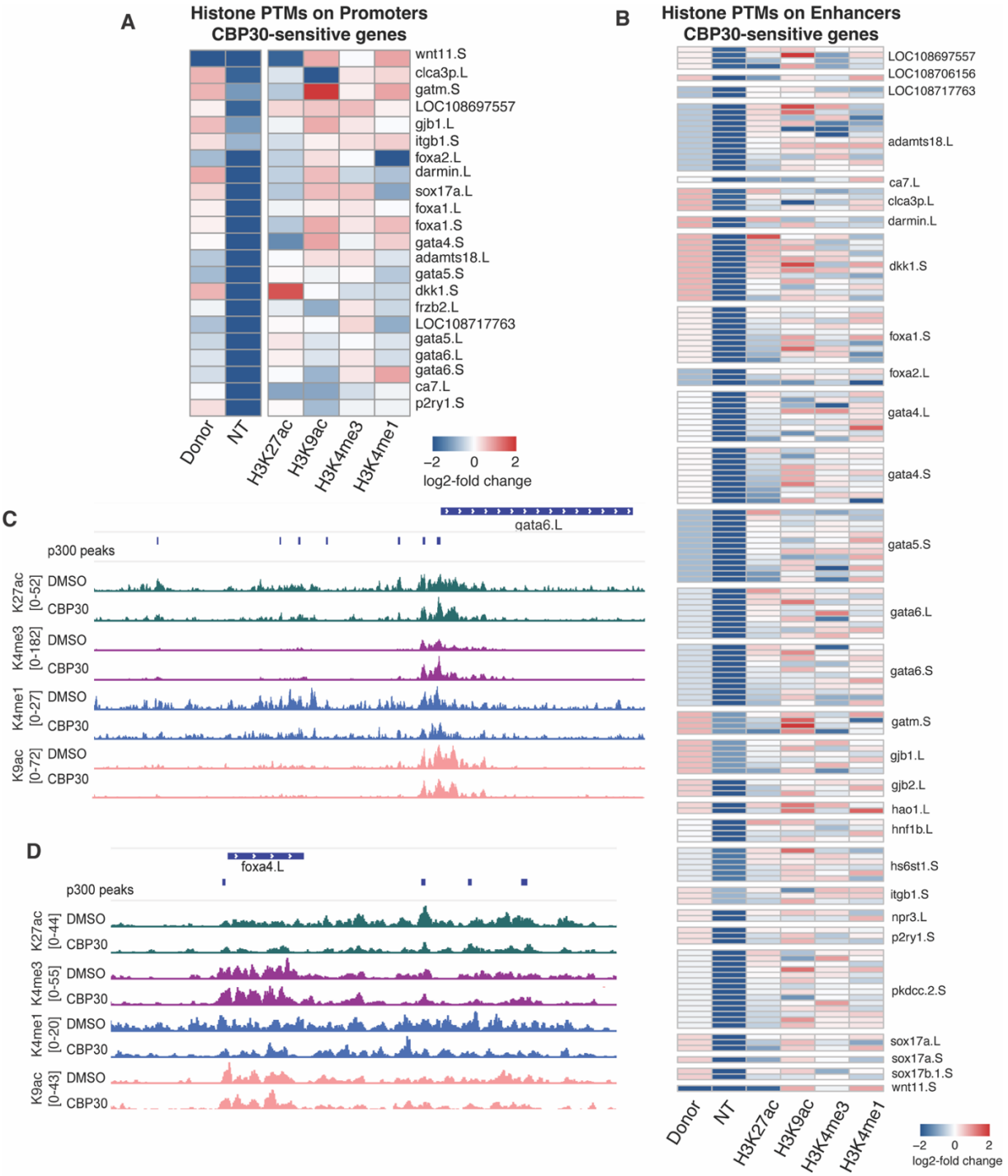

Figure *41*). Together, these findings point towards distinct contributions of H3K27ac on enhancers and H3K4me3 on promoters in the maintenance of transcriptional memory during nuclear reprogramming.

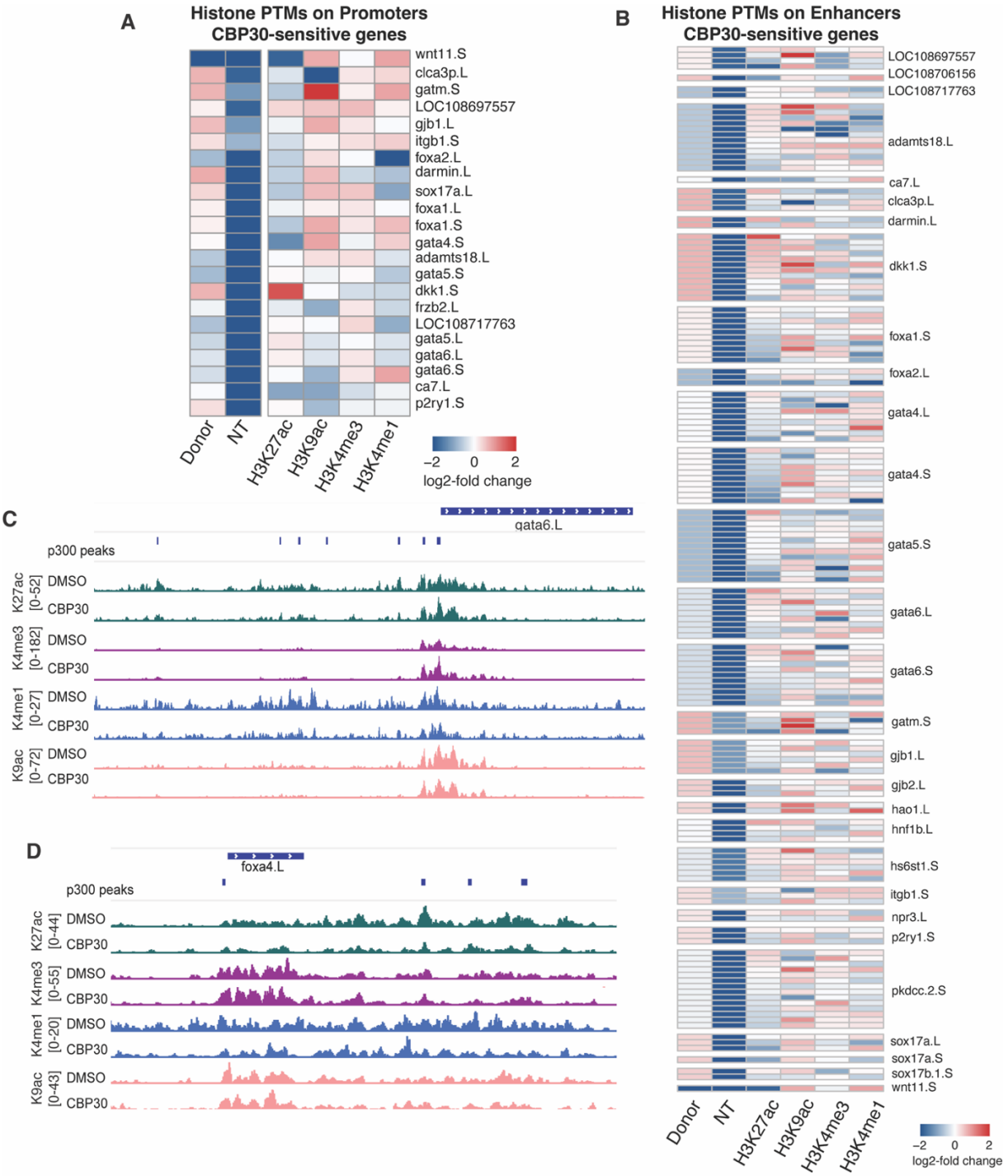

Figure 41: Histone post-translational modifications (PTMs) on regulatory elements of CBP30-sensitive genes. (A) Heatmap showing log2-fold changes in histone modifications on promoters of CBP30-sensitive genes, comparing donor nuclei, NT embryos, and various histone marks (H3K27ac, H3K9ac, H3K4me3, H3K4me1). (B) Heatmap displaying log2-fold changes in histone modifications on enhancers of CBP30-sensitive genes. (C-D) Genome browser snapshots showing signal tracks of H3K27ac, H3K4me3, H3K4me1, and H3K9ac in DMSO and CBP30-treated donor nuclei at representative loci: (C) gata6.L, a CBP30-sensitive gene and (D) foxa4.L, a CBP30-insensitive gene.

4.4.4. Genome-wide profiling of candidate histone modifications in p300/CBP HAT domain inhibitor-treated endoderm

My previous analysis revealed that similar proportions of A-485 sensitive genes are proximal to enhancers, unlike the CBP30-sensitive gene set (Figure 34). Considering that I observed a moderate but significant decrease in ON-memory expression in NT embryos from donor(CBP30) or donor(A-485) nuclei, I hypothesized that the CBP30 and A-485 treatments may have affected H3K27ac levels on distinct genomic sites in donor nuclei. Therefore, I performed CUT&RUN for DMSO and A-485 treated endoderm donor nuclei as described above and analyzed the differential occupancy of H3K27ac using the set of p300-peaks from Stevens *et al.* (2017) as the reference peak set.

To obtain a global view of the H3K27ac binding around p300-sites under DMSO, CBP30 and A-485 conditions, I performed principal component analysis (Figure 42). When comparing DMSO and CBP30 samples, I observed clear separation along PC1, with one of the replicates separating from the other three and grouping closer to the control samples. On the other hand, three of the four replicates from A-485 conditions grouped closer to DMSO samples, suggesting that the global differences in H3K27ac occupancy around p300-sites may not be as prominent as for CBP30 samples.

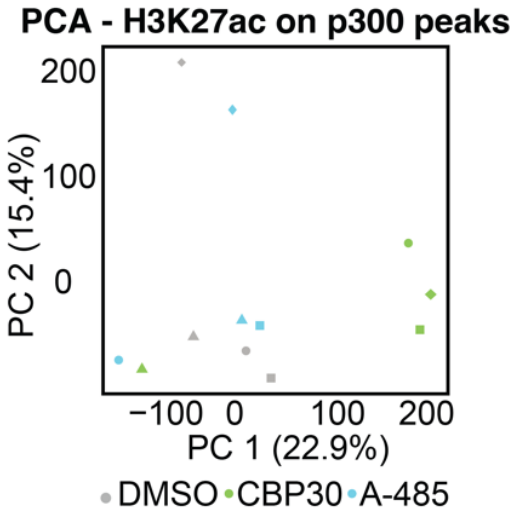

Figure 42: Principal component analysis comparing H3K27ac counts sampled on p300-peaks genome-wide for DMSO, CBP30 and A-485 endoderm donor cells. The x-axis shows PC scores of PC1 explaining 22.9% of the variance, and the y-axis shows the PC scores of PC2, explaining 15.4% of the variance. Each distinct shape of the datapoints represents an independent biological replicate. DMSO samples are shown as gray symbols, CBP30 green and A-485 blue.

Next, I performed differential peak analysis to assess the H3K27ac signal changes around p300 sites upon A-485 treatment in endoderm donor nuclei (Figure 43A). This revealed 404 p300-sites with increased and 461 sites with decreased H3K27ac levels in A-485 samples (p-value < 0.05) (Figure 43B). Furthermore, we analyzed the genomic localization of the p300-sites with altered H3K27ac levels, revealing similar proportions of promoter *versus* non-promoter peaks in the sets of p300-peaks with either increased or decreased H3K27ac levels (Figure 43C), suggesting that A-485 treatment could target histone acetylation at both enhancers and promoters.

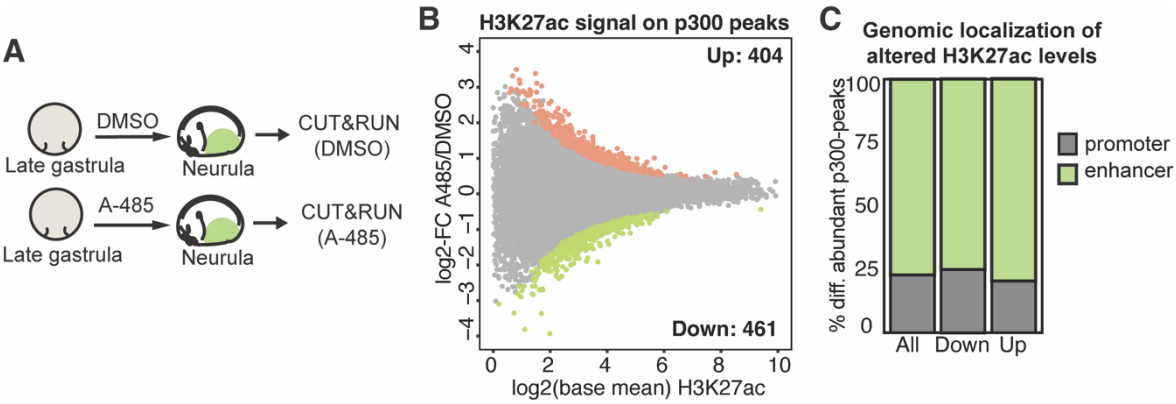

Figure 43: Genome-wide analysis of H3K27ac changes upon A-485 treatment in endoderm donor nuclei. (A) CUT&RUN in donor embryos treated with DMSO or A-485. Endoderm tissues (green) were isolated for CUT&RUN against H3K27ac. (B) MA-plot comparing H3K27ac levels in donor(A-485) vs. donor(DMSO) endoderm on p300-peaks. Y-axis: mean log2FC (A-485/DMSO); x-axis: base mean H3K27ac. Gray: all p300-peaks; green: p300-peaks with decreased H3K27ac levels (p-value <0.05), orange: p300-peaks with increased H3K27ac levels (p-value <0.05). (C) Genomic distribution of 865 differentially abundant (DA) p300-peaks with H3K27ac, of which 461 DA p300-peaks with decreased and 404 p300-peaks with increased H3K27ac levels on enhancers (green) or promoters (gray).

Furthermore, I wondered if the gene expression changes observed in donor(A-485) and NT(A-485) correlate with the changes in H3K27ac around p300-sites detected via CUT&RUN. Comparing the log2-fold change values for ON-memory genes in donor(A-485) vs. donor(DMSO) endoderm revealed a weak but positive correlation with H3K27ac changes around p300-marked promoters (

Figure *44*A). However, when comparing the ON-memory gene expression changes in NT(A-485) vs. NT(DMSO) ectoderm and the changes in H3K27ac levels on p300-marked promoters in donor(A-485) *vs*. donor(DMSO) endoderm, I did not detect any correlation. Furthermore, I did not detect any significant correlations between ON-memory gene expression in NT or donor samples when comparing them with H3K27ac changes on non-promoter p300-sites (

Figure *44*A). Similarly, I did not detect any correlations between expression changes of reprogrammed-down genes in NT or donor samples when comparing them to H3K27ac changes in donor nuclei (

Figure *44*B). Therefore, I hypothesized that the changes elicited by A-485 on these sites may be subtle and only detected when focusing on subsets of ON-memory genes.

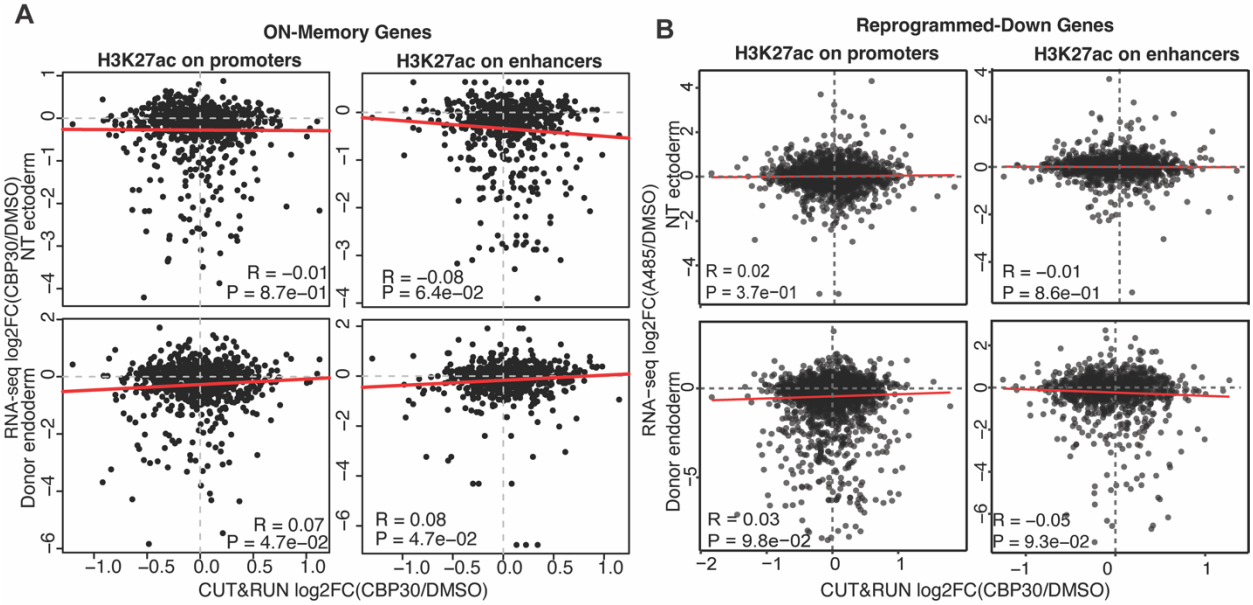

Figure 44: Changes in H3K27ac levels on enhancers upon A-485 treatment in endoderm donor nuclei do not correlate with gene expression changes in the ectoderm of NT(CBP30) embryos. (A-B) Scatter plots comparing the log2FC in (A) ON-memory or (B) Reprogrammed-Down gene expression for NT(A-485/DMSO) or donor(A-485/DMSO), against log2FC in H3K27ac signal for donor(A-485/DMSO) on promoters and active enhancers. Pearson's correlation coefficients and p-values are shown within each box.

To assess the overlap between p300-sites with altered H3K27ac levels and gene expression changes, I then classified ON-memory genes based on their gene expression changes in NT(A-485) vs. NT(DMSO) embryos and donor(A-485) vs. donor(DMSO) embryos and performed enrichment analysis (Figure 45A). This did not reveal any significant over- or under-representation of sites with altered H3K27ac among the subsets of ON-memory genes which were differentially expressed between A-485 and DMSO samples in NT and donor tissues (Figure 45A). I next compared the H3K27ac signal levels on p300-marked promoter and enhancer sites, revealing a decrease in H3K27ac on the promoters of A-485 sensitive ON-memory genes, albeit non-significant (Figure 45B). In contrast, the H3K27ac signal on the promoters of A-485 insensitive ON-memory genes and reprogrammed-down genes remained unaltered (Figure 45B). On enhancers, I did not detect any changes in H3K27ac signal upon A-485 treatment for the groups of A-485

sensitive and insensitive ON-memory genes, reprogrammed-down genes or the rest of the genes (Figure 45C). These analyses showed no significant association between A-485–induced changes in H3K27ac at p300-marked promoters or enhancers and the expression of ON-memory or reprogrammed genes, suggesting that altered H3K27ac alone cannot fully account for the transcriptional effects observed in NT embryos.

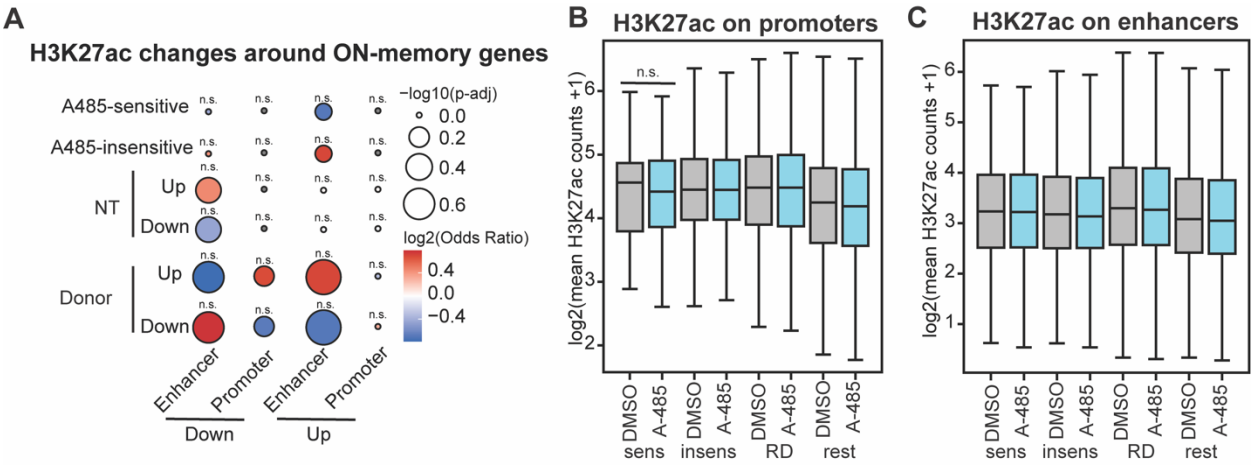

Figure 45: H3K27ac changes upon A-485 treatment in donor nuclei do not correlate with ON-memory gene expression changes in NT(A-485) embryos (A) Balloon plot comparing subsets of ON-memory genes based on gene expression changes in donor(A-485/DMSO), or in NT(A-485/DMSO), against changes in H3K27ac levels on promoters or enhancers. Balloon sizes: -log10 p-adj; colors: log2 odds ratio. (B) Boxplot comparing H3K27ac levels in donor(DMSO) and donor(A-485) on promoters of treatment-sensitive ON-memory genes (n=56 peaks), treatment-insensitive ON-memory genes (n=708), RD genes (n=14841), and Rest (n=33256). Wilcoxon rank-sum test. (C) Boxplot comparing H3K27ac levels between donor(DMSO) and donor(A-485) on enhancers proximal to treatment-sensitive ON-memory genes (n= 412 peaks, p-value = n.s.), treatment-insensitive ON-memory genes (n= 4392), RD genes (n= 2654), and Rest (n= 8993).

Taken together, the CUT&RUN analysis focusing on H3K27ac around p300-sites was not sufficient to explain the decreased ON-memory gene expression in NT embryos observed in our transcriptome analysis, thus prompting us to look into the effects of A-485 treatment on other histone modifications in endoderm donor nuclei (Figure 46).

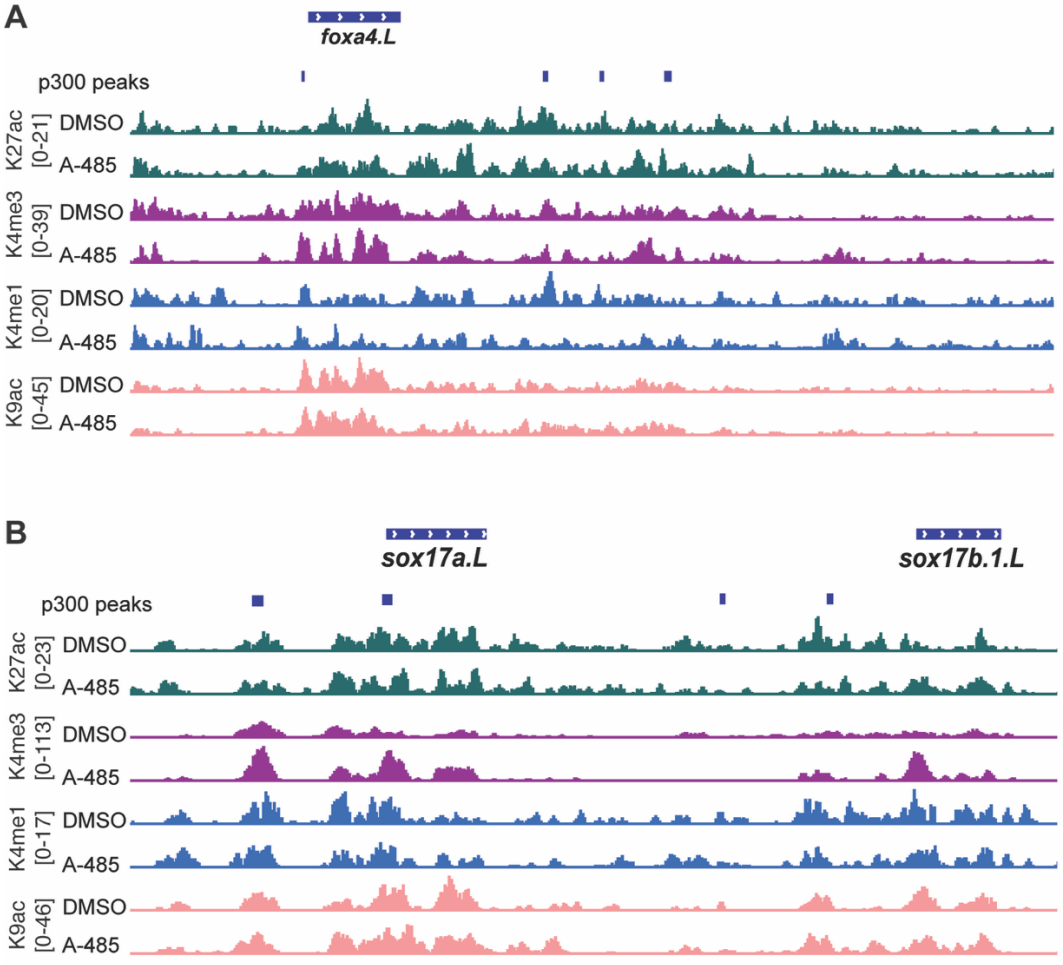

Figure 46: Analysis of histone modifications in A-485 treated endoderm donor nuclei. (A-B) Genome browser snapshots showing signal tracks of H3K27ac, H3K4me3, H3K4me1, and H3K9ac in DMSO and A-485-treated donor nuclei at representative loci: (A) *foxa4.L*, an A485-insensitive gene and (B) *sox17a.L* and *sox17b.1.L*, A-485 sensitive genes.

First, I analyzed H3K4me3 levels around the promoters of ON-memory, reprogrammed-down and rest genes. Interestingly, I found that H3K4me3 levels were increased on the promoters of A-485 insensitive, reprogrammed-down and rest genes, while H3K4me3 levels remained unaltered at the promoters of A-485 sensitive genes (Figure 47A). As observed in my CBP30-focused analysis, I also found that the genes insensitive to A-485 treatment had elevated H3K4me3 signal on the promoters compared to A-485 sensitive genes (Figure 47A). In addition, A-485 sensitive genes demonstrated lower H3K4me3 levels on their promoters compared to reprogrammed-down genes. I further analyzed the correlation between ON-memory gene expression in donor or NT samples, and changes in H3K4me3 levels on promoters. I did not detect any correlation between gene expression changes in donor nuclei and H3K4me3 signal changes upon A-485 treatment (Figure 47B). Interestingly, we found a significant positive correlation

between gene expression changes in NT(A-485) nuclei and H3K4me3 changes in donor(A-485) nuclei (Figure 47B), hinting that H3K4me3 on promoters may have contributed to maintaining reprogramming-resistant gene expression under A-485 conditions.

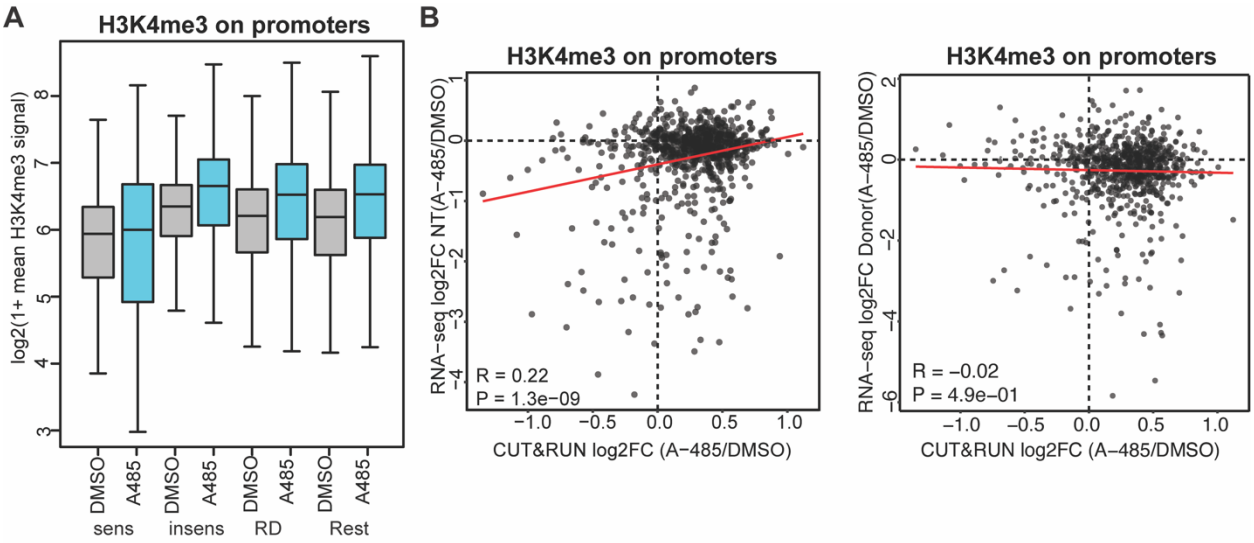

Figure 47: H3K4me3 levels do not change on the promoters of A-485 sensitive genes upon A-485 treatment in donor nuclei. (A) Boxplot comparing H3K4me3 levels in donor(DMSO) and donor(A-485) on promoters of treatment-sensitive ON-memory genes (n=56 peaks), treatment-insensitive ON-memory genes (n=708), RD genes (n=14841 peaks), and Rest (n=33256 peaks). Wilcoxon rank-sum test. (B) Scatter plots comparing the log2FC for ON-memory gene expression for NT(A-485/DMSO) or donor(A-485/DMSO), against log2FC in H3K4me3 signal for donor(A-485/DMSO) on promoters and active enhancers. Pearson's correlation coefficients and p-values are shown within each box.

Second, I analyzed the H3K4me1 levels on non-promoter p300-sites upon A-485 treatment, which did not reveal any detectable differences across the sets of A-485 sensitive, insensitive, reprogrammed-down and the rest of the genes (Figure 48).

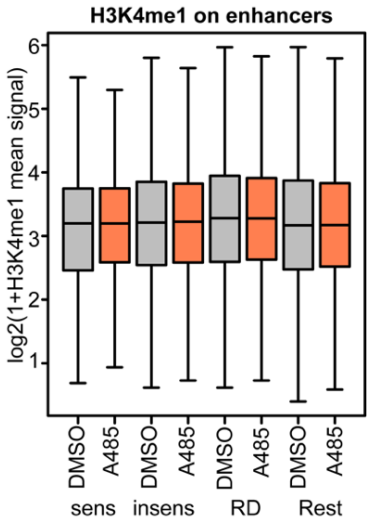

Figure 48: H3K4me1 levels on putative enhancers do not change upon A-485 treatment in donor nuclei. Boxplot comparing H3K4me1 levels around putative enhancers of ON-memory treatment-sensitive, insensitive, reprogrammed-down and rest genes. Wilcoxon rank-sum test, all pairwise comparisons n.s.

Finally, I compared H3K9ac levels on the promoters and enhancers around ON-memory, reprogrammed-down and rest genes in DMSO and A-485 samples. While the subset of A485-sensitive ON-memory genes did not reveal any difference between DMSO and A-485 on the promoters, the sets of A-485 insensitive, reprogrammed-down and rest genes revealed a mild decrease (Figure 49A). In contrast, I found mild increase in H3K9ac levels across the non-promoter sites associated with the A-485 sensitive, insensitive, reprogrammed-down and the rest of the genes (Figure 49B).

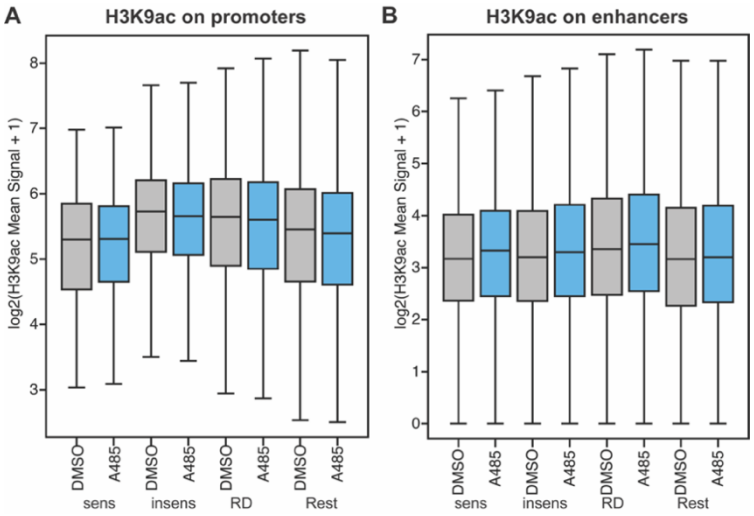

Figure 49: H3K9ac levels on promoters or putative enhancers do not change upon A-485 treatment in donor nuclei. (A-B) Boxplot comparing H3K9ac levels around (A) promoters or (B)

putative enhancers of ON-memory treatment-sensitive, insensitive, reprogrammed-down and rest genes. Wilcoxon rank-sum test, all pairwise comparisons n.s.

In summary, the CUT&RUN analysis of histone modifications, in particular H3K27ac around p300 sites in A-485 samples, was insufficient to fully explain the decreased ON-memory gene expression observed in NT embryos in our transcriptome analysis. While some correlations were identified, particularly with H3K4me3, the overall histone modification patterns upon A-485 treatment could not be linked to the findings from our transcriptome results, suggesting effects elicited by the A-485 inhibitor which have not been uncovered by the experiments in the present study.

5. Discussion and Outlook

Cell-fate reprogramming holds great promise for autologous cell replacement therapies, regenerative medicine and disease modeling, yet remains inefficient (Götz & Torres-Padilla, 2025; Gurdon & Melton, 2008; Mall & Wernig, 2017; Yamanaka & Blau, 2010). In particular, the success of somatic cell nuclear transfer is limited by epigenetic memory of the donor cell nucleus, which prevents the establishment of the correct transcriptome in the resulting cell type and maintains aberrant expression patters indicative of the donor cell type (Hörmanseder, 2021). In the present study, we leveraged a machine learning model 'Digital Reprogramming' to identify novel epigenetic marks of transcriptional memory in reprogramming, such as H3K27ac (Janeva et al., 2025). I performed *in vivo* perturbations of histone acetylation by inhibiting p300/CBP in donor nuclei before reprogramming and analyzed the transcriptome of the resulting NT embryos. Perturbing H3K27ac via p300/CBP inhibition correlated with loss of H3K27ac mainly on enhancers in donor endoderm and a moderate decrease of ON-memory gene expression in NT ectoderm. In summary, the present study points towards H3K27ac on enhancers as a novel contributor to the maintenance of active transcriptional states in reprogramming.

5.1. Generating endoderm donor nuclei with perturbed histone acetylation for nuclear transfer

To investigate the role of H3K27ac, or more broadly, histone acetylation as a barrier to the reprogramming process, we established a p300/CBP inhibitor treatment setup, that allowed me to obtain viable donor nuclei with reduced histone acetylation levels for NT. A limitation of this approach is the promiscuous nature of p300/CBP and its many substrates in a cell, including histone and non-histone proteins, such as TFs, tubulin proteins and transcriptional co-factors (Dancy & Cole, 2015; Weinert et al., 2018). Thus, it remains possible, that other substrates of p300/CBP could be affected by inhibitor treatment in donor embryos. In order to address these limitations of the pharmacological inhibition approach, I limited the duration of the inhibitor treatments to 6 hours. Moreover, I used two different p300/CBP inhibitors, which target distinct domains of the protein, the bromodomain and the catalytic HAT domain.

First, p300/CBP bromodomain inhibitors have been reported to be selective in reducing H3K27ac levels in tissue culture systems (Ebrahimi et al., 2019; Raisner et al., 2018). Raisner *et al.* used a related p300/CBP bromodomain inhibitor to CBP30 and performed histone mass-spectrometry analyzing PTMs on histones H3 and H4, revealing

a decrease in H3K27ac levels, but not other histone modifications. This is in agreement with our findings, which indicated that CBP30 treatment in donor embryos mainly reduced H3K27ac levels. A noteworthy consideration of the mass-spectrometry analyses performed by Raisner *et al.* and our group, is that only histones H3 and H4 were analyzed. In light of recent reports suggesting functional roles for p300/CBP-mediated acetylation on the N-terminus of histone H2B (Narita et al., 2021), for example, it would be important to conduct mass-spectrometry analyses in the future that includes additional core histones and histone variants. Furthermore, analyses of the cellular acetylome, i.e. analyzing all acetylated proteins in a cell, would be a compelling experiment to perform in order to understand the effects of p300/CBP bromodomain inhibition on non-histone substrates. Such analyses would comprehensively illuminate the putative off-target effects by small-molecule treatments.

It is important to note, though, that the bromodomain of p300/CBP binds acetylated histones, thereby facilitating substrate recruitment and playing a regulatory role in the further deposition of the mark and transcriptional co-factor recruitment (Dhalluin et al., 1999; Zaware & Zhou, 2019; Zeng & Zhou, 2002). Thus, by inhibiting the p300/CBP bromodomain, the recruitment of p300/CBP to chromatin may be affected and the architectural role of p300/CBP perturbed (Weinert et al., 2018). Due to this, it may be difficult to attribute any effects on reprogramming outcomes to a role of the bromodomain itself or the decrease of histone acetylation. To address this concern, I utilized A-485 (Lasko et al., 2017), an acetyl-CoA competitive inhibitor targeting the p300/CBP HAT domain. As expected, our mass-spectrometry analyses revealed broadly reduced histone acetylation levels on H3K27 and other histone H3 and H4 lysine residues. While this approach did not allow for selective targeting of H3K27ac in donor nuclei, it provided an experimental approach for testing the contribution of overall histone acetylation to transcriptional ON-memory in NT-reprogramming.

Importantly, neither of the two compounds analyzed here affected the global levels of H3K4me3, H3K4me1 or H3K36me3, which were predicted to be reprogramming barriers by our Digital Reprogramming analyses (Janeva et al., 2025). While I could not fully rule out off-target effects of the compounds used to perturb histone acetylation in donor nuclei prior to reprograming, the use of distinct classes of inhibitors, mass-spectrometry analysis and the possibility to restrict the duration of the treatment so as to obtain viable endoderm donor nuclei, provided a reasonable and feasible experimental strategy to interrogate the role of histone acetylation in the reprogramming process while minimizing confounding effects.

5.2. Transcriptome analysis revealed decreased ON-memory gene expression in NT ectoderm from perturbed donor nuclei

Taking advantage of the p300/CBP inhibitor treated embryos, we performed NT-reprogramming using endoderm donor nuclei with reduced histone acetylation. I then analyzed the ectoderm of the resulting NT embryos to quantify the aberrant expression of ON-memory genes maintained from the donor nucleus to the wrong cell type of the NT-embryo. With both modes of p300/CBP inhibition in donor nuclei, I observed a moderate decrease in the average expression of ON-memory genes and reduced counts of ON-memory genes in the ectoderm of NT embryos from perturbed donor cells. Importantly, I found that the ON-memory genes in the ectoderm of NT embryos from perturbed donors were aberrantly expressed to a lower extent than in NT embryos from control, as compared to IVF embryos as a baseline, suggesting a 'weakened' ON-memory phenotype.

Crucially, analysis of the ON-memory genes that could be rescued by p300/CBP inhibition in donor nuclei, revealed significantly reduced expression levels of key endoderm TFs, such as *sox17a*, *sox17b, gata4-6, foxa1, foxa2* and *darmin/endodermin* (Jansen et al., 2022; Mukherjee et al., 2020; Sinner et al., 2006). Previous work from our group has shown that the epigenetic status of these genes is stabilized by a broad H3K4me3 domain in the donor nucleus (Hörmanseder et al., 2017), thus mediating transcriptional memory in the NT embryo. While depletion of H3K4me3 via overexpression of the histone demethylase Kdm5b resulted in a global reduction of ON-memory and strongly improved developmental outcome of the NT embryos, the effects of p300/CBP manipulation were mild in comparison. Additionally, depleting H3K4me3 in donor nuclei also improved OFF-memory in NT embryos, which was not the case when perturbing p300/CBP in donor nuclei prior to reprogramming. I, nevertheless, observed an improvement in the developmental outcome of NT embryos from CBP30-treated donor nuclei, suggesting that improving ON-memory alone, even to a moderate extent, is beneficial for reprogramming. I suggest that the improved developmental outcome of the NT(CBP30) embryos may be due to the corrected ON-memory status of key endoderm lineage TFs. Indeed, in a recent study from our group it was shown that even the manipulation of one key ON-memory gene, *sox17b,* was sufficient to rescue the aberrant differentiation phenotype in the ectodermal linage of NT embryos (Zikmund et al., 2025). Thus, it is possible that a hierarchical relationship exists between different classes of ON-memory genes, in which the persistent expression of a set of ON-memory genes promotes the expression of downstream target genes, thus jointly forming the aberrant transcriptome of NT embryos.

While our findings demonstrate that reducing H3K27ac levels in donor nuclei via p300/CBP inhibition can improve ON-memory and developmental outcomes, this raises important questions about the broader role of histone acetylation in nuclear reprogramming. Previous approaches have taken the opposite strategy, using histone deacetylase (HDAC) inhibitors to improve reprogramming efficiency in various systems. Treatments of NT embryos and iPSCs with histone deacetylase (HDAC) inhibitors have been previously used to improve reprogramming by increasing pluripotency gene activation (G. Chen et al., 2020; Hou et al., 2014, 2014; Huangfu, Maehr, et al., 2008; Huangfu, Osafune, et al., 2008; Iager et al., 2008, 2008; Jin et al., 2017; Kretsovali et al., 2012; Mali et al., 2010; Staszkiewicz et al., 2013). It has therefore been suggested that high levels of histone acetylation are beneficial for nuclear reprogramming. This is not in conflict with our observation. I propose that reducing H3K27ac only in the donor cell, leaving the histone acetyltransferase activities unperturbed after NT, allows successful inactivation of ON-memory genes in the resulting NT embryos. A subsequent treatment of NT embryos with HDAC inhibitors may then improve the activation of OFF-memory genes during reprogramming. This hypothesis would be of interest for future experiments.

In the context of iPSC reprogramming, the p300/CBP bromodomain inhibitor CBP30 was used to reduce H3K27ac levels in fibroblasts (Ebrahimi et al., 2019). When applied during the early stages of reprogramming, CBP30 treatment decreased the expression of fibroblast-specific genes, leaving the activation of pluripotency genes unperturbed and improved iPSC reprogramming. While in iPSC reprogramming such treatments are usually applied over the course of several days and take place with ongoing transcription, it is difficult to discern, whether such a perturbation improved reprogramming due to reduced cellular memory of the somatic cell or improving the establishment of the target transcriptome. To address such questions, the *Xenopus* nuclear transfer system offers an unparalleled advantage. In fact, a key difference between NT in *Xenopus* and iPSC reprogramming is that TF-mediated reprogramming is accompanied by ongoing transcription, while early *Xenopus* embryos undergo 12 cycles of rapid cell divisions in a transcription-free window before ZGA (Hörmanseder et al., 2013; Kimelman et al., 1987). Therefore, in our experimental setup, the perturbation of p300/CBP and H3K27ac in the donor cell is achieved first. Then, using NT, a zygote with unperturbed p300/CBP activities is formed, and the cloned zygote divides several times in the absence of transcription until ZGA when transcription occurs again. Thus, by perturbing histone acetylation in the donor nuclei before reprogramming, our experimental approach allows to dissect the contribution of the donor cell chromatin state from restarting transcription in the newly formed NT embryo, in turn allowing us to scrutinize histone acetylation as a potential player in epigenetic memory.

5.3. H3K27ac-decrease on enhancers correlates with loss of ON-memory in NT-reprogramming

I detected significant H3K27ac enrichment on ON-memory gene promoters and proximal p300-sites or putative enhancers linked to ON-memory genes. Accordingly, I found that the ON-memory genes that became permissive to reprogramming upon p300/CBP bromodomain perturbation in the donor nuclei showed significant enrichment for proximity to an enhancer. Moreover, genome-wide analysis using CUT&RUN revealed depleted H3K27ac on enhancers coupled to ON-memory genes sensitive to p300/CBP bromodomain inhibition, and a positive correlation between H3K27ac levels on active enhancers, and ON-memory gene expression in NT embryos.

Recent studies (Sankar et al., 2022; T. Zhang et al., 2020) have challenged the previously attributed role of H3K27ac on active enhancers (Creyghton et al., 2010; Rada-Iglesias et al., 2011). Using histone mutagenesis, Sankar *et al*. observed minimal effects on active transcription under steady states, but only upon challenging cell identities by inducing differentiation (Sankar et al., 2022). In our system, where briefly targeting the p300/CBP bromodomain mostly led to decreased H3K27ac levels on enhancers, I found that gene expression in donor nuclei did not correlate with changes in H3K27ac levels. Only after SCNT, when I challenged the steady state by inducing nuclear reprogramming, I detected a correlation between gene expression in NT ectoderm and H3K27ac changes in the donor cell. While our approach chemically targets p300/CBP, it cannot be ruled out that there are effects due to altered chromatin accessibility or overall changes in the nuclear acetylome (Weinert et al., 2018). However, the brief treatment window and our histone mass-spectrometry data showing high selectivity for H3K27ac help minimize such off-target effects. Therefore, our results align with findings that H3K27ac perturbation has minimal impact under steady-state conditions while suggesting that H3K27ac maintains cell state stability and, when removed, introduces a vulnerability for cell fates that could be exploited for cellular reprogramming.

Our enhancer prediction approach, leveraging H3K4me1, H3K27ac, p300 binding and gene expression data, provided a solid foundation for this analysis in the *Xenopus* system (Ing-Simmons, 2021). Importantly, our approach identified genes to be putatively regulated by enhancers, such as *sox17a, sox17b, foxa4 and gata6* among others, aligning with previous reports in *Xenopus* embryos (Paraiso et al., 2019). As our enhancer identification approach mostly captured proximal enhancers and could not comprehensively identify distal enhancers, we hypothesize that distal regulatory interactions and loops between enhancers and promoters may add an additional layer of regulation in the context of transcriptional memory. It would be of interest for future studies

to perform *in vivo* experiments to identify enhancers in various tissues used as donor cells in *Xenopus* NT, such as 3D genome profiling and identification of enhancer-promoter contacts, combined with perturbation approaches, to further address the contribution of enhancers, as well as enhancer-promoter contacts in transcriptional ON-memory.

CUT&RUN analysis of donor nuclei treated with the p300/CBP bromodomain inhibitor CBP30 revealed that perturbing H3K27ac on predicted enhancers correlated with reduced ON-memory in NT embryos. Interestingly, I observed that the genes which maintained their ON-memory expression in NT embryos despite loss of H3K27ac on enhancers, displayed significantly higher H3K4me3 signal on their promoters than those that became permissive to reprogramming upon treatment. Importantly, the genes that lost ON-memory in NT embryos under CBP30 conditions maintained their expression in donor nuclei even under the treatment conditions, as reported for the reduction of H3K4me3 upon Kdm5b overexpression in donor nuclei (Hörmanseder et al., 2017). Previous work has suggested that genes essential for maintaining the lineage identity of cells may be controlled by defined chromatin states, such as broad H3K4me3/H3K27ac domains (Beacon et al., 2021; Benayoun et al., 2014; Hörmanseder et al., 2017) and enhancers (Hnisz et al., 2013; Kent et al., 2023; Paraiso et al., 2019). Thus, the present work and the work of Hörmanseder *et al.* (2017), which show that perturbing H3K27ac on enhancers and H3K4me3 on promoters allows donor cells to maintain the gene expression *status quo* in donor nuclei. However, the loss of ON-memory upon exposure to the reprogramming activities of the egg points towards H3K4me3 and H3K27ac as a synergistic mechanism maintaining cell fates. Thus, future work could address a combinatorial approach in perturbing both H3K4me3 and H3K27ac in donor nuclei and testing the reprogramming outcomes.

Surveying the p300/CBP HAT domain inhibition correlations with the observed loss of ON-memory has been less conclusive. While I observed a reduction in H3K27ac on the promoters of treatment-sensitive genes, this was statistically not significant. Moreover, I did not observe reduced H3K27ac levels on enhancers. Thus, this raises questions in light of our mass-spectrometry quantification revealing a 1.8-fold decrease in global H3K27ac levels. In part, this discrepancy can be explained by the less quantitative nature of immunoprecipitation-based chromatin profiling methods, in contrast to mass-spectrometry based quantifications of histone PTMs (K. Chen et al., 2016; Eberl et al., 2011; Han & and Garcia, 2013; Meyer & Liu, 2014). In addition, the genomic effects of A-485 treatment may have been underestimated by our approach in which the set of p300-peaks was used as a reference peak set for sampling H3K27ac signal and performing differential peak analysis and should be addressed with a different strategy. Finally, it is noteworthy that the inhibitor treatments, as well as the subsequent mass-

spectrometry and immunoblot analyses were performed on whole embryos, while CUT&RUN was performed on dissected endoderm tissues, which comprise the inner mass of the embryo. Therefore, in case of the CBP30 treatment for which we observed a better agreement of our genomic and biochemical analyses, it may be that the small molecule penetrance was overall better than for A-485, such that the reduction in H3K27ac levels measured on average in the whole embryo is greater than in the endoderm. This concern could be addressed by performing histone PTM mass-spectrometry or Western Blot analyses on dissected endoderm and ectoderm tissues from A-485 treatment and measuring the H3K27ac levels.

In summary, the present study suggests a correlation between H3K27ac on enhancers, and to some extent promoters, in donor nuclei and transcriptional memory of an active state in nuclear reprogramming. It would be of significant interest in future studies to test this correlation in a locus-specific manner by utilizing dCas9-coupled histone deacetylases (Cai et al., 2023) and targeting them to promoter and enhancer elements of ON-memory genes.

5.4. Nature *vs.* nuisance: mechanistic basis for histone acetylation and transcriptional memory?

While the present work has focused on transcriptional memory through the lens of reprogramming and has viewed it as ‘a nuisance’, its occurrence ‘in nature’ is of essence for multicellular organisms, as it ensures the maintenance of cellular identity from mother to daughter cells across generations. Indeed, dividing cells possess mechanisms that ensure the faithful propagation of transcriptional memory across cell divisions and therefore stabilize cell fates to prevent their aberrant changes (Bellec et al., 2022; Palozola et al., 2019; Stewart-Morgan et al., 2020). Thus, it is conceivable that the mechanisms that safeguard cell identities and maintain transcriptional memory pose a barrier to the successful erasure of such memories and the establishment of new cell identities (Brumbaugh et al., 2019; Hörmanseder, 2021; Nashun et al., 2015). In the following section, mechanistic possibilities for the contribution of H3K27ac to the maintenance of transcriptional memory will be discussed on the basis of existing reports in the context of mitosis and development.

Current models of transcriptional memory across mitosis describe several complementary ‘bookmarking’ mechanisms that ensure faithful reactivation of gene expression upon mitotic exit (Palozola et al., 2019). Among such mechanisms, the key described players are TFs, histone modifications or low levels of ongoing transcription

during mitosis (Gonzalez et al., 2021; Palozola et al., 2019). While global histone acetylation decreases dramatically during mitosis, emerging evidence indicates that H3K27ac exhibits locus-specific retention patterns that may serve bookmarking functions. Studies in pluripotent stem cells and other mammalian cell lines have demonstrated that H3K27ac selectively marks promoters of housekeeping genes and enhancers of cell identity genes during mitosis (Behera et al., 2019; Y. Liu et al., 2017; Palozola et al., 2019; Pelham-Webb et al., 2021). Histone methylation also contributes to the mitotic bookmarking landscape, with H3K4me3 retained on promoters and H3K4me1 on enhancers (Kang et al., 2020), potentially serving as anchors for re-establishing TADs that disassemble during mitosis (Oomen et al., 2019). Additionally, select transcription factors remain bound to mitotic chromosomes, including key cell identity factors that co-localize with H3K27ac sites (Gonzalez et al., 2021). The bookmarking function may also extend to histone-modifying enzymes themselves, as suggested by studies identifying p300 as a potential bookmarking factor at candidate promoters (M. M. Wong et al., 2014), though genome-wide confirmation of these results is lacking. Considering the complex interplay of various putatively bookmarking mechanisms, such as TFs, histone-modifying enzymes and histone modifications, it is a significant challenge to dissect the causal relationships. For instance, in the case of H3K27ac, it may be that the mark itself plays a role in reactivating transcription upon mitosis, or the persistence of TFs on chromatin may aid the recruitment of p300, thus being rapidly re-deposited (Ferrie et al., 2024). Thus, future studies addressing the question of how transcriptional memory is maintained across mitosis are necessary.

Given all this, H3K27ac may be a 'symptom' of a broader mechanism maintaining cellular memory rather than an independent player. This interpretation aligns with our observations that enriched H3K27ac levels in donor nuclei correlate with reprogramming resistance and that when perturbing it in donor nuclei, it correlates with merely a moderate improvement of reprogramming outcomes. Indeed, the persistence of this mark in specific genomic regions may reflect a more complex regulatory network that maintains cell identity across cellular transitions, which remains to be studied in the future. In the context of our NT-reprogramming model, the observed correlation between H3K27ac and transcriptional memory, despite the transcription-free window in early *Xenopus* embryos, hints at a putative transcription-independent mechanism to maintain histone acetylation and instruct aberrant memory gene expression. For instance, our previous observations in which H3K4-methylation was identified as a key player in transcriptional ON-memory in reprogramming have been followed up by the discovery that H3K4-methylation is maintained from the male gamete to the fertilized embryo in a transcription-free manner to ensure proper ZGA (Hörmanseder et al., 2017; M. Oak et al., 2025). Thus, it may be possible that a similar developmental mechanism is ‘hijacked’ by the somatic nucleus

when introduced to the egg and aberrant chromatin states are maintained in the NT embryo, ultimately resulting in aberrant transcription states after ZGA. While studies that characterize p300/CBP recruitment and activity, as well as H3K27ac profiles in the transcription-free window of *Xenopus* embryos are lacking, a recent study has reported that inhibiting HDAC1 in *Xenopus* embryos before ZGA leads to developmental arrest (J. J. Zhou et al., 2023). Moreover, Zhou *et al.* suggested that balanced acetylation is essential to maintain correct expression levels in each germ layer, thereby controlling lineage identity in developing embryos. It is conceivable that such an acetylome imbalance could be at play in the NT embryo. Testing this hypothesis would require chromatin profiling or histone mass-spectrometry in the NT embryo, which has thus far been limited by the scarce number of embryos that can be obtained via NT. It will be key to address this in the future by taking advantage of low-input approaches.

5.5. Two sides of a coin: Epigenetic memory and clinical application of reprogrammed cells

While the present study investigated epigenetic memory through the lens of a barrier that hinders reprogramming, sought to be eliminated, such epigenetic memory represents two sides of the coin when it comes to applications for regenerative medicine (Hörmanseder et al., 2021). For example, the persistent epigenetic memory of the donor cell can hinder the establishment of fully functional reprogrammed cell types of lineages unrelated to the cell of origin. Such observations have been made in mouse SCNT embryos, whereby the developmental failure of SCNT embryos was attributed to epigenetic memory (W. Liu et al., 2016), as well as in frog SCNT embryos, where our group showed that ON-memory of the endoderm cell fate can affect the differentiation potential of specific cell types in the ectoderm lineage (Zikmund et al., 2025).

Similarly, in mammalian iPSC systems, it has been shown that epigenetic memory of the somatic donor cell can bias the differentiation potential of iPSCs (Polo et al., 2010). This finding suggests that cell types of related lineages could be used to generate iPSC to be further differentiated into the desired cell type, potentially generating reprogrammed cells with high fidelity and higher resemblance to *in vivo* cell types. For example, higher success rates for generating retina cells have been reported when using iPSCs derived from rod photoreceptors, rather than fibroblast-derived cells (Hiler et al., 2015). Thus, epigenetic memory could be harnessed to streamline the production of clinically relevant cell types for tissue replacement therapies, potentially reducing the time, cost, and variability associated with directing iPSC differentiation toward unrelated lineages. Conversely, when broad multipotency is desired, or when generating cell types distant from the donor cell origin, this same epigenetic memory becomes a hindrance that must be overcome through extended culture periods or active chromatin remodeling

approaches. However, extended passaging of iPSC-lines can be a risky road to take, as it has been shown that this can introduce genomic instability (Yoshihara et al., 2017). Thus, understanding and potentially controlling the degree of epigenetic memory retention in iPSCs could enable tailored reprogramming strategies that either preserve or erase donor cell identity depending on the intended therapeutic application.

5.6. Proposed model: H3K4me3 on promoters and H3K27ac on enhancers act in concert to mediate ON-memory in reprogramming

In summary, the present work suggests that H3K27ac acts as a previously unidentified barrier to reprogramming via NT, potentially acting in synergy with H3K4me3. In previous work, perturbing H3K4-methylation in donor nuclei resulted in substantially stronger rescue of ON-memory and the developmental outcome of cloned embryos (Hörmanseder et al., 2017) when compared to p300/CBP inhibition. Moreover, the p300/CBP approach did not render all ON-memory genes permissive to reprogramming, resulting in a subset of ‘treatment-insensitive’ ON-memory genes with significantly higher H3K4me3 levels on their promoters compared to the group of ‘treatment-sensitive’ genes. Thus, we propose a hierarchical relationship between these two chromatin modifications in mediating reprogramming resistance. In this model, H3K4me3 on promoters poses the primary reprogramming barrier and mediator of ON-memory, while H3K27ac on enhancers plays a reinforcing role to stabilize the expression of a subset of ON-memory genes important for donor cell identity (Janeva et al., 2025). It would be subject of future work to address the effects of combinatorial targeting of H3K4-methylation and H3K27ac in donor nuclei on nuclear reprogramming.

6. Materials and Methods

6.1. Experimental procedures

Xenopus laevis husbandry

Adult *Xenopus Laevis* were obtained from Nasco (901 Janesville Avenue, P.O. Box 901, Fort Atkinson, WI 53538-0901, USA) and Xenopus1 (Xenopus1, Corp. 5654 Merkel Rd. Dexter, MI. 48130). All frog maintenance and care were conducted according to the German Animal Welfare Act. Research animals were used following guidelines approved and licensed by ROB-55.2-2532.Vet_02-23-126.

Inducing ovulation in *Xenopus laevis* females

To induce egg-laying in *Xenopus laevis* females, a low dose of the human chorionic gonadotropin (hCG) hormone (45 U per frog) was injected into the dorsal lymph sack 3-5 days prior to the time point when egg-laying is needed, followed by injection with an inductive dose of the hCG hormone (500 U per frog) 14-17 hours before egg-laying (Sive et al., 2000). The frogs were then kept at 16°C overnight. For egg collection, female frogs were kept in a high-salt solution (1x MMR: 100 mM NaCl, 2 mM KCl, 1 mM MgSO4, 2 mM CaCl2, 0.1 mM EDTA, 5 mM HEPES (pH 7.8)) and allowed to release the eggs naturally, without manual agitation.

Testis collection from *Xenopus laevis*

Sexually mature males from *X. laevis* were sacrificed using an overdose of the anesthetic tricaine. Testis was collected by dissection.

In vitro fertilization (IVF)

Eggs were *in vitro* fertilized by mixing with a sperm slurry in a Petri dish, incubating for 2 min at RT and flooding with distilled water, then dejellied using 2% cysteine solution pH 7.8 (adjusted using NaOH), washed 3 times with 0.1x MMR and transferred into 0.1x MMR for culturing until the desired stage for endoderm donor cell preparation.

p300/CBP inhibitor treatments

IVF-derived gastrulae (NF stage 12) were treated with 40 µM SGC-CBP30 (Sigma, SML1133), 30 µM A-485 (Tocris, #6387) or DMSO in 0.1x MMR at 23°C until they

reached neurula stage (stage 18). The embryos were collected at synchronized stages to eliminate influences from different cell numbers or developmental stages. The embryos were either used as donors for nuclear transfer as described above, or frozen for further experiments.

Donor cell preparation for Nuclear Transfer

Endoderm was dissected from neurula-stage embryos (NF stage 18) and allowed to dissociate into single cells in calcium- and magnesium-free 1x modified Barth saline (MBS, 88 mM NaCl, 1mM KCl, 10mM HEPES, 2.5 mM $NaHCO_3$, pH 7.4) with 1 mM EDTA and 0.1% BSA in a Petri dish coated with 0.1% agarose in H_2O. Donor cells were immediately used for NT.

Nuclear Transfer (NT) and embryo culture

Nuclear transfer was performed as described previously (Gurdon et al., 1958). Endoderm donor cells were partly disrupted by suction into a glass capillary needle and injected into an egg enucleated by UV exposure in a UV-crosslinker (CL-1000 Analytik Jena, exposure setting 2000). Nuclear transfer was performed immediately upon enucleating the acceptor eggs. The injected eggs were then placed in 1x MMR and the medium was changed to 0.1x MMR after cleavage of the embryos. Alongside, IVF embryos were cultured as control overnight at 16°C until they reached the blastula stage. Then, NT embryos morphologically indistinguishable from IVF controls were selected for subsequent experiments. For gene expression analyses in gastrulae, NT and IVF embryos with the same blastopore size were selected to ensure equal developmental stages. The embryonic ectoderm (animal cap) was excised from each embryo and snap-frozen on dry ice for RNA isolation (Hörmanseder et al., 2017). To score the developmental outcome, the NT and IVF embryos were cultured in 0.1x MMR at 16°C until they reached the neurula stage and then at 23°C until the feeding tadpole stage.

Western Blot

Whole control and inhibitor-treated embryos were collected at NF stage 18 and lysed in 10 µl E1 buffer (50 mM HEPES-KOH pH 7.5, 140 mM NaCl, 0.1 mM EDTA pH 8.0, 10% glycerol, 0.5% Igepal CA-630, 0.25% Triton X-100, 1% beta-mercaptoethanol) per embryo and then centrifuged at 3500 rpm at 4°C for 2 min to separate the nuclear and cytosolic fraction. For chromatin extraction, the nuclear fraction (pellet) was solubilized in 10 µl E1 buffer per embryo by vigorously agitating and vortexing. Laemmli buffer (BIO-RAD, #1610747) containing 10% beta-mercaptoethanol was added, the samples were denatured at 95°C for 10 min and centrifuged at maximum speed for 10 min. The

chromatin extract was separated on a 4-20% gradient gel (BIO-RAD, Mini-PROTEAN TGX #4561096) and transferred onto a PVDF membrane (Thermo Scientific, 88518) for 1.5 h at 30 V. The membrane was blocked using 5% bovine serum albumin (BSA) and incubated overnight using 1:1000 dilution of primary antibodies against histone modifications or H4 as a loading control (see table for antibody details). Protein detection was performed using IRDye-coupled secondary antibodies (IRDye 800CW #926-68022, IRDye 680LT #926-32213, Licor) and imaged on a Licor Odyssey LT machine.

Mass-spectrometry

50 whole embryos at stage 18, pharmacologically treated as described above, were collected in a 2 ml Eppendorf tube, washed 3 times with embryo extraction buffer (10 mM HEPES-KOH pH 7.7, 100 mM KCl, 50 mM sucrose, 1 mM $MgCl_2$, 0.1 mM $CaCl_2$) by gently inverting the tube, centrifuged at 700 g for 1 min and frozen upon liquid removal at -80°C. To separate the nuclear fraction, the embryos were centrifuged for 10 min at 17000 rpm at 4°C. The nuclei (liquid phase) were carefully removed using a P200 pipette tip, while avoiding the lipids (white ring on top of the liquid phase), and transferred to a fresh Eppendorf tube. The nuclear fraction was washed twice with 500 µl SuNASP (250 mM sucrose, 75 mM NaCl, 0.5 mM spermidine, 0.15 mM spermine) and centrifuged for 5 min at 3500 g at 4°C, without disturbing the nuclear pellet. To extract the histones, the nuclei were solubilized in 600 µl RIPA buffer (50 mM Tris-HCl pH 7.4, 1% Igepal CA-630, 0.25% sodium deoxycholate, 150 mM NaCl, 1 mM EDTA, 0.1% SDS, 0.5 mM DTT, 5 mM sodium butyrate, 1x protease inhibitor) and centrifuged at 14,000 g for 10 min at 4°C. The supernatant was removed, taking care to remove excess lipids or debris. The samples were incubated on ice in 100 µl RIPA, centrifuged as described above and the supernatant was removed. The pellet containing histone extract was solubilized in 50 µl E1 buffer as described for Western Blot, mixed with Laemmli buffer, and separated on a 4-20% gradient polyacrylamide gel. Coomassie-stained bands of H3 and H4 were excised from the gels and stored in Milli-Q H_2O in 2 ml Eppendorf tubes at 4°C until mass-spectrometry analysis.

Gel pieces containing histones were washed with 100 mM ammonium bicarbonate, dehydrated with acetonitrile, chemically propionylated with propionic anhydride, and digested overnight with trypsin. Tryptic peptides were extracted sequentially with 70% acetonitrile/0.25% TFA and acetonitrile, filtered using C8-StageTips, vacuum concentrated, and reconstituted in 15µl of 0.1% FA.

For LC-MS/MS purposes, desalted peptides were injected in an Ultimate 3000 RSLCnano system (Thermo) and separated in a 25-cm analytical column (75µm ID, 1.6µm C18, IonOpticks) with a 50-min gradient from 2 to 37% acetonitrile in 0.1% formic acid. The

effluent from the HPLC was directly electrosprayed into a Qexactive HF (Thermo) operated in data-dependent mode to automatically switch between full scan MS and MS/MS acquisition with the following parameters: survey full scan MS spectra (from m/z 375–1600) were acquired with resolution R=60,000 at m/z 400 (AGC target of 3x106). The 10 most intense peptide ions with charge states between 2 and 5 were sequentially isolated to a target value of 1x105, and fragmented at 27% normalized collision energy. Typical mass spectrometric conditions were: spray voltage, 1.5 kV; no sheath and auxiliary gas flow; heated capillary temperature, 250ºC; ion selection threshold, 33.000 counts.

Data analysis was performed with Skyline (version 21.2) by using doubly and triply charged peptide masses for extracted ion chromatograms. Automatic selection of peaks was manually curated based on the relative retention times and fragmentation spectra as shown by the results from Proteome Discoverer 1.4. Integrated peak values were exported for further calculations. The relative abundance of an observed modified peptide was calculated as the percentage of the overall peptide.

Chromatin Immunoprecipitation (ChIP)

ChIP was performed as described previously (Gentsch & Smith, 2014; Hörmanseder et al., 2017) Endoderm from 75 stage 18 embryos per ChIP sample was dissected in 0.1x MMR and collected on ice in 2 ml Eppendorf tubes. The tissue was then fixed in 1% paraformaldehyde (PFA) diluted in 0.1x MMR at RT for 20 min while twisting the tube. The fixation was quenched using a glycine solution in PBS at a final concentration of 125 mM for 5 min at RT, followed by four washes with ice-cold 0.1x MMR for 5 min each under frequent twisting. Finally, the tissue was equilibrated in 500 µl ice-cold HEG (50 mM HEPES-KOH pH 7.5, 1 mM EDTA pH 8.0, 20% glycerol) solution for 5 min, the tissue was allowed to settle at the bottom of the tube, the liquid removed and frozen at -80°C.

For nuclear extraction, fixed tissue samples were allowed to thaw on ice and resuspended in 2 ml E1 buffer (50 mM HEPES-KOH pH 7.5, 140 mM NaCl, 1 mM EDTA pH 8.0, 10% glycerol, 0.5% NP40, 0.25% Triton-X, 1 M DTT, 1x protease inhibitor) to homogenize the tissue, followed by centrifugation at 3500 rpm for 2 min at 4°C. The supernatant was then removed, including the lipid fraction attached to the side of the Eppendorf tube. This step was repeated once more, and followed by 3 washing steps with E2 buffer (10 mM TRIS pH 8.0, 200 mM NaCl, 1 mM EDTA pH 8.0, 0.5 mM EGTA pH 8.0, 1x protease inhibitor), and two washing steps with E3 buffer (10 mM TRIS pH 8.0, 200 mM NaCl, 1 mM EDTA pH 8.0, 0.5 mM EGTA pH 8.0, 0.1% sodium deoxycholate, 0.5% sodium lauroylsarcosine, 1x protease inhibitor), as described. Finally, the tissue was resuspended in 700 µl E3 buffer for chromatin fragmentation via sonication. The chromatin was fragmented on a

Bioruptor Pico (Diagenode) in 15 ml conical tubes (Diagenode) for 25 cycles (30 s ON, 30 s OFF). The fragmented chromatin was transferred to fresh tubes and centrifuged for 5 min at 4°C at full speed. The chromatin supernatant fraction was collected, and 10% of the extract were set aside for the input fraction and reverse-crosslinked in 150 µl total volume of STOP buffer (40 mM TRIS pH 8.0, 10 mM EDTA pH 8.0, 1% SDS), supplemented with 0.3 µg/µl proteinase K and 7.5 µl of 5 M NaCl, at 65°C overnight under constant shaking. The samples were subsequently incubated with 3 µl of 10 mg/ml DNase-free RNase for 1 hour at 37°C. The input DNA was extracted using a Qiagen MiniElute PCR Purification Kit according to the manufacturer's instructions. Before proceeding with the ChIP reaction, the input fragment size distribution was validated on a Tape Station.

To set up the ChIP reaction, sheep anti-rabbit Dynabeads (Invitrogen) were washed and blocked with 30 µl PBS supplemented with 0.1% BSA in 30 µl per reaction for 5 min per wash on ice, followed by a wash step with buffer E2 supplemented with 1% Triton-X 100 and 1x protease inhibitors. Finally, the beads were resuspended in 25 µl buffer E2 + 1% Triton-X 100 per ChIP reaction and 25 µl of the bead solution was added to each chromatin lysate samples, followed by the addition of 2 µl antibody (anti-H3K27ac #8137 Cell Signaling Technologies). The ChIP reactions were incubated overnight at 4°C under constant rotation. The following day, the ChIP samples were washed six times with 500 µl ice-cold RIPA buffer (50 mM HEPES-KOH pH 7.5, 500 mM LiCl, 1 mM EDTA pH 8.0, 1% NP40, 0.7% sodium deoxycholate, 1x protease inhibitor), followed by two washes with 500 µl ice-cold TEN buffer (10 mM TRIS pH 8.0, 1 mM EDTA pH 8.0, 150 mM NaCl). The immunoprecipitated chromatin was then reverse cross-linked and RNase digested, as described above for the input samples, and DNA was extracted.

Chromatin Immunoprecipitation-quantitative Polymerase Chain Reaction (ChIP-qPCR)

ChIP reactions and input samples were diluted 1:20 and 4 µL were used for subsequent qPCR analysis using primer pairs described in Table 1 at 0.5 µM with iTaq Univer SYBR Green Supermix (BIO-RAD), in a two-step PCR cycle: 94°C for 15 s and 60°C for 60 s. Reactions were performed in a total volume of 20 µl.

Table 2: Primers used for ChIP-qPCR assay

Target	Forward Primer	Reverse Primer
leprot.S_TSS	AGGCAGTCCTATAAGGCCGA	CGAGTGACAGGCCGAGTAAG
hao1_TSS	TAGCGGATAACGTTGACGCA	GTATGGGGTTGTGAGGAGCC
Sox17a_Exon1	CCTCTTGCGCTCGTCCTTT	TCCGCCGACCCATGAAT

Gata5_TSS	CCGTACAGGAGAAGTGGGGT	GTGTTTGCTAAAGGTGGGACC
Foxa4_TSS	ACTGGAAGGTCTTCTTGTTGGG	TTGACTCTATTTAGCATGTTCTGGA
a2m_TSS	GCAGGGGGTGTTGTTGCTTA	TGCCAGAGACCATCGTTTGTT

Cleavage Under Target & Release Using Nuclease (CUT&RUN)

CUT&RUN was performed as described previously (Phelps et al., 2023; Skene et al., 2018), with some adjustments. For nuclear extraction, neurula stage (NF stage 18) embryos were manually devitellinized and incubated in Newport 2.0 buffer (J. A. Briggs et al., 2018) to facilitate tissue dissociation, by gently agitating the supernatant, but not disturbing the tissue. The nuclei were extracted by resuspending in 1 ml ice-cold nuclear extraction buffer (20mM HEPES-KOH, pH 7.9, 10mM KCl, 500 µM spermidine, 0.1% Triton X-100, 20% glycerol), and subsequently resuspended in 600 µl nuclear extraction buffer. 150 µl concanavalin A beads (Epicypher, 21-1401) were resuspended in 850 µl binding buffer (20 mM HEPES-KOH pH 7.9, 10 mM KCl, 1mM $CaCl_2$, 1mM $MnCl_2$) per sample and activated by washing twice with 1 ml binding buffer. The nuclei were added to 300 µl bead suspension under gentle vortexing and incubated for 10 min at RT while rotating to allow binding of the nuclei to the beads. The supernatant was discarded and the nuclei were incubated in 1 ml blocking buffer (20 mM HEPES-KOH pH 7.5, 150 mM NaCl, 0.5 mM spermidine, 0.1% BSA, 2 mM EDTA,1x protease inhibitor) for 5 min at RT, then incubated in 1:100 primary antibody solution overnight at 4°C. The following antibodies were used as primary antibodies for CUT&RUN: anti-H3K27ac #8137 Cell Signaling Technologies, anti-H3K4me3 ab8580 abcam, anti-H3K4me1 ab9995 abcam, anti-H3K9ac ab4441 abcam. Next, the antibody-bound nuclei were washed twice using 1 ml wash buffer (20 mM HEPES-KOH pH 7.5, 150 mM NaCl, 0.5 mM spermidine, 0.1% BSA, 1x protease inhibitor). To facilitate pAG-MNase (Epicypher) binding to the primary antibody, samples were incubated under rotation at 4°C for 1 h, washed twice using wash buffer and resuspended in 150 µl wash buffer. To activate the MNase digestion reaction, 3 µl 100 mM CaCl2 was added to each sample and incubated at 0°C for 30 min, then quenched using 2x STOP buffer (200 mM NaCl, 20 mM EDTA, 4 mM EGTA, 50 µg/mL RNase A, 40 µg/mL glycogen), containing 1 ng exogenous spike-in DNA (E. coli, Epicypher). To release chromatin fragments, the samples were incubated at 37°C for 20 min, following centrifugation at 16.000 g for 5 min at 4°C. The supernatant containing soluble chromatin fragments was mixed with SDS and proteinase K at 70°C for 10 min and subjected to on-column DNA purification (QIAGEN, MiniElute PCR Purification Kit).

CUT&RUN library preparation

CUT&RUN sequencing libraries were prepared using NEB Ultra II DNA library prep kit (NEB, #E7645), following the manufacturer's instructions, using 12 PCR amplification

cycles with CUT&RUN-specific cycling parameters (45 s 98°C for polymerase activation, 14 cycles of 15 s 98°C DNA melting and 10 s 60°C primer annealing and short extension, 1 min 72°C final extension), without size selection. The libraries were sequenced on a NovaSeq X+ sequencing platform.

Total ribonucleic acid (RNA) extraction

Embryonic tissues were collected, dissected, and stored at -80°C. Total RNA was isolated using the RNeasy Mini Kit (QIAGEN, 74104) according to the manufacturer's instructions. To lyse the embryonic tissue, samples were vortexed on high speed for 10 min at 4°C. DNase digestion was performed according to the manufacturer's instructions, using RNase-free DNase (QIAGEN, 79254). RNA was eluted in 35 µl nuclease-free H_2O.

mRNA-sequencing library preparation

Total RNA was quantified on a Qubit fluorometer, and the sample quality was assessed on a TapeStation before library preparation. Per sample, 400 ng total RNA of animal cap (ectoderm) tissue and 300 ng of endoderm donor tissue were used to isolate mRNA using the NEBNext Poly(A) mRNA Magnetic Isolation Module (NEB, E7490). Sequencing libraries were generated using the NEBNext Ultra II Directional RNA Library Prep Kit for Illumina (NEB, E7760), following the manufacturer's instructions, using 12-13 PCR amplification cycles. Libraries were multiplexed and sequenced on a NextSeq 6000 platform.

6.2. Bioinformatic analyses

RNA-seq Data Processing and Differential Expression Analysis

Paired sequencing reads were processed using Kallisto (v0.48) for pseudoalignment and quantification of transcript abundance. Transcript and annotation files were downloaded from Xenbase (v10.1) for *Xenopus laevis* (transcripts and annotation). After quantification, transcript-level abundances were imported using 'tximport' and converted to a 'SummarizedExperiment' object in R (v4.3.1). Datasets of two independent batches were merged and subjected to differential expression analysis performed with DESeq2 (v1.40.2).

Filtering strategy for memory class and reprogrammed genes

For RNA-seq experiments addressing the effects of p300/CBP inhibition on ON-memory, log2 fold changes (log2FC) and adjusted p-values (p-adj) were calculated using DEseq2

(Love et al., 2014). The gene lists were then filtered as follows (note that 3FC corresponds to log2FC ≈ 1.5). The filtering strategy follows (Hörmanseder et al., 2017)

Differentially expressed genes (DEG) Donor/IVF: p-adj (Donor/IVF) < 0.05
DEG Donor/IVF and NT/IVF: p-adj (Donor/IVF) < 0.05 & p-adj (NT/IVF) < 0.05
ON-memory genes: p-adj (Donor/IVF) < 0.05, log2FC (Donor/IVF) > 0, p-adj (NT/IVF) < 0.05, log2FC(NT/IVF) > 0, TPM(Donor) >1.
OFF-memory genes: p-adj (Donor/IVF) < 0.05, log2FC (Donor/IVF) < 0, p-adj (NT/IVF) < 0.05, log2FC(NT/IVF) < 0
Reprogrammed-Down: p-adj (Donor/IVF) < 0.05, log2FC (Donor/IVF) >0, p-adj (Donor/NT) < 0.05, log2FC (Donor/NT) > 0.05, TPM (Donor) >1. Transcripts with p-adj (NT/IVF) < 0.05 were excluded.
Reprogrammed-Up: p-adj (Donor/IVF) < 0.05, log2FC (Donor/IVF) < 0, p-adj (Donor/NT) < 0.05, log2FC (Donor/NT) < 0.05, p-adj (NT/IVF) > 0.05.
In the experiments comparing the effect of p300/CBP inhibitor treatment vs. control, filtering the ON-memory genes was performed separately in each condition.
Differentially expressed genes (DEG) Donor(DMSO)/IVF: p-adj (Donor(DMSO)/IVF) < 0.05
DEG Donor(DMSO)/IVF and NT(DMSO)/IVF: p-adj (Donor(DMSO)/IVF) < 0.05 & p-adj (NT(DMSO)/IVF) < 0.05
ON-memory genes (DMSO): p-adj (Donor(DMSO)/IVF) < 0.05, log2FC (Donor(DMSO)/IVF) > 0, p-adj (NT(DMSO)/IVF) < 0.05, log2FC(NT(DMSO)/IVF) > 0, TPM(Donor(DMSO)) >1.
OFF-memory genes (DMSO): p-adj (Donor(DMSO)/IVF) < 0.05, log2FC (Donor(DMSO)/IVF) < 0, p-adj (NT(DMSO)/IVF) < 0.05, log2FC(NT(DMSO)/IVF) < 0
Reprogrammed-Down (DMSO): p-adj (Donor(DMSO)/IVF) < 0.05, log2FC (Donor(DMSO)/IVF) >0, p-adj (Donor(DMSO)/NT(DMSO)) < 0.05, log2FC (Donor(DMSO)/NT(DMSO)) > 0.05, TPM (Donor(DMSO)) >1. Transcripts with p-adj (NT(DMSO)/IVF) < 0.05 were excluded.
Reprogrammed-Up (DMSO): p-adj (Donor(DMSO)/IVF) < 0.05, log2FC (Donor(DMSO)/IVF) < 0, p-adj (Donor(DMSO)/NT(DMSO)) < 0.05, log2FC (Donor(DMSO)/NT(DMSO)) < 0.05, p-adj (NT(DMSO)/IVF) > 0.05.

The same filtering strategy was applied for samples generated upon CBP30 and A-485 treatment.

Plots for gene expression

Heatmaps – Expression values for each condition were normalized to the mean expression of IVF controls. Log2-transformed fold changes were calculated for each

condition relative to IVF mean expression. These values were plotted using heatmap.2 from the R package gplots, with clustering by rows and columns and default settings: complete as agglomeration method and Euclidean distance as similarity measure. Z-scores were calculated per row, using the scaling function in heatmap.2.

MA-plots – The log2FC between genes expressed in NT and IVFs was plotted against the log2-transformed TPM-expression values (log2 TPM+1) in the endoderm donor cells. MA-plots were created using base R.

Boxplots – The distribution of mean expression levels of the different gene sets is represented as boxplots, whereby the line represents the median, the box edges indicate the lower and upper percentiles (25^{th} and 75^{th} respectively), and the whiskers represent the minimum and maximum values. Boxplots were created using default settings in base R. p-values comparing differences in gene expression between the different gene sets were calculated using a two-sided unpaired Wilcoxon rank-sum test in R.

Principal component analysis (PCA) plots - Principal Component Analysis was performed on TPM gene expression data. Genes with zero variance were removed. The data was centered and scaled prior to PCA. Finally, PCA was performed using the prcomp() package and visualized using ggplot2() in R.

ChIP-seq analysis for enhancer annotation

For the endoderm H3K27ac ChIP-seq analysis, peaks were called using MACS2(Y. Zhang et al., 2008) (v2.2.8) with the "--broad" option. Due to low enrichment and minimal peak calls, replicate 2 was excluded from further analysis. Common peaks between replicates 1 and 3 were identified and merged using bedtools (v2.31.0), resulting in a total of 7915 peaks. These peaks were further classified into 4851 promoter peaks (+/- 500bp) and 3064 non-promoter peaks (distant from promoters by more than 500bp). To predict active enhancers in *Xenopus laevis* endoderm, previously published p300 ChIP-seq data (Stevens et al., 2017) from NF stage 20 foregut and hindgut were analyzed. Foregut and hindgut peaks were concatenated (cat), sorted (sort -k1,1 -k2,2n) and merged using bedtools merge, resulting in 61418 peaks on the main chromosomes. Subsequently, we identified 1306 H3K27ac+ and p300+ putative enhancers, supported by detected H3K4me1 signal on these sites. Enhancer-gene pairing was performed as described previously (Ing-Simmons, 2021).

CUT&RUN analysis

Sequencing reads were aligned to the *Xenopus laevis* genome (XENLA_10.1) and a spike-in genome (*Escherichia coli*, GCA_001606525) using Bowtie2 (v2.4). The

alignment process excluded discordant and mixed reads, with paired-end reads mapped to the reference genome. Aligned reads were converted to BAM format and filtered to retain only properly paired alignments. Normalization scaling factors were computed using deepTools (v3.5.3) based on the read distribution across genomic regions. HOMER (v4.11) was used for peak identification. Broad peaks were called using histone-style parameters and converted to BED format for downstream analysis. Differential peak analysis for H3K27ac signal was performed on the p300 ChIP-seq peak set from Stevens et al. (Stevens et al., 2017) as a reference peak set using DEseq2 (Love et al., 2014) (v1.46.0). Enhancer and promoters were annotated as described above.

Boxplots comparing DEseq2 normalized counts on differentially abundant peaks across gene sets of interest were generated in base R (v4.4.2), whereby the line represents the median, the box edges indicate the lower and upper percentiles (25^{th} and 75^{th} respectively), and the whiskers represent the minimum and maximum values.

MA-plots, balloon plots, stacked bar charts, and scatter plots were generated using ggplot2 in R. Heatmaps comparing enrichment or correlations were generated using pheatmap in R.

Heatmaps comparing global coverage distribution across conditions were generated in R using the package EnrichedHeatmap (Z. Gu et al., 2018), using the function normalizeToMatrix to calculate the coverage over genomic features. The coverage from biological replicates was averaged and normalize to *E. coli* spike-in.

7. Appendix – Tables

Table 3: Overview of biological replicates in transcriptome assays

Differential expression analysis (RNA-seq)				
		CBP30 experiments (Figure 3, S3)		
Embryo tissue	Treatment	#1	#2	#3
Donor (endoderm)	DMSO CBP30	2 2	2 2	2 1
NT (ectoderm)	DMSO CBP30	4 3	3 5	6 3
IVF (ectoderm)	N/A	4	3	4
		A-485 experiments (Figure 3, S3)		
		#1	#2	#3
Donor(endoderm)	A-485	2	2	2
NT (ectoderm)	A-485	3	6	3
IVF (ectoderm)	N/A	4	4	4

Donor: endoderm donor nuclei; NT: ectoderm of nuclear transfer embryos; IVF: ectoderm of *in vitro* fertilized embryos; CBP30: p300/CBP bromodomain inhibitor; A-485 p300 histone acetyltransferase domain inhibitor. One tissue was harvested from one embryo as an individual sample.

Table 3: Overview of gene expression changes in p300/CBP inhibitor treated donor cells (CBP30 - bromodomain inhibitor, or A-485 - catalytic domain inhibitor)

	Number of transcripts	% of transcripts	Filter applied
Total transcripts	36994	100	TPM >1 in either donor, IVF or NT samples
DE donor DMSO vs. donor CBP30	3282	8,8	p-adj < 0.05
DE donor DMSO vs. donor A-485	5493	14,8	p-adj < 0.05

Donor: endoderm donor nuclei; NT: ectoderm of nuclear transfer embryos; IVF: ectoderm of *in vitro* fertilized embryos; DE: differentially expressed; TPM: transcripts per million; p-adj: adjusted p-value.

Table 4: Overview of memory and reprogrammed gene sets upon filtering

	DMSO		CBP30		A-485	
	Number of transcripts	% of total transcripts	Number of transcripts	% of total transcripts	Number of transcripts	% of total transcripts
Total transcripts	36994	100	36994	100	36994	100
DE Donor vs. IVF	20314	54,9	19336	52,2	19379	52,4
DE Donor vs. IVF & DE NT	17662	47,7	16773	45,3	16456	44,5
ON-memory	1360	3,6	1071	2,9	1253	3,4
OFF-memory	1315	3,55	1413	3,8	1525	4,1
RD	5906	15,9	5186	14,0	5153	13,9
RU	3754	10,1	6223	16,8	5787	15,6

Donor: endoderm donor nuclei; NT: ectoderm of nuclear transfer embryos; IVF: ectoderm of *in vitro* fertilized embryos; DE: differentially expressed; RD: reprogrammed-down genes; RU: reprogrammed-up genes. The filtering strategy is described in the Materials and Methods section

Table 5: Overview of embryo counts in the developmental outcome assay

Developmental outcome assay – Results of quantifications			
Developmental stage	NT(DMSO)	NT(CBP30)	IVF
NT (number of injections)	720	720	N/A
Cleaved	109	131	325
Gastrulae	50	65	263
Neurulae	11	24	235
Tadpole	7	13	227

References

Ancona, M., & Gross, M. (2017). A unified view of gradient-based attribution methods for Deep Neural Networks. *Neural Information Processing Systems*, *Section 3*.

AOKI, F. (2022). Zygotic gene activation in mice: Profile and regulation. *The Journal of Reproduction and Development*, *68*(2), 79–84. https://doi.org/10.1262/jrd.2021-129

Aoki, F., Worrad, D. M., & Schultz, R. M. (1997). Regulation of transcriptional activity during the first and second cell cycles in the preimplantation mouse embryo. *Developmental Biology*, *181*(2), 296–307. https://doi.org/10.1006/dbio.1996.8466

Apostolou, E., & Hochedlinger, K. (2013). Chromatin dynamics during cellular reprogramming. *Nature*, *502*(7472), 462–471. https://doi.org/10.1038/nature12749

Apostolou, E., & Stadtfeld, M. (2018). Cellular trajectories and molecular mechanisms of iPSC reprogramming. *Current Opinion in Genetics & Development*, *52*, 77–85. https://doi.org/10.1016/j.gde.2018.06.002

Atlasi, Y., & Stunnenberg, H. G. (2017). The interplay of epigenetic marks during stem cell differentiation and development. *Nature Reviews Genetics*, *18*(11), 643–658. https://doi.org/10.1038/nrg.2017.57

Bannister, A. J., & Kouzarides, T. (1996). The CBP co-activator is a histone acetyltransferase. *Nature*, *384*(6610), 641–643. https://doi.org/10.1038/384641a0

Bannister, A. J., & Kouzarides, T. (2011). Regulation of chromatin by histone modifications. *Cell Research*, *21*(3), 381–395. https://doi.org/10.1038/cr.2011.22

Baumann, V., Wiesbeck, M., Breunig, C. T., Braun, J. M., Köferle, A., Ninkovic, J., Götz, M., & Stricker, S. H. (2019). Targeted removal of epigenetic barriers during transcriptional reprogramming. *Nature Communications*, *10*(1), 2119. https://doi.org/10.1038/s41467-019-10146-8

Beacon, T. H., Delcuve, G. P., López, C., Nardocci, G., Kovalchuk, I., Van Wijnen, A. J., & Davie, J. R. (2021). The dynamic broad epigenetic (H3K4me3, H3K27ac) domain as a mark of essential genes. *Clinical Epigenetics*, *13*(1), 138. https://doi.org/10.1186/s13148-021-01126-1

Beck, C. W., Izpisúa Belmonte, J. C., & Christen, B. (2009). Beyond early development: Xenopus as an emerging model for the study of regenerative mechanisms. *Developmental Dynamics*, *238*(6), 1226–1248. https://doi.org/10.1002/dvdy.21890

Behera, V., Stonestrom, A. J., Hamagami, N., Hsiung, C. C., Keller, C. A., Giardine, B., Sidoli, S., Yuan, Z.-F., Bhanu, N. V., Werner, M. T., Wang, H., Garcia, B. A., Hardison, R. C., & Blobel, G. A. (2019). Interrogating Histone Acetylation and BRD4 as Mitotic Bookmarks of Transcription. *Cell Reports*, *27*(2), 400-415.e5. https://doi.org/10.1016/j.celrep.2019.03.057

Bell, C. C., Faulkner, G. J., & Gilan, O. (2024). Chromatin-based memory as a self-stabilizing influence on cell identity. *Genome Biology*, *25*(1), 320. https://doi.org/10.1186/s13059-024-03461-x

Bellec, M., Dufourt, J., Hunt, G., Lenden-Hasse, H., Trullo, A., Zine El Aabidine, A., Lamarque, M., Gaskill, M. M., Faure-Gautron, H., Mannervik, M., Harrison, M. M., Andrau, J.-C., Favard, C., Radulescu, O., & Lagha, M. (2022). The control of transcriptional memory by stable mitotic bookmarking. *Nature Communications*, *13*(1), 1176. https://doi.org/10.1038/s41467-022-28855-y

Benayoun, B. A., Pollina, E. A., Ucar, D., Mahmoudi, S., Karra, K., Wong, E. D., Devarajan, K., Daugherty, A. C., Kundaje, A. B., Mancini, E., Hitz, B. C., Gupta, R., Rando, T. A., Baker, J. C., Snyder, M. P., Cherry, J. M., & Brunet, A. (2014). H3K4me3 breadth is

linked to cell identity and transcriptional consistency. *Cell*, *158*(3), 673–688. https://doi.org/10.1016/j.cell.2014.06.027
Berninger, B., Costa, M. R., Koch, U., Schroeder, T., Sutor, B., Grothe, B., & Götz, M. (2007). Functional Properties of Neurons Derived from *In Vitro* Reprogrammed Postnatal Astroglia. *The Journal of Neuroscience*, *27*(32), 8654–8664. https://doi.org/10.1523/JNEUROSCI.1615-07.2007
Blau, H. M., & Blakely, B. T. (1999). Plasticity of cell fate: Insights from heterokaryons. *Seminars in Cell & Developmental Biology*, *10*(3), 267–272. https://doi.org/10.1006/scdb.1999.0311
Blau, H. M., Chiu, C.-P., & Webster, C. (1983). Cytoplasmic activation of human nuclear genes in stable heterocaryons. *Cell*, *32*(4), 1171–1180. https://doi.org/10.1016/0092-8674(83)90300-8
Blau, H. M., Pavlath, G. K., Hardeman, E. C., Chiu, C.-P., Silberstein, L., Webster, S. G., Miller, S. C., & Webster, C. (n.d.). *Plasticity of the Differentiated State*.
Blelloch, R., Wang, Z., Meissner, A., Pollard, S., Smith, A., & Jaenisch, R. (2006). Reprogramming Efficiency Following Somatic Cell Nuclear Transfer Is Influenced by the Differentiation and Methylation State of the Donor Nucleus. *STEM CELLS*, *24*(9), 2007–2013. https://doi.org/10.1634/stemcells.2006-0050
Bondarieva, A., & Tachibana, K. (2024). Genome folding and zygotic genome activation in mammalian preimplantation embryos. *Current Opinion in Genetics & Development*, *89*, 102268. https://doi.org/10.1016/j.gde.2024.102268
Briggs, J. A., Weinreb, C., Wagner, D. E., Megason, S., Peshkin, L., Kirschner, M. W., & Klein, A. M. (2018). The dynamics of gene expression in vertebrate embryogenesis at single-cell resolution. *Science*, *360*(6392), eaar5780. https://doi.org/10.1126/science.aar5780
Briggs, R., & King, T. J. (1952). Transplantation of Living Nuclei From Blastula Cells into Enucleated Frogs' Eggs. *Proceedings of the National Academy of Sciences of the United States of America*, *38*(5), 455–463. https://doi.org/10.1073/pnas.38.5.455
Brown, K. E., & Fisher, A. G. (2021). Reprogramming lineage identity through cell–cell fusion. *Current Opinion in Genetics & Development*, *70*, 15–23. https://doi.org/10.1016/j.gde.2021.04.004
Brumbaugh, J., Di Stefano, B., & Hochedlinger, K. (2019). Reprogramming: Identifying the mechanisms that safeguard cell identity. *Development*, *146*(23), dev182170. https://doi.org/10.1242/dev.182170
Buganim, Y., Faddah, D. A., Cheng, A. W., Itskovich, E., Markoulaki, S., Ganz, K., Klemm, S. L., van Oudenaarden, A., & Jaenisch, R. (2012). Single-Cell Expression Analyses during Cellular Reprogramming Reveal an Early Stochastic and a Late Hierarchic Phase. *Cell*, *150*(6), 1209–1222. https://doi.org/10.1016/j.cell.2012.08.023
Buganim, Y., Faddah, D. A., & Jaenisch, R. (2013). Mechanisms and models of somatic cell reprogramming. *Nature Reviews Genetics*, *14*(6), 427–439. https://doi.org/10.1038/nrg3473
Cai, R., Lv, R., Shi, X., Yang, G., & Jin, J. (2023). CRISPR/dCas9 Tools: Epigenetic Mechanism and Application in Gene Transcriptional Regulation. *International Journal of Molecular Sciences*, *24*(19), 14865. https://doi.org/10.3390/ijms241914865
Calo, E., & Wysocka, J. (2013). Modification of Enhancer Chromatin: What, How, and Why? *Molecular Cell*, *49*(5), 825–837. https://doi.org/10.1016/j.molcel.2013.01.038
Campbell, K. H. S., Loi, P., Otaegui, P. J., & Wilmut, I. (1996). *Cell cycle co-ordination in embryo cloning by nuclear transfer*.
Campbell, K. H. S., McWhir, J., Ritchie, W. A., & Wilmut, I. (1996). Sheep cloned by nuclear transfer from a cultured cell line. *Nature*, *380*(6569), 64–66. https://doi.org/10.1038/380064a0

Chan, M. M., Smith, Z. D., Egli, D., Regev, A., & Meissner, A. (2012). Mouse ooplasm confers context-specific reprogramming capacity. *Nature Genetics*, *44*(9), 978–980. https://doi.org/10.1038/ng.2382

Chang, C.-C., Gao, S., Sung, L.-Y., Corry, G. N., Ma, Y., Nagy, Z. P., Tian, X. C., & Rasmussen, T. P. (2010). Rapid elimination of the histone variant MacroH2A from somatic cell heterochromatin after nuclear transfer. *Cellular Reprogramming*, *12*(1), 43–53. https://doi.org/10.1089/cell.2009.0043

Chen, G., Guo, Y., Li, C., Li, S., & Wan, X. (2020). Small Molecules that Promote Self-Renewal of Stem Cells and Somatic Cell Reprogramming. *Stem Cell Reviews and Reports*, *16*(3), 511–523. https://doi.org/10.1007/s12015-020-09965-w

Chen, J., Chen, X., Li, M., Liu, X., Gao, Y., Kou, X., Zhao, Y., Zheng, W., Zhang, X., Huo, Y., Chen, C., Wu, Y., Wang, H., Jiang, C., & Gao, S. (2016). Hierarchical Oct4 Binding in Concert with Primed Epigenetic Rearrangements during Somatic Cell Reprogramming. *Cell Reports*, *14*(6), 1540–1554. https://doi.org/10.1016/j.celrep.2016.01.013

Chen, J., Ghazawi, F. M., & Li, Q. (2010). Interplay of bromodomain and histone acetylation in the regulation of p300-dependent genes. *Epigenetics*, *5*(6), 509–515. https://doi.org/10.4161/epi.5.6.12224

Chen, K., Hu ,Zheng, Xia ,Zheng, Zhao ,Dongyu, Li ,Wei, & and Tyler, J. K. (2016). The Overlooked Fact: Fundamental Need for Spike-In Control for Virtually All Genome-Wide Analyses. *Molecular and Cellular Biology*, *36*(5), 662–667. https://doi.org/10.1128/MCB.00970-14

Chen, M., Zhu, Q., Li, C., Kou, X., Zhao, Y., Li, Y., Xu, R., Yang, L., Yang, L., Gu, L., Wang, H., Liu, X., Jiang, C., & Gao, S. (2020). Chromatin architecture reorganization in murine somatic cell nuclear transfer embryos. *Nature Communications*, *11*(1), 1813. https://doi.org/10.1038/s41467-020-15607-z

Chen, T., Ueda, Y., Dodge, J. E., Wang, Z., & Li, E. (2003). Establishment and maintenance of genomic methylation patterns in mouse embryonic stem cells by Dnmt3a and Dnmt3b. *Molecular and Cellular Biology*, *23*(16), 5594–5605. https://doi.org/10.1128/MCB.23.16.5594-5605.2003

Chronis, C., Fiziev, P., Papp, B., Butz, S., Bonora, G., Sabri, S., Ernst, J., & Plath, K. (2017). Cooperative Binding of Transcription Factors Orchestrates Reprogramming. *Cell*, *168*(3), 442-459.e20. https://doi.org/10.1016/j.cell.2016.12.016

Comet, I., Riising, E. M., Leblanc, B., & Helin, K. (2016). Maintaining cell identity: PRC2-mediated regulation of transcription and cancer. *Nature Reviews Cancer*, *16*(12), 803–810. https://doi.org/10.1038/nrc.2016.83

Condic, M. L. (2014). Totipotency: What It Is and What It Is Not. *Stem Cells and Development*, *23*(8), 796–812. https://doi.org/10.1089/scd.2013.0364

Creyghton, M. P., Cheng, A. W., Welstead, G. G., Kooistra, T., Carey, B. W., Steine, E. J., Hanna, J., Lodato, M. A., Frampton, G. M., Sharp, P. A., Boyer, L. A., Young, R. A., & Jaenisch, R. (2010). Histone H3K27ac separates active from poised enhancers and predicts developmental state. *Proceedings of the National Academy of Sciences*, *107*(50), 21931–21936. https://doi.org/10.1073/pnas.1016071107

Dancy, B. M., & Cole, P. A. (2015). Protein Lysine Acetylation by p300/CBP. *Chemical Reviews*, *115*(6), 2419–2452. https://doi.org/10.1021/cr500452k

Davis, R. L., Weintraub, H., & Lassar, A. B. (1987). Expression of a single transfected cDNA converts fibroblasts to myoblasts. *Cell*, *51*(6), 987–1000. https://doi.org/10.1016/0092-8674(87)90585-x

Day, R. C., & Beck, C. W. (2011). Transdifferentiation from cornea to lens in Xenopus laevis depends on BMP signalling and involves upregulation of Wnt signalling. *BMC Developmental Biology*, *11*(1), 54. https://doi.org/10.1186/1471-213X-11-54

Dhalluin, C., Carlson, J. E., Zeng, L., He, C., Aggarwal, A. K., & Zhou, M.-M. (1999). *Structure and ligand of a histone acetyltransferase bromodomain*. *399*.
Djekidel, M. N., Inoue, A., Matoba, S., Suzuki, T., Zhang, C., Lu, F., Jiang, L., & Zhang, Y. (2018). Reprogramming of Chromatin Accessibility in Somatic Cell Nuclear Transfer Is DNA Replication Independent. *Cell Reports*, *23*(7), Article 7. https://doi.org/10.1016/j.celrep.2018.04.036
Doi, A., Park, I.-H., Wen, B., Murakami, P., Aryee, M. J., Irizarry, R., Herb, B., Ladd-Acosta, C., Rho, J., Loewer, S., Miller, J., Schlaeger, T., Daley, G. Q., & Feinberg, A. P. (2009). Differential methylation of tissue- and cancer-specific CpG island shores distinguishes human induced pluripotent stem cells, embryonic stem cells and fibroblasts. *Nature Genetics*, *41*(12), 1350–1353. https://doi.org/10.1038/ng.471
Eberl, H. C., Mann, M., & Vermeulen, M. (2011). Quantitative Proteomics for Epigenetics. *ChemBioChem*, *12*(2), 224–234. https://doi.org/10.1002/cbic.201000429
Ebrahimi, A., Sevinç, K., Gürhan Sevinç, G., Cribbs, A. P., Philpott, M., Uyulur, F., Morova, T., Dunford, J. E., Göklemez, S., Arı, Ş., Oppermann, U., & Önder, T. T. (2019). Bromodomain inhibition of the coactivators CBP/EP300 facilitate cellular reprogramming. *Nature Chemical Biology*, *15*(5), 519–528. https://doi.org/10.1038/s41589-019-0264-z
Elsdale, T. R., Gurdon, J. B., & Fischberg, M. (1960). A Description of the Technique for Nuclear Transplantation in *Xenopus laevis*. *Development*, *8*(4), 437–444. https://doi.org/10.1242/dev.8.4.437
Escobar, T. M., Loyola, A., & Reinberg, D. (2021). Parental nucleosome segregation and the inheritance of cellular identity. *Nature Reviews Genetics*, *22*(6), 379–392. https://doi.org/10.1038/s41576-020-00312-w
Ferrell, J. E. (1999). Xenopus oocyte maturation: New lessons from a good egg. *BioEssays: News and Reviews in Molecular, Cellular and Developmental Biology*, *21*(10), 833–842. https://doi.org/10.1002/(SICI)1521-1878(199910)21:10<833::AID-BIES5>3.0.CO;2-P
Ferrie, J. J., Karr, J. P., Graham, T. G. W., Dailey, G. M., Zhang, G., Tjian, R., & Darzacq, X. (2024). P300 is an obligate integrator of combinatorial transcription factor inputs. *Molecular Cell*, *84*(2), 234-243.e4. https://doi.org/10.1016/j.molcel.2023.12.004
Freeman, G. (1963). Lens regeneration from the cornea in Xenopus laevis. *Journal of Experimental Zoology*, *154*(1), 39–65. https://doi.org/10.1002/jez.1401540105
Ganier, O., Bocquet, S., Peiffer, I., Brochard, V., Arnaud, P., Puy, A., Jouneau, A., Feil, R., Renard, J.-P., & Méchali, M. (2011). Synergic reprogramming of mammalian cells by combined exposure to mitotic *Xenopus* egg extracts and transcription factors. *Proceedings of the National Academy of Sciences*, *108*(42), 17331–17336. https://doi.org/10.1073/pnas.1100733108
Gao, R., Wang, C., Gao, Y., Xiu, W., Chen, J., Kou, X., Zhao, Y., Liao, Y., Bai, D., Qiao, Z., Yang, L., Wang, M., Zang, R., Liu, X., Jia, Y., Li, Y., Zhang, Y., Yin, J., Wang, H., … Gao, S. (2018). Inhibition of Aberrant DNA Re-methylation Improves Post-implantation Development of Somatic Cell Nuclear Transfer Embryos. *Cell Stem Cell*, *23*(3), 426-435.e5. https://doi.org/10.1016/j.stem.2018.07.017
Gentsch, G. E., & Smith, J. C. (2014). Investigating Physical Chromatin Associations Across the *Xenopus* Genome by Chromatin Immunoprecipitation. *Cold Spring Harbor Protocols*, *2014*(5), pdb.prot080614. https://doi.org/10.1101/pdb.prot080614
Gonzalez, I., Molliex, A., & Navarro, P. (2021). Mitotic memories of gene activity. *Current Opinion in Cell Biology*, *69*, 41–47. https://doi.org/10.1016/j.ceb.2020.12.009
Götz, M., & Torres-Padilla, M.-E. (2025). Stem cells as role models for reprogramming and repair. *Science*, *388*(6746), eadp2959. https://doi.org/10.1126/science.adp2959
Graham, C. F., Arms, K., & Gurdon, J. B. (1966). The induction of DNA synthesis by frog egg cytoplasm. *Developmental Biology*, *14*(3), 349–381. https://doi.org/10.1016/0012-1606(66)90020-0

Greenberg, M. V. C., & Bourc'his, D. (2019). The diverse roles of DNA methylation in mammalian development and disease. *Nature Reviews Molecular Cell Biology*, *20*(10), 590–607. https://doi.org/10.1038/s41580-019-0159-6

Gu, T.-P., Guo, F., Yang, H., Wu, H.-P., Xu, G.-F., Liu, W., Xie, Z.-G., Shi, L., He, X., Jin, S., Iqbal, K., Shi, Y. G., Deng, Z., Szabó, P. E., Pfeifer, G. P., Li, J., & Xu, G.-L. (2011). The role of Tet3 DNA dioxygenase in epigenetic reprogramming by oocytes. *Nature*, *477*(7366), 606–610. https://doi.org/10.1038/nature10443

Gu, Z., Eils, R., Schlesner, M., & Ishaque, N. (2018). EnrichedHeatmap: An R/Bioconductor package for comprehensive visualization of genomic signal associations. *BMC Genomics*, *19*(1), 234. https://doi.org/10.1186/s12864-018-4625-x

Guo, Z., Zhang, L., Wu, Z., Chen, Y., Wang, F., & Chen, G. (2014). In Vivo Direct Reprogramming of Reactive Glial Cells into Functional Neurons after Brain Injury and in an Alzheimer's Disease Model. *Cell Stem Cell*, *14*(2), 188–202. https://doi.org/10.1016/j.stem.2013.12.001

Gurdon, J. B. (1960a). The Developmental Capacity of Nuclei Taken from Differentiating Endoderm Cells of *Xenopus Laevis*. *Development*, *8*(4), 505–526. https://doi.org/10.1242/dev.8.4.505

Gurdon, J. B. (1960b). The developmental capacity of nuclei taken from differentiating endoderm cells of Xenopus laevis. *Journal of Embryology and Experimental Morphology*, *8*, 505–526.

Gurdon, J. B. (1960c). The Effects of Ultraviolet Irradiation on Uncleaved Eggs of *Xenopus laevis*. *Journal of Cell Science*, *S3-101*(55), 299–311. https://doi.org/10.1242/jcs.s3-101.55.299

Gurdon, J. B. (1968). Changes in somatic cell nuclei inserted into growing and maturing amphibian oocytes. *Development*, *20*(3), 401–414. https://doi.org/10.1242/dev.20.3.401

Gurdon, J. B. (2013). The Egg and the Nucleus: A Battle for Supremacy (Nobel Lecture). *Angewandte Chemie International Edition*, *52*(52), 13890–13899. https://doi.org/10.1002/anie.201306722

Gurdon, J. B., Elsdale, T. R., & Fischberg, M. (1958). Sexually Mature Individuals of Xenopus laevis from the transplantation of single somatic nuclei. *Nature*, *182*(4627), 65–66. https://doi.org/10.1038/182065a0

Gurdon, J. B., & Melton, D. A. (2008). Nuclear Reprogramming in Cells. *Science*, *322*(5909), 1811–1815. https://doi.org/10.1126/science.1160810

Gurdon, J. B., & Uehlinger, V. (1966). "Fertile" Intestine Nuclei. *Nature*, *210*(5042), 1240–1241. https://doi.org/10.1038/2101240a0

Gurdon, J. B., & Wilmut, I. (2011). Nuclear Transfer to Eggs and Oocytes. *Cold Spring Harbor Perspectives in Biology*, *3*(6), a002659–a002659. https://doi.org/10.1101/cshperspect.a002659

Halley-Stott, R. P., Pasque, V., Astrand, C., Miyamoto, K., Simeoni, I., Jullien, J., & Gurdon, J. B. (2010). Mammalian nuclear transplantation to Germinal Vesicle stage Xenopus oocytes – A method for quantitative transcriptional reprogramming. *Methods*, *51*(1), 56–65. https://doi.org/10.1016/j.ymeth.2010.01.035

Halley-Stott, R. P., Pasque, V., & Gurdon, J. B. (2013). Nuclear reprogramming. *Development*, *140*(12), 2468–2471. https://doi.org/10.1242/dev.092049

Han, Y., & and Garcia, B. A. (2013). Combining Genomic and Proteomic Approaches for Epigenetics Research. *Epigenomics*, *5*(4), 439–452. https://doi.org/10.2217/epi.13.37

Hanna, J. H., Saha, K., & Jaenisch, R. (2010). Pluripotency and Cellular Reprogramming: Facts, Hypotheses, Unresolved Issues. *Cell*, *143*(4), 508–525. https://doi.org/10.1016/j.cell.2010.10.008

Hansson, J., Rafiee, M. R., Reiland, S., Polo, J. M., Gehring, J., Okawa, S., Huber, W., Hochedlinger, K., & Krijgsveld, J. (2012). Highly Coordinated Proteome Dynamics during

Reprogramming of Somatic Cells to Pluripotency. *Cell Reports*, *2*(6), 1579–1592. https://doi.org/10.1016/j.celrep.2012.10.014
Heintzman, N. D., Hon, G. C., Hawkins, R. D., Kheradpour, P., Stark, A., Harp, L. F., Ye, Z., Lee, L. K., Stuart, R. K., Ching, C. W., Ching, K. A., Antosiewicz-Bourget, J. E., Liu, H., Zhang, X., Green, R. D., Lobanenkov, V. V., Stewart, R., Thomson, J. A., Crawford, G. E., … Ren, B. (2009). Histone modifications at human enhancers reflect global cell-type-specific gene expression. *Nature*, *459*(7243), 108–112. https://doi.org/10.1038/nature07829
Heintzman, N. D., Stuart, R. K., Hon, G., Fu, Y., Ching, C. W., Hawkins, R. D., Barrera, L. O., Van Calcar, S., Qu, C., Ching, K. A., Wang, W., Weng, Z., Green, R. D., Crawford, G. E., & Ren, B. (2007). Distinct and predictive chromatin signatures of transcriptional promoters and enhancers in the human genome. *Nature Genetics*, *39*(3), 311–318. https://doi.org/10.1038/ng1966
Heinz, S., Romanoski, C. E., Benner, C., & Glass, C. K. (2015). The selection and function of cell type-specific enhancers. *Nature Reviews Molecular Cell Biology*, *16*(3), 144–154. https://doi.org/10.1038/nrm3949
Hiler, D., Chen, X., Hazen, J., Kupriyanov, S., Carroll, P. A., Qu, C., Xu, B., Johnson, D., Griffiths, L., Frase, S., Rodriguez, A. R., Martin, G., Zhang, J., Jeon, J., Fan, Y., Finkelstein, D., Eisenman, R. N., Baldwin, K., & Dyer, M. A. (2015). Quantification of Retinogenesis in 3D Cultures Reveals Epigenetic Memory and Higher Efficiency in iPSCs Derived from Rod Photoreceptors. *Cell Stem Cell*, *17*(1), 101–115. https://doi.org/10.1016/j.stem.2015.05.015
Hnisz, D., Abraham, B. J., Lee, T. I., Lau, A., Saint-André, V., Sigova, A. A., Hoke, H. A., & Young, R. A. (2013). Super-Enhancers in the Control of Cell Identity and Disease. *Cell*, *155*(4), 934–947. https://doi.org/10.1016/j.cell.2013.09.053
Holmqvist, P.-H., & Mannervik, M. (2013). Genomic occupancy of the transcriptional co-activators p300 and CBP. *Transcription*, *4*(1), 18–23. https://doi.org/10.4161/trns.22601
Hopwood, N. D., & Gurdon, J. B. (1990). Activation of muscle genes without myogenesis by ectopic expression of MyoD in frog embryo cells. *Nature*, *347*(6289), 197–200. https://doi.org/10.1038/347197a0
Horb, M. E., Shen, C.-N., Tosh, D., & Slack, J. M. W. (2003). Experimental Conversion of Liver to Pancreas. *Current Biology*, *13*(2), 105–115. https://doi.org/10.1016/S0960-9822(02)01434-3
Horb, M. E., & Slack, J. M. W. (2001). Endoderm Specification and Differentiation in Xenopus Embryos. *Developmental Biology*, *236*(2), 330–343. https://doi.org/10.1006/dbio.2001.0347
Hörmanseder, E. (2021). Epigenetic memory in reprogramming. *Current Opinion in Genetics & Development*, *70*, 24–31. https://doi.org/10.1016/j.gde.2021.04.007
Hörmanseder, E., Simeone, A., Allen, G. E., Bradshaw, C. R., Figlmüller, M., Gurdon, J., & Jullien, J. (2017). H3K4 Methylation-Dependent Memory of Somatic Cell Identity Inhibits Reprogramming and Development of Nuclear Transfer Embryos. *Cell Stem Cell*, *21*(1), 135-143.e6. https://doi.org/10.1016/j.stem.2017.03.003
Hörmanseder, E., Tischer, T., & Mayer, T. U. (2013). Modulation of cell cycle control during oocyte-to-embryo transitions. *The EMBO Journal*, *32*(16), 2191–2203. https://doi.org/10.1038/emboj.2013.164
Hou, L., Ma, F., Yang, J., Riaz, H., Wang, Y., Wu, W., Xia, X., Ma, Z., Zhou, Y., Zhang, L., Ying, W., Xu, D., Zuo, B., Ren, Z., & Xiong, Y. (2014). Effects of Histone Deacetylase Inhibitor Oxamflatin on *In Vitro* Porcine Somatic Cell Nuclear Transfer Embryos. *Cellular Reprogramming*, *16*(4), 253–265. https://doi.org/10.1089/cell.2013.0058
Huang, P., Zhang, L., Gao, Y., He, Z., Yao, D., Wu, Z., Cen, J., Chen, X., Liu, C., Hu, Y., Lai, D., Hu, Z., Chen, L., Zhang, Y., Cheng, X., Ma, X., Pan, G., Wang, X., & Hui, L. (2014).

Direct Reprogramming of Human Fibroblasts to Functional and Expandable Hepatocytes. *Cell Stem Cell*, *14*(3), 370–384. https://doi.org/10.1016/j.stem.2014.01.003
Huang, Y., Zhang, J., Li, X., Wu, Z., Xie, G., Wang, Y., Liu, Z., Jiao, M., Zhang, H., Shi, B., Wang, Y., & Zhang, Y. (2023). Chromatin accessibility memory of donor cells disrupts bovine somatic cell nuclear transfer blastocysts development. *The FASEB Journal*, *37*(9), e23111. https://doi.org/10.1096/fj.202300131RRR
Huangfu, D., Maehr, R., Guo, W., Eijkelenboom, A., Snitow, M., Chen, A. E., & Melton, D. A. (2008). Induction of pluripotent stem cells by defined factors is greatly improved by small-molecule compounds. *Nature Biotechnology*, *26*(7), 795–797. https://doi.org/10.1038/nbt1418
Huangfu, D., Osafune, K., Maehr, R., Guo, W., Eijkelenboom, A., Chen, S., Muhlestein, W., & Melton, D. A. (2008). Induction of pluripotent stem cells from primary human fibroblasts with only Oct4 and Sox2. *Nature Biotechnology*, *26*(11), 1269–1275. https://doi.org/10.1038/nbt.1502
Iager, A. E., Ragina, N. P., Ross, P. J., Beyhan, Z., Cunniff, K., Rodriguez, R. M., & Cibelli, J. B. (2008). Trichostatin A Improves Histone Acetylation in Bovine Somatic Cell Nuclear Transfer Early Embryos. *Cloning and Stem Cells*, *10*(3), 371–380. https://doi.org/10.1089/clo.2007.0002
Ieda, M., Fu, J.-D., Delgado-Olguin, P., Vedantham, V., Hayashi, Y., Bruneau, B. G., & Srivastava, D. (2010). Direct Reprogramming of Fibroblasts into Functional Cardiomyocytes by Defined Factors. *Cell*, *142*(3), 375–386. https://doi.org/10.1016/j.cell.2010.07.002
Ing-Simmons, E. (2021). Independence of chromatin conformation and gene regulation during Drosophila dorsoventral patterning. *Nature Genetics*, *53*.
Inoue, A., Shen, L., Matoba, S., & Zhang, Y. (2015). Haploinsufficiency, but Not Defective Paternal 5mC Oxidation, Accounts for the Developmental Defects of Maternal Tet3 Knockouts. *Cell Reports*, *10*(4), 463–470. https://doi.org/10.1016/j.celrep.2014.12.049
Inoue, K., Ogonuki, N., Kamimura, S., Inoue, H., Matoba, S., Hirose, M., Honda, A., Miura, K., Hada, M., Hasegawa, A., Watanabe, N., Dodo, Y., Mochida, K., & Ogura, A. (2020). Loss of H3K27me3 imprinting in the Sfmbt2 miRNA cluster causes enlargement of cloned mouse placentas. *Nature Communications*, *11*(1), 2150. https://doi.org/10.1038/s41467-020-16044-8
Iqbal, K., Jin, S.-G., Pfeifer, G. P., & Szabó, P. E. (2011). Reprogramming of the paternal genome upon fertilization involves genome-wide oxidation of 5-methylcytosine. *Proceedings of the National Academy of Sciences*, *108*(9), 3642–3647. https://doi.org/10.1073/pnas.1014033108
Jackson, M., Krassowska, A., Gilbert, N., Chevassut, T., Forrester, L., Ansell, J., & Ramsahoye, B. (2004). Severe global DNA hypomethylation blocks differentiation and induces histone hyperacetylation in embryonic stem cells. *Molecular and Cellular Biology*, *24*(20), 8862–8871. https://doi.org/10.1128/MCB.24.20.8862-8871.2004
Janeva, A., Penfold, C. A., Llorente-Armijo, S., Li, H., Zikmund, T., Stock, M., Jullien, J., Straub, T., Forne, I., Imhof, A., Vaquerizas, J. M., Gurdon, J. B., & Hoermanseder, E. B. (2025). *Digital Reprogramming Decodes Epigenetic Barriers of Cell Fate Changes*. https://doi.org/10.1101/2025.01.22.634227
Jansen, C., Paraiso, K. D., Zhou, J. J., Blitz, I. L., Fish, M. B., Charney, R. M., Cho, J. S., Yasuoka, Y., Sudou, N., Bright, A. R., Wlizla, M., Veenstra, G. J. C., Taira, M., Zorn, A. M., Mortazavi, A., & Cho, K. W. Y. (2022). Uncovering the mesendoderm gene regulatory network through multi-omic data integration. *Cell Reports*, *38*(7). https://doi.org/10.1016/j.celrep.2022.110364
Jin, J.-X., Lee, S., Taweechaipaisankul, A., Kim, G. A., & Lee, B. C. (2017). The HDAC Inhibitor LAQ824 Enhances Epigenetic Reprogramming and In Vitro Development of Porcine

SCNT Embryos. *Cellular Physiology and Biochemistry*, *41*(3), 1255–1266. https://doi.org/10.1159/000464389
Jukam, D., Shariati, S. A. M., & Skotheim, J. M. (2017). Zygotic Genome Activation in Vertebrates. *Developmental Cell*, *42*(4), 316–332. https://doi.org/10.1016/j.devcel.2017.07.026
Jullien, J., Åstrand, C., Halley-Stott, R. P., Garrett, N., & Gurdon, J. B. (2010). Characterization of somatic cell nuclear reprogramming by oocytes in which a linker histone is required for pluripotency gene reactivation. *Proceedings of the National Academy of Sciences*, *107*(12), 5483–5488. https://doi.org/10.1073/pnas.1000599107
Jullien, J., Astrand, C., Szenker, E., Garrett, N., Almouzni, G., & Gurdon, J. B. (2012). HIRA dependent H3.3 deposition is required for transcriptional reprogramming following nuclear transfer to Xenopus oocytes. *Epigenetics & Chromatin*, *5*(1), 17. https://doi.org/10.1186/1756-8935-5-17
Jullien, J., Miyamoto, K., Pasque, V., Allen, G. E., Bradshaw, C. R., Garrett, N. J., Halley-Stott, R. P., Kimura, H., Ohsumi, K., & Gurdon, J. B. (2014). Hierarchical Molecular Events Driven by Oocyte-Specific Factors Lead to Rapid and Extensive Reprogramming. *Molecular Cell*, *55*(4), 524–536. https://doi.org/10.1016/j.molcel.2014.06.024
Jullien, J., Vodnala, M., Pasque, V., Oikawa, M., Miyamoto, K., Allen, G., David, S. A., Brochard, V., Wang, S., Bradshaw, C., Koseki, H., Sartorelli, V., Beaujean, N., & Gurdon, J. (2017). Gene Resistance to Transcriptional Reprogramming following Nuclear Transfer Is Directly Mediated by Multiple Chromatin-Repressive Pathways. *Molecular Cell*, *65*(5), 873-884.e8. https://doi.org/10.1016/j.molcel.2017.01.030
Kang, Y.-K., Koo, D.-B., Park, J.-S., Choi, Y.-H., Chung, A.-S., Lee, K.-K., & Han, Y.-M. (2001). Aberrant methylation of donor genome in cloned bovine embryos. *Nature Genetics*, *28*(2), 173–177. https://doi.org/10.1038/88903
Kent, D., Marchetti, L., Mikulasova, A., Russell, L. J., & Rico, D. (2023). Broad H3K4me3 domains: Maintaining cellular identity and their implication in super-enhancer hijacking. *BioEssays*, *45*(10), 2200239. https://doi.org/10.1002/bies.202200239
Kidder, B. L., Hu, G., Yu, Z.-X., Liu, C., & Zhao, K. (2013). Extended Self-Renewal and Accelerated Reprogramming in the Absence of Kdm5b. *Molecular and Cellular Biology*, *33*(24), 4793–4810. https://doi.org/10.1128/MCB.00692-13
Kim, K., Doi, A., Wen, B., Ng, K., Zhao, R., Cahan, P., Kim, J., Aryee, M. J., Ji, H., Ehrlich, L. I. R., Yabuuchi, A., Takeuchi, A., Cunniff, K. C., Hongguang, H., McKinney-Freeman, S., Naveiras, O., Yoon, T. J., Irizarry, R. A., Jung, N., … Daley, G. Q. (2010). Epigenetic memory in induced pluripotent stem cells. *Nature*, *467*(7313), 285–290. https://doi.org/10.1038/nature09342
Kim, K., Zhao, R., Doi, A., Ng, K., Unternaehrer, J., Cahan, P., Huo, H., Loh, Y.-H., Aryee, M. J., Lensch, M. W., Li, H., Collins, J. J., Feinberg, A. P., & Daley, G. Q. (2011). Donor cell type can influence the epigenome and differentiation potential of human induced pluripotent stem cells. *Nature Biotechnology*, *29*(12), 1117–1119. https://doi.org/10.1038/nbt.2052
Kimelman, D., Kirschner, M., & Scherson, T. (1987). The events of the midblastula transition in Xenopus are regulated by changes in the cell cycle. *Cell*, *48*(3), 399–407. https://doi.org/10.1016/0092-8674(87)90191-7
King, T. J., & DiBerardino, M. A. (1965). Transplantation of nuclei from the frog renal adenocarcinoma. I. Development of tumor nuclear-transplant embryos. *Annals of the New York Academy of Sciences*, *126*(1), 115–126. https://doi.org/10.1111/j.1749-6632.1965.tb14271.x
Kishigami, S., & Wakayama, T. (2009). Somatic cell nuclear transfer in the mouse. *Methods in Molecular Biology (Clifton, N.J.)*, *518*, 207–218. https://doi.org/10.1007/978-1-59745-202-1_15

Kretsovali, A., Hadjimichael, C., & Charmpilas, N. (2012). Histone Deacetylase Inhibitors in Cell Pluripotency, Differentiation, and Reprogramming. *Stem Cells International*, *2012*, 1–10. https://doi.org/10.1155/2012/184154

Kulessa, H., Frampton, J., & Graf, T. (1995). GATA-1 reprograms avian myelomonocytic cell lines into eosinophils, thromboblasts, and erythroblasts. *Genes & Development*, *9*(10), 1250–1262. https://doi.org/10.1101/gad.9.10.1250

Ladstätter, S., & Tachibana, K. (2018). Genomic insights into chromatin reprogramming to totipotency in embryos. *Journal of Cell Biology*, *218*(1), 70–82. https://doi.org/10.1083/jcb.201807044

Lasko, L. M., Jakob, C. G., Edalji, R. P., Qiu, W., Montgomery, D., Digiammarino, E. L., Hansen, T. M., Risi, R. M., Frey, R., Manaves, V., Shaw, B., Algire, M., Hessler, P., Lam, L. T., Uziel, T., Faivre, E., Ferguson, D., Buchanan, F. G., Martin, R. L., … Bromberg, K. D. (2017). Discovery of a selective catalytic p300/CBP inhibitor that targets lineage-specific tumours. *Nature*, *550*(7674), 128–132. https://doi.org/10.1038/nature24028

Lavagnolli, T., Gupta, P., Hörmanseder, E., Mira-Bontenbal, H., Dharmalingam, G., Carroll, T., Gurdon, J. B., Fisher, A. G., & Merkenschlager, M. (2015). Initiation and maintenance of pluripotency gene expression in the absence of cohesin. *Genes & Development*, *29*(1), 23–38. https://doi.org/10.1101/gad.251835.114

Lemaitre, J.-M., Danis, E., Pasero, P., Vassetzky, Y., & Méchali, M. (2005). Mitotic Remodeling of the Replicon and Chromosome Structure. *Cell*, *123*(5), 787–801. https://doi.org/10.1016/j.cell.2005.08.045

Li, G.-P., White, K. L., & Bunch, T. D. (2004). Review of enucleation methods and procedures used in animal cloning: State of the art. *Cloning and Stem Cells*, *6*(1), 5–13. https://doi.org/10.1089/15362300460743781

Lim, B., Domsch, K., Mall, M., & Lohmann, I. (2024). Canalizing cell fate by transcriptional repression. *Molecular Systems Biology*, *20*(3), 144–161. https://doi.org/10.1038/s44320-024-00014-z

Lister, R., Pelizzola, M., Kida, Y. S., Hawkins, R. D., Nery, J. R., Hon, G., Antosiewicz-Bourget, J., O'Malley, R., Castanon, R., Klugman, S., Downes, M., Yu, R., Stewart, R., Ren, B., Thomson, J. A., Evans, R. M., & Ecker, J. R. (2011). Hotspots of aberrant epigenomic reprogramming in human induced pluripotent stem cells. *Nature*, *471*(7336), 68–73. https://doi.org/10.1038/nature09798

Liu, W., Liu, X., Wang, C., Gao, Y., Gao, R., Kou, X., Zhao, Y., Li, J., Wu, Y., Xiu, W., Wang, S., Yin, J., Liu, W., Cai, T., Wang, H., Zhang, Y., & Gao, S. (2016). Identification of key factors conquering developmental arrest of somatic cell cloned embryos by combining embryo biopsy and single-cell sequencing. *Cell Discovery*, *2*(1), 16010. https://doi.org/10.1038/celldisc.2016.10

Liu, Y., Pelham-Webb, B., Di Giammartino, D. C., Li, J., Kim, D., Kita, K., Saiz, N., Garg, V., Doane, A., Giannakakou, P., Hadjantonakis, A.-K., Elemento, O., & Apostolou, E. (2017). Widespread Mitotic Bookmarking by Histone Marks and Transcription Factors in Pluripotent Stem Cells. *Cell Reports*, *19*(7), 1283–1293. https://doi.org/10.1016/j.celrep.2017.04.067

Liu, Y., Wu, F., Zhang, L., Wu, X., Li, D., Xin, J., Xie, J., Kong, F., Wang, W., Wu, Q., Zhang, D., Wang, R., Gao, S., & Li, W. (2018). Transcriptional defects and reprogramming barriers in somatic cell nuclear reprogramming as revealed by single-embryo RNA sequencing. *BMC Genomics*, *19*(1), Article 1. https://doi.org/10.1186/s12864-018-5091-1

Long, C., Li, H., Li, X., Yang, W., & Zuo, Y. (2021). Nuclear Transfer Arrest Embryos Show Massive Dysregulation of Genes Involved in Transcription Pathways. *International Journal of Molecular Sciences*, *22*(15), 8187. https://doi.org/10.3390/ijms22158187

Love, M. I., Huber, W., & Anders, S. (2014). Moderated estimation of fold change and dispersion for RNA-seq data with DESeq2. *Genome Biology*, *15*(12), 550. https://doi.org/10.1186/s13059-014-0550-8

Lu, F., & Zhang, Y. (2015). Cell totipotency: Molecular features, induction, and maintenance. *National Science Review*, *2*(2), 217–225. https://doi.org/10.1093/nsr/nwv009

Luger, K., Mäder, A. W., Richmond, R. K., Sargent, D. F., & Richmond, T. J. (1997). Crystal structure of the nucleosome core particle at 2.8 A resolution. *Nature*, *389*(6648), 251–260. https://doi.org/10.1038/38444

Mai, T., Markov, G. J., Brady, J. J., Palla, A., Zeng, H., Sebastiano, V., & Blau, H. M. (2018). NKX3-1 is required for induced pluripotent stem cell reprogramming and can replace OCT4 in mouse and human iPSC induction. *Nature Cell Biology*, *20*(8), 900–908. https://doi.org/10.1038/s41556-018-0136-x

Mali, P., Chou, B.-K., Yen, J., Ye, Z., Zou, J., Dowey, S., Brodsky, R. A., Ohm, J. E., Yu, W., Baylin, S. B., Yusa, K., Bradley, A., Meyers, D. J., Mukherjee, C., Cole, P. A., & Cheng, L. (2010). Butyrate Greatly Enhances Derivation of Human Induced Pluripotent Stem Cells by Promoting Epigenetic Remodeling and the Expression of Pluripotency-Associated Genes. *Stem Cells*, *28*(4), 713–720. https://doi.org/10.1002/stem.402

Mall, M., & Wernig, M. (2017). The novel tool of cell reprogramming for applications in molecular medicine. *Journal of Molecular Medicine*, *95*(7), 695–703. https://doi.org/10.1007/s00109-017-1550-4

Manning, E. T., Ikehara, T., Ito, T., Kadonaga, J. T., & Kraus, W. L. (2001). p300 Forms a Stable, Template-Committed Complex with Chromatin: Role for the Bromodomain. *Molecular and Cellular Biology*, *21*(12), 3876–3887. https://doi.org/10.1128/MCB.21.12.3876-3887.2001

Mansour, A. A., Gafni, O., Weinberger, L., Zviran, A., Ayyash, M., Rais, Y., Krupalnik, V., Zerbib, M., Amann-Zalcenstein, D., Maza, I., Geula, S., Viukov, S., Holtzman, L., Pribluda, A., Canaani, E., Horn-Saban, S., Amit, I., Novershtern, N., & Hanna, J. H. (2012). The H3K27 demethylase Utx regulates somatic and germ cell epigenetic reprogramming. *Nature*, *488*(7411), 409–413. https://doi.org/10.1038/nature11272

Matoba, S., Liu, Y., Lu, F., Iwabuchi, K. A., Shen, L., Inoue, A., & Zhang, Y. (2014a). Embryonic development following somatic cell nuclear transfer impeded by persisting histone methylation. *Cell*, *159*(4), Article 4. https://doi.org/10.1016/j.cell.2014.09.055

Matoba, S., Liu, Y., Lu, F., Iwabuchi, K. A., Shen, L., Inoue, A., & Zhang, Y. (2014b). Embryonic development following somatic cell nuclear transfer impeded by persisting histone methylation. *Cell*, *159*(4), 884–895. https://doi.org/10.1016/j.cell.2014.09.055

Matoba, S., Wang, H., Jiang, L., Lu, F., Iwabuchi, K. A., Wu, X., Inoue, K., Yang, L., Press, W., Lee, J. T., Ogura, A., Shen, L., & Zhang, Y. (2018). Loss of H3K27me3 Imprinting in Somatic Cell Nuclear Transfer Embryos Disrupts Post-Implantation Development. *Cell Stem Cell*, *23*(3), 343-354.e5. https://doi.org/10.1016/j.stem.2018.06.008

Matoba, S., & Zhang, Y. (2018). Somatic Cell Nuclear Transfer Reprogramming: Mechanisms and Applications. *Cell Stem Cell*, *23*(4), 471–485. https://doi.org/10.1016/j.stem.2018.06.018

Meissner, A., Mikkelsen, T. S., Gu, H., Wernig, M., Hanna, J., Sivachenko, A., Zhang, X., Bernstein, B. E., Nusbaum, C., Jaffe, D. B., Gnirke, A., Jaenisch, R., & Lander, E. S. (2008). Genome-scale DNA methylation maps of pluripotent and differentiated cells. *Nature*, *454*(7205), 766–770. https://doi.org/10.1038/nature07107

Melis, D. A., & Jaakkola, T. (2018). *Towards Robust Interpretability with Self-Explaining Neural Networks*.

Meyer, C. A., & Liu, X. S. (2014). Identifying and mitigating bias in next-generation sequencing methods for chromatin biology. *Nature Reviews Genetics*, *15*(11), 709–721. https://doi.org/10.1038/nrg3788

Mikkelsen, T. S., Hanna, J., Zhang, X., Ku, M., Wernig, M., Schorderet, P., Bernstein, B. E., Jaenisch, R., Lander, E. S., & Meissner, A. (2008). Dissecting direct reprogramming through integrative genomic analysis. *Nature*, *454*(7200), 49–55. https://doi.org/10.1038/nature07056

Millán-Zambrano, G., Burton, A., Bannister, A. J., & Schneider, R. (2022). Histone post-translational modifications—Cause and consequence of genome function. *Nature Reviews Genetics*, *23*(9), 563–580. https://doi.org/10.1038/s41576-022-00468-7

Miyamoto, K. (2019). Various nuclear reprogramming systems using egg and oocyte materials. *Journal of Reproduction and Development*, *65*(3), 203–208. https://doi.org/10.1262/jrd.2019-002

Miyamoto, K., Pasque, V., Jullien, J., & Gurdon, J. B. (2011). Nuclear actin polymerization is required for transcriptional reprogramming of *Oct4* by oocytes. *Genes & Development*, *25*(9), 946–958. https://doi.org/10.1101/gad.615211

Miyamoto, K., Teperek, M., Yusa, K., Allen, G. E., Bradshaw, C. R., & Gurdon, J. B. (2013). Nuclear Wave1 Is Required for Reprogramming Transcription in Oocytes and for Normal Development. *Science*, *341*(6149), 1002–1005. https://doi.org/10.1126/science.1240376

Morgan, M. A. J., & Shilatifard, A. (2020). Reevaluating the roles of histone-modifying enzymes and their associated chromatin modifications in transcriptional regulation. *Nature Genetics*, *52*(12), 1271–1281. https://doi.org/10.1038/s41588-020-00736-4

Morris, S. A., Shibata, Y., Noma, K., Tsukamoto, Y., Warren, E., Temple, B., Grewal, S. I. S., & Strahl, B. D. (2005). Histone H3 K36 Methylation Is Associated with Transcription Elongation in *Schizosaccharomyces pombe*. *Eukaryotic Cell*, *4*(8), 1446–1454. https://doi.org/10.1128/EC.4.8.1446-1454.2005

Mukherjee, S., Chaturvedi, P., Rankin, S. A., Fish, M. B., Wlizla, M., Paraiso, K. D., MacDonald, M., Chen, X., Weirauch, M. T., Blitz, I. L., Cho, K. W., & Zorn, A. M. (2020). Sox17 and β-catenin co-occupy Wnt-responsive enhancers to govern the endoderm gene regulatory network. *eLife*, *9*, e58029. https://doi.org/10.7554/eLife.58029

Nakatani, T. (2025). Dynamics of replication timing during mammalian development. *Trends in Genetics*, *0*(0). https://doi.org/10.1016/j.tig.2025.01.010

Nakatani, T., Lin, J., Ji, F., Ettinger, A., Pontabry, J., Tokoro, M., Altamirano-Pacheco, L., Fiorentino, J., Mahammadov, E., Hatano, Y., Van Rechem, C., Chakraborty, D., Ruiz-Morales, E. R., Arguello Pascualli, P. Y., Scialdone, A., Yamagata, K., Whetstine, J. R., Sadreyev, R. I., & Torres-Padilla, M.-E. (2022). DNA replication fork speed underlies cell fate changes and promotes reprogramming. *Nature Genetics*, *54*(3), 318–327. https://doi.org/10.1038/s41588-022-01023-0

Nakatsukasa, Y., Yamada, Y., & Yamada, Y. (2025). Research of *in vivo* reprogramming toward clinical applications in regenerative medicine: A concise review. *Regenerative Therapy*, *28*, 12–19. https://doi.org/10.1016/j.reth.2024.11.008

Narita, T., Ito, S., Higashijima, Y., Chu, W. K., Neumann, K., Walter, J., Satpathy, S., Liebner, T., Hamilton, W. B., Maskey, E., Prus, G., Shibata, M., Iesmantavicius, V., Brickman, J. M., Anastassiadis, K., Koseki, H., & Choudhary, C. (2021). Enhancers are activated by p300/CBP activity-dependent PIC assembly, RNAPII recruitment, and pause release. *Molecular Cell*, *81*(10), 2166-2182.e6. https://doi.org/10.1016/j.molcel.2021.03.008

Nashun, B., Hill, P. W., & Hajkova, P. (2015). Reprogramming of cell fate: Epigenetic memory and the erasure of memories past. *The EMBO Journal*, *34*(10), 1296–1308. https://doi.org/10.15252/embj.201490649

Ng, R. K., & Gurdon, J. B. (2005). Epigenetic memory of active gene transcription is inherited through somatic cell nuclear transfer. *Proceedings of the National Academy of Sciences*, *102*(6), 1957–1962. https://doi.org/10.1073/pnas.0409813102

Ng, R. K., & Gurdon, J. B. (2008a). Epigenetic inheritance of cell differentiation status. *Cell Cycle*, *7*(9), 1173–1177. https://doi.org/10.4161/cc.7.9.5791

Ng, R. K., & Gurdon, J. B. (2008b). Epigenetic memory of an active gene state depends on histone H3.3 incorporation into chromatin in the absence of transcription. *Nature Cell Biology*, *10*(1), 102–109. https://doi.org/10.1038/ncb1674

Nieuwkoop, J. F., P. D. (Ed.). (2020). *Normal Table of Xenopus Laevis (Daudin): A Systematical & Chronological Survey of the Development from the Fertilized Egg till the End of Metamorphosis*. Garland Science. https://doi.org/10.1201/9781003064565

Oak, M. S., & Hörmanseder, E. (2022). Using Xenopus to Understand Pluripotency and to Reprogram Cells for Therapeutic Use. In S. A. Moody & A. Fainsod, *Xenopus* (1st ed., pp. 325–335). CRC Press. https://doi.org/10.1201/9781003050230-26

Oak, M., Stock, M., Mezes, M., Straub, T., Hynes-Allen, A., van den Ameele, J., Forne, I., Ettinger, A., Imhof, A., Scialdone, A., & Hörmanseder, E. (2025). *H3K4 methylation-promoted transcriptional memory ensures faithful zygotic genome activation and embryonic developmen*. https://doi.org/10.1101/2025.01.20.633863

Ogryzko, V. V., Schiltz, R. L., Russanova, V., Howard, B. H., & Nakatani, Y. (1996). The Transcriptional Coactivators p300 and CBP Are Histone Acetyltransferases. *Cell*, *87*(5), 953–959. https://doi.org/10.1016/S0092-8674(00)82001-2

Ohi, Y., Qin, H., Hong, C., Blouin, L., Polo, J. M., Guo, T., Qi, Z., Downey, S. L., Manos, P. D., Rossi, D. J., Yu, J., Hebrok, M., Hochedlinger, K., Costello, J. F., Song, J. S., & Ramalho-Santos, M. (2011). Incomplete DNA methylation underlies a transcriptional memory of somatic cells in human iPS cells. *Nature Cell Biology*, *13*(5), 541–549. https://doi.org/10.1038/ncb2239

Olbrich, T., Vega-Sendino, M., Tillo, D., Wu, W., Zolnerowich, N., Pavani, R., Tran, A. D., Domingo, C. N., Franco, M., Markiewicz-Potoczny, M., Pegoraro, G., FitzGerald, P. C., Kruhlak, M. J., Lazzerini-Denchi, E., Nora, E. P., Nussenzweig, A., & Ruiz, S. (2021). CTCF is a barrier for 2C-like reprogramming. *Nature Communications*, *12*(1), 4856. https://doi.org/10.1038/s41467-021-25072-x

Onder, T. T., Kara, N., Cherry, A., Sinha, A. U., Zhu, N., Bernt, K. M., Cahan, P., Mancarci, B. O., Unternaehrer, J., Gupta, P. B., Lander, E. S., Armstrong, S. A., & Daley, G. Q. (2012). Chromatin-modifying enzymes as modulators of reprogramming. *Nature*, *483*(7391), 598–602. https://doi.org/10.1038/nature10953

Oomen, M. E., Hansen, A. S., Liu, Y., Darzacq, X., & Dekker, J. (2019). CTCF sites display cell cycle–dependent dynamics in factor binding and nucleosome positioning. *Genome Research*, *29*(2), 236–249. https://doi.org/10.1101/gr.241547.118

Ortega, E., Rengachari, S., Ibrahim, Z., Hoghoughi, N., Gaucher, J., Holehouse, A. S., Khochbin, S., & Panne, D. (2018). Transcription factor dimerization activates the p300 acetyltransferase. *Nature*, *562*(7728), 538–544. https://doi.org/10.1038/s41586-018-0621-1

Palozola, K. C., Lerner, J., & Zaret, K. S. (2019). A changing paradigm of transcriptional memory propagation through mitosis. *Nature Reviews. Molecular Cell Biology*, *20*(1), 55–64. https://doi.org/10.1038/s41580-018-0077-z

Papp, B., & Plath, K. (2013). Epigenetics of reprogramming to induced pluripotency. *Cell*, *152*(6), 1324–1343. https://doi.org/10.1016/j.cell.2013.02.043

Paraiso, K. D., Blitz, I. L., Coley, M., Cheung, J., Sudou, N., Taira, M., & Cho, K. W. Y. (2019). Endodermal Maternal Transcription Factors Establish Super-Enhancers during Zygotic Genome Activation. *Cell Reports*, *27*(10), 2962-2977.e5. https://doi.org/10.1016/j.celrep.2019.05.013

Park, S., Stanfield, R. L., Martinez-Yamout, M. A., Dyson, H. J., Wilson, I. A., & Wright, P. E. (2017). Role of the CBP catalytic core in intramolecular SUMOylation and control of histone H3 acetylation. *Proceedings of the National Academy of Sciences*, *114*(27). https://doi.org/10.1073/pnas.1703105114

Pasini, D., Malatesta, M., Jung, H. R., Walfridsson, J., Willer, A., Olsson, L., Skotte, J., Wutz, A., Porse, B., Jensen, O. N., & Helin, K. (2010). Characterization of an antagonistic switch between histone H3 lysine 27 methylation and acetylation in the transcriptional regulation of Polycomb group target genes. *Nucleic Acids Research*, *38*(15), 4958–4969. https://doi.org/10.1093/nar/gkq244

Pasque, V., Halley-Stott, R. P., Gillich, A., Garrett, N., & Gurdon, J. B. (2011). Epigenetic stability of repressed states involving the histone variant macroH2A revealed by nuclear transfer to Xenopus oocytes. *Nucleus*, *2*(6), 533–539. https://doi.org/10.4161/nucl.2.6.17799

Pasque, V., Jullien, J., Miyamoto, K., Halley-Stott, R. P., & Gurdon, J. B. (2011). Epigenetic factors influencing resistance to nuclear reprogramming. *Trends in Genetics*, *27*(12), 516–525. https://doi.org/10.1016/j.tig.2011.08.002

Pelham-Webb, B., Polyzos, A., Wojenski, L., Kloetgen, A., Li, J., Di Giammartino, D. C., Sakellaropoulos, T., Tsirigos, A., Core, L., & Apostolou, E. (2021). H3K27ac bookmarking promotes rapid post-mitotic activation of the pluripotent stem cell program without impacting 3D chromatin reorganization. *Molecular Cell*, *81*(8), 1732-1748.e8. https://doi.org/10.1016/j.molcel.2021.02.032

Perrimon, N., Pitsouli, C., & Shilo, B.-Z. (2012). Signaling Mechanisms Controlling Cell Fate and Embryonic Patterning. *Cold Spring Harbor Perspectives in Biology*, *4*(8), a005975. https://doi.org/10.1101/cshperspect.a005975

Phelps, W. A., Hurton, M. D., Ayers, T. N., Carlson, A. E., Rosenbaum, J. C., & Lee, M. T. (2023). Hybridization led to a rewired pluripotency network in the allotetraploid Xenopus laevis. *eLife*, *12*, e83952. https://doi.org/10.7554/eLife.83952

Polejaeva, I. A., Chen, S.-H., Vaught, T. D., Page, R. L., Mullins, J., Ball, S., Dai, Y., Boone, J., Walker, S., Ayares, D. L., Colman, A., & Campbell, K. H. S. (2000). Cloned pigs produced by nuclear transfer from adult somatic cells. *Nature*, *407*(6800), 86–90. https://doi.org/10.1038/35024082

Polo, J. M., Anderssen, E., Walsh, R. M., Schwarz, B. A., Nefzger, C. M., Lim, S. M., Borkent, M., Apostolou, E., Alaei, S., Cloutier, J., Bar-Nur, O., Cheloufi, S., Stadtfeld, M., Figueroa, M. E., Robinton, D., Natesan, S., Melnick, A., Zhu, J., Ramaswamy, S., & Hochedlinger, K. (2012). A Molecular Roadmap of Reprogramming Somatic Cells into iPS Cells. *Cell*, *151*(7), 1617–1632. https://doi.org/10.1016/j.cell.2012.11.039

Polo, J. M., Liu, S., Figueroa, M. E., Kulalert, W., Eminli, S., Tan, K. Y., Apostolou, E., Stadtfeld, M., Li, Y., Shioda, T., Natesan, S., Wagers, A. J., Melnick, A., Evans, T., & Hochedlinger, K. (2010). Cell type of origin influences the molecular and functional properties of mouse induced pluripotent stem cells. *Nature Biotechnology*, *28*(8), 848–855. https://doi.org/10.1038/nbt.1667

Prather, R. S., Barnes, F. L., Sims, M. M., Robl, J. M., Eyestone, W. H., & First, N. L. (1987). Nuclear transplantation in the bovine embryo: Assessment of donor nuclei and recipient oocyte. *Biology of Reproduction*, *37*(4), 859–866. https://doi.org/10.1095/biolreprod37.4.859

Rada-Iglesias, A., Bajpai, R., Swigut, T., Brugmann, S. A., Flynn, R. A., & Wysocka, J. (2011). A unique chromatin signature uncovers early developmental enhancers in humans. *Nature*, *470*(7333), 279–283. https://doi.org/10.1038/nature09692

Raisner, R., Kharbanda, S., Jin, L., Jeng, E., Chan, E., Merchant, M., Haverty, P. M., Bainer, R., Cheung, T., Arnott, D., Flynn, E. M., Romero, F. A., Magnuson, S., & Gascoigne, K. E. (2018). Enhancer Activity Requires CBP/P300 Bromodomain-Dependent Histone H3K27 Acetylation. *Cell Reports*, *24*(7), 1722–1729. https://doi.org/10.1016/j.celrep.2018.07.041

Rao, A., & LaBonne, C. (2018). Histone Deacetylase activity plays an essential role in establishing and maintaining the vertebrate neural crest. *Development*, dev.163386. https://doi.org/10.1242/dev.163386

Rao, R. A., Dhele, N., Cheemadan, S., Ketkar, A., Jayandharan, G. R., Palakodeti, D., & Rampalli, S. (2015). Ezh2 mediated H3K27me3 activity facilitates somatic transition during human pluripotent reprogramming. *Scientific Reports*, *5*(1), 8229. https://doi.org/10.1038/srep08229

Reik, W. (2007). Stability and flexibility of epigenetic gene regulation in mammalian development. *Nature*, *447*(7143), 425–432. https://doi.org/10.1038/nature05918

Reinberg, D., & Vales, L. D. (2018). Chromatin domains rich in inheritance. *Science (New York, N.Y.)*, *361*(6397), Article 6397. https://doi.org/10.1126/science.aat7871

Russo, V. E., Martienssen, R. A., & Riggs, A. D. (1996). *Epigenetic mechanisms of gene regulation.*

Rybouchkin, A., Kato, Y., & Tsunoda, Y. (2006). Role of Histone Acetylation in Reprogramming of Somatic Nuclei Following Nuclear Transfer1. *Biology of Reproduction*, *74*(6), 1083–1089. https://doi.org/10.1095/biolreprod.105.047456

Samavarchi-Tehrani, P., Golipour, A., David, L., Sung, H., Beyer, T. A., Datti, A., Woltjen, K., Nagy, A., & Wrana, J. L. (2010). Functional Genomics Reveals a BMP-Driven Mesenchymal-to-Epithelial Transition in the Initiation of Somatic Cell Reprogramming. *Cell Stem Cell*, *7*(1), 64–77. https://doi.org/10.1016/j.stem.2010.04.015

Sankar, A., Mohammad, F., Sundaramurthy, A. K., Wang, H., Lerdrup, M., Tatar, T., & Helin, K. (2022). Histone editing elucidates the functional roles of H3K27 methylation and acetylation in mammals. *Nature Genetics*, *54*(6), 754–760. https://doi.org/10.1038/s41588-022-01091-2

Santos-Rosa, H., Schneider, R., Bannister, A. J., Sherriff, J., Bernstein, B. E., Emre, N. C. T., Schreiber, S. L., Mellor, J., & Kouzarides, T. (2002). Active genes are tri-methylated at K4 of histone H3. *Nature*, *419*(6905), Article 6905. https://doi.org/10.1038/nature01080

Sato, Y., Hilbert, L., Oda, H., Wan, Y., Heddleston, J. M., Chew, T.-L., Zaburdaev, V., Keller, P., Lionnet, T., Vastenhouw, N., & Kimura, H. (2019). Histone H3K27 acetylation precedes active transcription during zebrafish zygotic genome activation as revealed by live-cell analysis. *Development*, *146*(19), dev179127. https://doi.org/10.1242/dev.179127

Schneuwly, S., Klemenz, R., & Gehring, W. J. (1987). Redesigning the body plan of Drosophila by ectopic expression of the homoeotic gene Antennapedia. *Nature*, *325*(6107), 816–818. https://doi.org/10.1038/325816a0

Scott, M. P., Weiner, A. J., Hazelrigg, T. I., Polisky, B. A., Pirrotta, V., Scalenghe, F., & Kaufman, T. C. (1983). The molecular organization of the Antennapedia locus of drosophila. *Cell*, *35*(3), 763–776. https://doi.org/10.1016/0092-8674(83)90109-5

Seto, E., & Yoshida, M. (2014). Erasers of Histone Acetylation: The Histone Deacetylase Enzymes. *Cold Spring Harbor Perspectives in Biology*, *6*(4), a018713–a018713. https://doi.org/10.1101/cshperspect.a018713

Shechter, D., Chitta, R. K., Xiao, A., Shabanowitz, J., Hunt, D. F., & Allis, C. D. (2009). A distinct H2A.X isoform is enriched in *Xenopus laevis* eggs and early embryos and is phosphorylated in the absence of a checkpoint. *Proceedings of the National Academy of Sciences*, *106*(3), 749–754. https://doi.org/10.1073/pnas.0812207106

Shen, L., Inoue, A., He, J., Liu, Y., Lu, F., & Zhang, Y. (2014). Tet3 and DNA Replication Mediate Demethylation of Both the Maternal and Paternal Genomes in Mouse Zygotes. *Cell Stem Cell*, *15*(4), 459–471. https://doi.org/10.1016/j.stem.2014.09.002

Shvedunova, M., & Akhtar, A. (2022). Modulation of cellular processes by histone and non-histone protein acetylation. *Nature Reviews Molecular Cell Biology*, *23*(5), 329–349. https://doi.org/10.1038/s41580-021-00441-y

Sinner, D., Kirilenko, P., Rankin, S., Wei, E., Howard, L., Kofron, M., Heasman, J., Woodland, H. R., & Zorn, A. M. (2006). Global analysis of the transcriptional network controlling Xenopus endoderm formation. *Development*, *133*(10), 1955–1966. https://doi.org/10.1242/dev.02358

Sive, H. L., Grainger, R. M., & Harland, R. M. (2000). *Early development of Xenopus laevis: A laboratory manual*. Cold Spring Harbor Laboratory Press.
Skene, P. J., Henikoff, J. G., & Henikoff, S. (2018). Targeted in situ genome-wide profiling with high efficiency for low cell numbers. *Nature Protocols*, *13*(5), 1006–1019. https://doi.org/10.1038/nprot.2018.015
Soufi, A., Donahue, G., & Zaret, K. S. (2012). Facilitators and Impediments of the Pluripotency Reprogramming Factors' Initial Engagement with the Genome. *Cell*, *151*(5), 994–1004. https://doi.org/10.1016/j.cell.2012.09.045
Soufi, A., Garcia, M. F., Jaroszewicz, A., Osman, N., Pellegrini, M., & Zaret, K. S. (2015). Pioneer Transcription Factors Target Partial DNA Motifs on Nucleosomes to Initiate Reprogramming. *Cell*, *161*(3), 555–568. https://doi.org/10.1016/j.cell.2015.03.017
Spitz, F., & Furlong, E. E. M. (2012). Transcription factors: From enhancer binding to developmental control. *Nature Reviews Genetics*, *13*(9), 613–626. https://doi.org/10.1038/nrg3207
Sridharan, R., Gonzales-Cope, M., Chronis, C., Bonora, G., McKee, R., Huang, C., Patel, S., Lopez, D., Mishra, N., Pellegrini, M., Carey, M., Garcia, B. A., & Plath, K. (2013). Proteomic and genomic approaches reveal critical functions of H3K9 methylation and Heterochromatin Protein-1γ in reprogramming to pluripotency. *Nature Cell Biology*, *15*(7), 872–882. https://doi.org/10.1038/ncb2768
Staszkiewicz, J., Power, R. A., Harkins, L. L., Barnes, C. W., Strickler, K. L., Rim, J. S., Bondioli, K. R., & Eilersten, K. J. (2013). Silencing Histone Deacetylase–Specific Isoforms Enhances Expression of Pluripotency Genes in Bovine Fibroblasts. *Cellular Reprogramming*, *15*(5), 397–404. https://doi.org/10.1089/cell.2013.0026
Stevens, M. L., Chaturvedi, P., Rankin, S. A., Macdonald, M., Jagannathan, S., Yukawa, M., Barski, A., & Zorn, A. M. (2017). Genomic integration of Wnt/β-catenin and BMP/Smad1 signaling coordinates foregut and hindgut transcriptional program. *Development*, dev.145789. https://doi.org/10.1242/dev.145789
Stewart-Morgan, K. R., Petryk, N., & Groth, A. (2020). Chromatin replication and epigenetic cell memory. *Nature Cell Biology*, *22*(4), 361–371. https://doi.org/10.1038/s41556-020-0487-y
Szabo, E., Rampalli, S., Risueño, R. M., Schnerch, A., Mitchell, R., Fiebig-Comyn, A., Levadoux-Martin, M., & Bhatia, M. (2010). Direct conversion of human fibroblasts to multilineage blood progenitors. *Nature*, *468*(7323), 521–526. https://doi.org/10.1038/nature09591
Takahashi, K., Tanabe, K., Ohnuki, M., Narita, M., Ichisaka, T., Tomoda, K., & Yamanaka, S. (2007). Induction of Pluripotent Stem Cells from Adult Human Fibroblasts by Defined Factors. *Cell*, *131*(5), 861–872. https://doi.org/10.1016/j.cell.2007.11.019
Takahashi, K., & Yamanaka, S. (2006). Induction of Pluripotent Stem Cells from Mouse Embryonic and Adult Fibroblast Cultures by Defined Factors. *Cell*, *126*(4), 663–676. https://doi.org/10.1016/j.cell.2006.07.024
Tamada, H., Thuan, N. V., Reed, P., Nelson, D., Katoku-Kikyo, N., Wudel, J., Wakayama, T., & Kikyo, N. (2006). Chromatin Decondensation and Nuclear Reprogramming by Nucleoplasmin. *MOL. CELL. BIOL.*, *26*.
Tao, J., Zhang, Y., Zuo, X., Hong, R., Li, H., Liu, X., Huang, W., Cao, Z., & Zhang, Y. (2017). DOT1L inhibitor improves early development of porcine somatic cell nuclear transfer embryos. *PLOS ONE*, *12*(6), e0179436. https://doi.org/10.1371/journal.pone.0179436
Tie, F., Banerjee, R., Stratton, C. A., Prasad-Sinha, J., Stepanik, V., Zlobin, A., Diaz, M. O., Scacheri, P. C., & Harte, P. J. (2009). CBP-mediated acetylation of histone H3 lysine 27 antagonizes *Drosophila* Polycomb silencing. *Development*, *136*(18), 3131–3141. https://doi.org/10.1242/dev.037127

Tokmakov, A. A., Iwasaki, T., Sato, K.-I., & Kamada, S. (2016). Reprogramming of somatic cells and nuclei by Xenopus oocyte and egg extracts. *The International Journal of Developmental Biology*, *60*(7-8–9), 289–296. https://doi.org/10.1387/ijdb.160163at

Tsunoda, Y., Yasui, T., Shioda, Y., Nakamura, K., Uchida, T., & Sugie, T. (1987). Full-term development of mouse blastomere nuclei transplanted into enucleated two-cell embryos. *Journal of Experimental Zoology*, *242*(2), 147–151. https://doi.org/10.1002/jez.1402420205

Ulferts, S., Lopes, M., Miyamoto, K., & Grosse, R. (2024). Nuclear actin dynamics and functions at a glance. *Journal of Cell Science*, *137*(6), jcs261630. https://doi.org/10.1242/jcs.261630

Vastenhouw, N. L., Cao, W. X., & Lipshitz, H. D. (2019). The maternal-to-zygotic transition revisited. *Development*, *146*(11), dev161471. https://doi.org/10.1242/dev.161471

Vierbuchen, T., Ostermeier, A., Pang, Z. P., Kokubu, Y., Südhof, T. C., & Wernig, M. (2010). Direct conversion of fibroblasts to functional neurons by defined factors. *Nature*, *463*(7284), 1035–1041. https://doi.org/10.1038/nature08797

Waddington, C. H. (2014). *The strategy of the genes*. Routledge.

Wakayama, T., Perry, A. C. F., Zuccotti, M., Johnson, K. R., & Yanagimachi, R. (1998). Full-term development of mice from enucleated oocytes injected with cumulus cell nuclei. *Nature*, *394*(6691), 369–374. https://doi.org/10.1038/28615

Wang, L.-Y., Li, Z.-K., Wang, L.-B., Liu, C., Sun, X.-H., Feng, G.-H., Wang, J.-Q., Li, Y.-F., Qiao, L.-Y., Nie, H., Jiang, L.-Y., Sun, H., Xie, Y.-L., Ma, S.-N., Wan, H.-F., Lu, F.-L., Li, W., & Zhou, Q. (2020). Overcoming Intrinsic H3K27me3 Imprinting Barriers Improves Post-implantation Development after Somatic Cell Nuclear Transfer. *Cell Stem Cell*, *27*(2), 315-325.e5. https://doi.org/10.1016/j.stem.2020.05.014

Wang, M., Chen, Z., & Zhang, Y. (2022). CBP /p300 and HDAC activities regulate H3K27 acetylation dynamics and zygotic genome activation in mouse preimplantation embryos. *The EMBO Journal*, *41*(22), e112012. https://doi.org/10.15252/embj.2022112012

Weinert, B. T., Narita, T., Satpathy, S., Srinivasan, B., Hansen, B. K., Schölz, C., Hamilton, W. B., Zucconi, B. E., Wang, W. W., Liu, W. R., Brickman, J. M., Kesicki, E. A., Lai, A., Bromberg, K. D., Cole, P. A., & Choudhary, C. (2018). Time-Resolved Analysis Reveals Rapid Dynamics and Broad Scope of the CBP/p300 Acetylome. *Cell*, *174*(1), 231-244.e12. https://doi.org/10.1016/j.cell.2018.04.033

Wen, D., Banaszynski, L. A., Liu, Y., Geng, F., Noh, K.-M., Xiang, J., Elemento, O., Rosenwaks, Z., Allis, C. D., & Rafii, S. (2014). Histone variant H3.3 is an essential maternal factor for oocyte reprogramming. *Proceedings of the National Academy of Sciences*, *111*(20), 7325–7330. https://doi.org/10.1073/pnas.1406389111

Wong, M. M., Byun, J. S., Sacta, M., Jin, Q., Baek, S., & Gardner, K. (2014). Promoter-Bound p300 Complexes Facilitate Post-Mitotic Transmission of Transcriptional Memory. *PLoS ONE*, *9*(6), e99989. https://doi.org/10.1371/journal.pone.0099989

Wong, W. T., Matrone, G., Tian, X., Tomoiaga, S. A., Au, K. F., Meng, S., Yamazoe, S., Sieveking, D., Chen, K., Burns, D. M., Chen, J. K., Blau, H. M., & Cooke, J. P. (2017). Discovery of novel determinants of endothelial lineage using chimeric heterokaryons. *eLife*, *6*, e23588. https://doi.org/10.7554/eLife.23588

Wossidlo, M., Arand, J., Sebastiano, V., Lepikhov, K., Boiani, M., Reinhardt, R., Schöler, H., & Walter, J. (2010). Dynamic link of DNA demethylation, DNA strand breaks and repair in mouse zygotes. *The EMBO Journal*, *29*(11), 1877–1888. https://doi.org/10.1038/emboj.2010.80

Wossidlo, M., Nakamura, T., Lepikhov, K., Marques, C. J., Zakhartchenko, V., Boiani, M., Arand, J., Nakano, T., Reik, W., & Walter, J. (2011). 5-Hydroxymethylcytosine in the mammalian zygote is linked with epigenetic reprogramming. *Nature Communications*, *2*(1), 241. https://doi.org/10.1038/ncomms1240

Wu, K., Fan, D., Zhao, H., Liu, Z., Hou, Z., Tao, W., Yu, G., Yuan, S., Zhu, X., Kang, M., Tian, Y., Chen, Z.-J., Liu, J., & Gao, L. (2023). Dynamics of histone acetylation during human early embryogenesis. *Cell Discovery*, *9*(1), 29. https://doi.org/10.1038/s41421-022-00514-y

Wu, X., Wu, X., & Xie, W. (2023). Activation, decommissioning, and dememorization: Enhancers in a life cycle. *Trends in Biochemical Sciences*, *48*(8), 673–688. https://doi.org/10.1016/j.tibs.2023.04.005

Xie, B., Zhang, H., Wei, R., Li, Q., Weng, X., Kong, Q., & Liu, Z. (2016). Histone H3 lysine 27 trimethylation acts as an epigenetic barrier in porcine nuclear reprogramming. *REPRODUCTION*, *151*(1), 9–16. https://doi.org/10.1530/REP-15-0338

Xie, H., Ye, M., Feng, R., & Graf, T. (2004). Stepwise reprogramming of B cells into macrophages. *Cell*, *117*(5), 663–676. https://doi.org/10.1016/s0092-8674(04)00419-2

Yamanaka, S., & Blau, H. M. (2010). Nuclear reprogramming to a pluripotent state by three approaches. *Nature*, *465*(7299), 704–712. https://doi.org/10.1038/nature09229

Yamauchi, Y., Ward, M. A., & Ward, W. S. (2009). *Asynchronous DNA replication and origin licensing in the mouse one‐cell embryo*. https://doi.org/10.1002/jcb.22117

Yang, G., Zhang, L., Liu, W., Qiao, Z., Shen, S., Zhu, Q., Gao, R., Wang, M., Wang, M., Li, C., Liu, M., Sun, J., Wang, L., Liu, W., Cui, X., Zhao, K., Zang, R., Chen, M., Liang, Z., … Jiang, C. (2021). Dux-Mediated Corrections of Aberrant H3K9ac during 2-Cell Genome Activation Optimize Efficiency of Somatic Cell Nuclear Transfer. *Cell Stem Cell*, *28*(1), 150-163.e5. https://doi.org/10.1016/j.stem.2020.09.006

Yang, L., Song, L., Liu, X., Bai, L., & Li, G. (2018). KDM 6A and KDM 6B play contrasting roles in nuclear transfer embryos revealed by MERVL reporter system. *EMBO Reports*, *19*(12), e46240. https://doi.org/10.15252/embr.201846240

Yang, L., Xu, X., Xu, R., Chen, C., Zhang, X., Chen, M., Kou, X., Zhao, Y., Wang, H., Liu, X., Gao, S., & Li, C. (2022). Aberrant nucleosome organization in mouse SCNT embryos revealed by ULI-MNase-seq. *Stem Cell Reports*, *17*(7), 1730–1742. https://doi.org/10.1016/j.stemcr.2022.05.020

Yoshihara, M., Hayashizaki, Y., & Murakawa, Y. (2017). Genomic Instability of iPSCs: Challenges Towards Their Clinical Applications. *Stem Cell Reviews*, *13*(1), 7–16. https://doi.org/10.1007/s12015-016-9680-6

Yu, J., Vodyanik, M. A., Smuga-Otto, K., Antosiewicz-Bourget, J., Frane, J. L., Tian, S., Nie, J., Jonsdottir, G. A., Ruotti, V., Stewart, R., Slukvin, I. I., & Thomson, J. A. (2007). *Induced Pluripotent Stem Cell Lines Derived from Human Somatic Cells*. *318*.

Zahn, N., James-Zorn, C., Ponferrada, V. G., Adams, D. S., Grzymkowski, J., Buchholz, D. R., Nascone-Yoder, N. M., Horb, M., Moody, S. A., Vize, P. D., & Zorn, A. M. (2022). Normal Table of Xenopus development: A new graphical resource. *Development*, *149*(14), dev200356. https://doi.org/10.1242/dev.200356

Zaret, K. S., & Carroll, J. S. (2011). Pioneer transcription factors: Establishing competence for gene expression. *Genes & Development*, *25*(21), 2227–2241. https://doi.org/10.1101/gad.176826.111

Zaret, K. S., & Mango, S. (2016). Pioneer Transcription Factors, Chromatin Dynamics, and Cell Fate Control. *Current Opinion in Genetics & Development*, *37*, 76–81. https://doi.org/10.1016/j.gde.2015.12.003

Zaware, N., & Zhou, M.-M. (2019). Bromodomain biology and drug discovery. *Nature Structural & Molecular Biology*, *26*(10), 870–879. https://doi.org/10.1038/s41594-019-0309-8

Zeng, L., & Zhou, M.-M. (2002). Bromodomain: An acetyl-lysine binding domain. *FEBS Letters*, *513*(1), 124–128. https://doi.org/10.1016/S0014-5793(01)03309-9

Zhang, K., Wu, D.-Y., Zheng, H., Wang, Y., Sun, Q.-R., Liu, X., Wang, L.-Y., Xiong, W.-J., Wang, Q., Rhodes, J. D. P., Xu, K., Li, L., Lin, Z., Yu, G., Xia, W., Huang, B., Du, Z., Yao, Y., Nasmyth, K. A., … Xie, W. (2020). Analysis of Genome Architecture during

SCNT Reveals a Role of Cohesin in Impeding Minor ZGA. *Molecular Cell*, *79*(2), 234-250.e9. https://doi.org/10.1016/j.molcel.2020.06.001

Zhang, T., Cooper, S., & Brockdorff, N. (2015). The interplay of histone modifications – writers that read. *EMBO Reports*, *16*(11), 1467–1481. https://doi.org/10.15252/embr.201540945

Zhang, T., Zhang, Z., Dong, Q., Xiong, J., & Zhu, B. (2020). Histone H3K27 acetylation is dispensable for enhancer activity in mouse embryonic stem cells. *Genome Biology*, *21*(1), 45. https://doi.org/10.1186/s13059-020-01957-w

Zhang, Y., Liu, T., Meyer, C. A., Eeckhoute, J., Johnson, D. S., Bernstein, B. E., Nusbaum, C., Myers, R. M., Brown, M., Li, W., & Liu, X. S. (2008). Model-based Analysis of ChIP-Seq (MACS). *Genome Biology*, *9*(9), R137. https://doi.org/10.1186/gb-2008-9-9-r137

Zhang, Z., Zhai, Y., Ma, X., Zhang, S., An, X., Yu, H., & Li, Z. (2018). Down-Regulation of H3K4me3 by MM-102 Facilitates Epigenetic Reprogramming of Porcine Somatic Cell Nuclear Transfer Embryos. *Cellular Physiology and Biochemistry : International Journal of Experimental Cellular Physiology, Biochemistry, and Pharmacology*, *45*(4), 1529–1540. https://doi.org/10.1159/000487579

Zhao, J., Hao, Y., Ross, J. W., Spate, L. D., Walters, E. M., Samuel, M. S., Rieke, A., Murphy, C. N., & Prather, R. S. (2010). Histone Deacetylase Inhibitors Improve *In Vitro* and *In Vivo* Developmental Competence of Somatic Cell Nuclear Transfer Porcine Embryos. *Cellular Reprogramming*, *12*(1), 75–83. https://doi.org/10.1089/cell.2009.0038

Zhao, K., Wang, M., Gao, S., & Chen, J. (2021). Chromatin architecture reorganization during somatic cell reprogramming. *Current Opinion in Genetics & Development*, *70*, 104–114. https://doi.org/10.1016/j.gde.2021.07.006

Zhou, C., Wang, Y., Zhang, J., Su, J., An, Q., Liu, X., Zhang, M., Wang, Y., Liu, J., & Zhang, Y. (2019). H3K27me3 is an epigenetic barrier while KDM6A overexpression improves nuclear reprogramming efficiency. *The FASEB Journal*, *33*(3), 4638–4652. https://doi.org/10.1096/fj.201801887R

Zhou, C., Zhang, J., Zhang, M., Wang, D., Ma, Y., Wang, Y., Wang, Y., Huang, Y., & Zhang, Y. (2020). Transcriptional memory inherited from donor cells is a developmental defect of bovine cloned embryos. *The FASEB Journal*, *34*(1), 1637–1651. https://doi.org/10.1096/fj.201900578RR

Zhou, J. J., Cho, J. S., Han, H., Blitz, I. L., Wang, W., & Cho, K. W. (2023). Histone deacetylase 1 maintains lineage integrity through histone acetylome refinement during early embryogenesis. *eLife*, *12*, e79380. https://doi.org/10.7554/eLife.79380

Zikmund, T., Fiorentino, J., Penfold, C., Stock, M., Shpudeiko, P., Agarwal, G., Langfeld, L., Petrova, K., Peshkin, L., Hamperl, S., Scialdone, A., & Hoermanseder, E. (2025). Differentiation success of reprogrammed cells is heterogeneous in vivo and modulated by somatic cell identity memory. *Stem Cell Reports*, *0*(0). https://doi.org/10.1016/j.stemcr.2025.102447

List of abbreviations

AUPR - Area Under Precision-Recall
ChIP-qPCR - Chromatin Immunoprecipitation followed by Quantitative Polymerase Chain Reaction
CMM - Chromatin Modification Module
CNN - Convolutional Neural Network
CUT&RUN - Cleavage Under Targets and Release Using Nuclease
DEG - Differentially Expressed Gene(s)
DHS - DNase I Hypersensitive Site
DMSO - Dimethyl Sulfoxide
DNA - Deoxyribonucleic Acid
ESC - Embryonic Stem Cell
FC - Fold Change
GEM - Gene Expression Module
GO - Gene Ontology
GV - Germinal Vesicle
H2AK119ub - Histone H2A Lysine 119 Ubiquitination
H3K18ac - Histone H3 Lysine 18 Acetylation
H3K23ac - Histone H3 Lysine 23 Acetylation
H3K27ac - Histone H3 Lysine 27 Acetylation
H3K27me3 - Histone H3 Lysine 27 Trimethylation
H3K36me3 - Histone H3 Lysine 36 Trimethylation
H3K4me1 - Histone H3 Lysine 4 Monomethylation
H3K4me3 - Histone H3 Lysine 4 Trimethylation
H3K79me3 - Histone H3 Lysine 79 Trimethylation
H3K9ac - Histone H3 Lysine 9 Acetylation
H3K9me3 - Histone H3 Lysine 9 Trimethylation
HAT - Histone Acetyltransferase
HDAC - Histone Deacetylase
HU - Hydroxyurea
iPSC - Induced Pluripotent Stem Cell
IVF - In Vitro Fertilization
KAT - Lysine Acetyltransferase
Kdm5b - Lysine Demethylase 5B
LC-MS/MS - Liquid Chromatography-Tandem Mass Spectrometry
log2FC - Log2 Fold Change
mESC - Mouse Embryonic Stem Cells
MPF - M-phase Promoting Factor
MS - Mass Spectrometry
NF-stage - Nieuwkoop-Faber Stage
nTL - Naïve Transfer Learning
NT - Nuclear Transfer

OSK - Oct4, Sox2, Klf4
OSKM - Oct4, Sox2, c-Myc, Klf4
PC - Principal Component
PCA - Principal Component Analysis
PCC - Premature Chromosome Condensation
Pol II - RNA Polymerase II
PPN - Pseudo-Pronuclei
PTM - Post-Translational Modification
RBP1 - RNA Polymerase B1
RD - Reprogrammed-Down (genes)
RF - Random Forest
RNA - Ribonucleic Acid
ROC - Receiver Operating Characteristic
RPKM - Reads Per Kilobase Million
RU - Reprogrammed-Up (genes)
SCNT - Somatic Cell Nuclear Transfer
$SrCl_2$ – Strontium chloride
TAD - Topologically Associating Domain
TBP - TATA-Binding Protein
TBP2 - TATA-Binding Protein 2
TF - Transcription Factor
TL - Transfer Learning
TPM - Transcripts Per Million
TSS - Transcription Start Site
UV - Ultraviolet
ZGA - Zygotic Genome Activation

Acknowledgements

First and foremost, I would like to thank Dr. Eva Hörmanseder for giving me the opportunity to work on this project and explore the world of chromatin and reprogramming during my PhD. Thank you for your guidance, support and faith in me throughout the years, as well as your tireless curiosity and passion for science. I learned a great deal from you during the years we spent working together, and I am grateful for that.

I would also like to thank my lab mates: Meghana, Marco, Tomas, and Huiwen, who all came before me, welcomed me, taught me and included me in our team. Thank you for being such team players and for sharing our scientific journey together.

In particular, I would like to thank Meghana with whom we soldiered on throughout the PhD journey, especially at the end stages with all the highs and lows, successes and lessons, and somehow always found a way to make things work. Being colleagues with you was a formative part of the PhD journey, which taught me a lot and I cherish it deeply.

I would also like to thank Prof. Maria-Elena Torres-Padilla for her supervision, insightful input for my project and continuous support. Thank you for making the IES such a vibrant and stimulating place to work in.

I thank my thesis advisory committee consisting of Prof. Maria-Elena Torres-Padilla, Prof. John Parsch and Prof. Kikue Tachibana. I truly appreciated and enjoyed the discussions and feedback on the project I received in the annual TAC meetings, which greatly improved my research and helped me grow as a scientist.

My deep gratitude goes also to Dr. Stephan Hamperl who has selflessly supported my work and my project throughout the years, with his insightful comments, great questions, encouraging feedback and always positive attitude. Furthermore, I thank the entire Hamperl lab for being such amazing lab neighbors who never hesitated to share their advice, materials, support and good spirits, it was truly a pleasure to have you by our side.

I also thank Prof. Kikue Tachibana and her group for welcoming us to their group seminars: your curiosity for our projects has been such a source of motivation and new impulses in the end-stages of this project and I am very grateful for this opportunity!

I thank Dr. Sara Llorente-Armijo for our productive and stimulating collaboration on identifying enhancers in *Xenopus* embryonic endoderm. Through this process, I learned

a great deal about bioinformatic analyses, which allowed us to push this project forward and gain new insights.

I thank Dr. Adam Burton for his keen interest in this project and his ‘tough’ questions, which always made me learn and think about my work from a new perspective.

I thank Dr. Chris Penfold for his work on the Digital Reprogramming model, which served as a basis for my project, as well as our work together on the manuscript.

I deeply thank the people and facilities that supported our work: the Genomics Facility of HMGU with Inti de la Rosa and Gertrud Eckstein, the ZfP at BMC LMU with Ignasi Forne, and the Bioinformatics Core and BMC LMU with Tobias Straub, the CAM at LMU, in particular, Monika Haberland and Selina Scheungrab for taking such good care of our frogs and supporting our experimental work.

The frog life wouldn’t have been half as joyous without the Rupps who shared everything with us and who were always such a source of advice, team spirit and friendliness. Janet, thank you for being our partner in crime!

I have been very fortunate and privileged to do this PhD in the CRC 1064 Chromatin Dynamics. This opportunity has been formative in many ways, but more than anything it gave me a strong sense of community and belonging. Thank you, Elizabeth Schroeder-Reiter, for always having an open door and open ear– it was a pleasure working with you and Prateek Yadav as a PhD representative.

I would like to thank my colleagues and friends from the IES, in particular Marlies, Clara, Mrinmoy, Antoine, Marcel, Marion, Fede – you have made every single day in the lab a fun one, and your support, friendship and conversations mean the world. I am proud of every single one of you and it is a privilege to know you.

My journey has also been blessed with many friendships and powerful women who each have their own path and never cease to amaze and inspire me. Fani, Ioana, Jona, Nadine, Erika, Ana, Huiwen – thank you for being who you are, and thank you for always being by my side, no matter where life took us.

Last but not least, I am extremely fortunate to have a family like mine to thank. My deepest gratitude goes to my parents Nadica and Pece who supported every step I took – from the day I signed up for German classes in 2008 to venturing off on my academic journey to Germany in 2016 until this very moment. Thank you for showing me the value of education and the power of finding your own path. Thank you for the endless hours you

listened to me, learned about what I do, understood me, loved me and supported me unconditionally. This is the reason I am who I am, and I am where I am. Being raised by you is my biggest privilege.

I thank my little sister Marija – thank you for teaching me a continuous lesson on courage in life, for being a ray of sunshine since day one, and for teaching me to take life with a little bit more lightness. You are an inspiration and a role model to me, and I watch you take the world by storm with immense pride.

I thank my dear grandparents Filip and Dubravka who taught me how to read and write, who made me fall in love with books and the joy of learning; my grandmother who left us too soon but taught me all I know on how to be a strong and kind woman; my grandfather who taught me how to persevere in every challenge life brings, and how to do it with a smile. Thank you for believing in me so unconditionally.

And finally, I thank everyone else from our large, loud, loving and growing family: Tanja, Irena, Trajce, Boki, Kiko, Tijana, Tamara, Filip. I am immensely rich for having all of you.

I thank my partner, Antonio Gonzalez, for bringing love and joy into my life. Thank you for being my tireless supporter and for empowering me along every step of this journey. Thank you for always reminding me of the bright and light side of life.

Finally, I thank my younger self. Thank you for being strong and brave. It is your shoulders I stand on today.